CHARACTERIZATION OF A G PROTEIN-COUPLED RECEPTOR ENCODED BY THE RHESUS MACAQUE VIRAL HOMOLOGUE OF HUMAN HERPESVIRUS 8 (HHV-8) / KAPOSI'S SARCOMA-ASSOCIATED HERPESVIRUS (KSHV)

by

Ryan D. Estep

A DISSERTATION

Presented to the Department of Molecular Microbiology and Immunology

and the Oregon Health and Science University School of Medicine

in partial fulfillment of the requirements for the degree of

Doctor of Philosophy

July 2004

School of Medicine
Oregon Health and Science University

CERTIFICATE OF APPROVAL

This is certify that the Ph.D. thesis of

Ryan D. Estep

has been approved

[redacted]
Scott Wong, Ph.D, *thesis advisor*

[redacted]
Richard Maurer, Ph.D, *committee member*

[redacted]
Jay Nelson, Ph.D, *committee member*

[redacted]
Klaus Frueh, Ph.D, *committee member*

TABLE OF CONTENTS

LIST OF FIGURES AND TABLES

Figure **Page Number(s)**

Table **Page Number**

ACKNOWLEDGEMENTS

First and foremost I would like to thank my advisor **Scott W. Wong**, for allowing me the opportunity to carry out my thesis research in his laboratory, and for providing me with continued support and mentorship that have allowed me to develop my skills as a scientist. His openness to my ideas and faith in my abilities have been key to my success, and his friendship and kindness will always be remembered. In addition, I would like to extend my gratitude to **Richard Maurer**, **Jay Nelson**, and **Klaus Frueh**, for donating their time and providing guidance as members of my thesis committee. Recognition also goes to the faculty and staff of the **Molecular Microbiology and Immunology Department** at OHSU, many of who have provided their assistance at many steps along the way. Thanks also go to the members of the **Wong Lab** for all of their help and support, and for providing an enjoyable and stimulating work environment.

My greatest thanks are reserved for my wife **Valerie L. Estep**, who has been instrumental to my success in graduate school. Her undying support, love, and understanding have helped me through many trying times, and for this I am extremely grateful. Also deserving of thanks are my parents, **Ronald M. and Beverly A. Estep**, and my brother **Brett A. Estep**, whose love and support for me has never waned, regardless of my endeavors, and who have helped me become the person I am today. In addition, many thanks go to my numerous close friends, and the many members of **The Plaep, Estep, Wetzel, Bangs, and Moen families**, who have provided their support and love.

My graduate school experience would not have been as memorable if not for the wonderful acquaintances I have made during my time at OHSU. Thus, I would like to

thank all of my fellow graduate students, whom I have had the pleasure of knowing as both friends and colleagues. Special mention goes to **Shaun Lee** and **Sean Kelly**, who have become dear friends, and with which I have shared many fun times during my graduate school years. Also, deserving of special note is **Carly Langlais**, my fellow lab-mate and friend, who I have enjoyed working with closely, and whose many helpful discussions and insights have been invaluable to me.

This thesis is dedicated to several people very close to me that have passed away in the past year, including my grandmother **Jacqulyn L. Plaep**, my grandfather **Donald M. Estep**, and my grandfather-in-law **Howard H. Bangs**. They have all touched my life in many ways, and I will cherish my memories of them always.

" *Facilius per partes in cognitionem totius adducimur.*"

(We are more easily led part by part to an understanding of the whole.)

– Seneca

"*The most beautiful experience we can have is the mysterious - the fundamental emotion which stands at the cradle of true art and true science.*"

– Albert Einstein

ABSTRACT

Human herpesvirus 8 (HHV-8)/Kaposi's sarcoma-associated herpesvirus (KSHV) is the causative agent of Kaposi's sarcoma (KS), as well as B cell malignancies such as primary effusion lymphoma (PEL) and multicentric Castleman's disease (MCD). Recently, a herpesvirus known as rhesus rhadinovirus (RRV) was identified in a rhesus macaque that had developed B cell hyperplasia. Upon sequencing of the entire RRV genome, the virus was found to be homologous to HHV-8. Importantly, RRV shares a majority of open reading frames (ORFs) with HHV-8, including one encoding a viral G protein-coupled receptor (vGPCR). The vGPCR encoded by ORF74 of HHV-8 has been shown to be a constitutively signaling receptor with transforming properties *in vitro* and *in vivo*, and has been suggested to play a role in HHV-8-associated disease development. Based on the similarity of RRV ORF74 to HHV-8 ORF74, we speculated that this ORF also encodes a vGPCR, and that the protein may have similar properties to the HHV-8 vGPCR. Therefore, studies were initiated to examine RRV ORF74, to determine the properties of this ORF and the encoded protein product. The work presented in this thesis demonstrates that RRV ORF74 encodes a vGPCR with similarity to the HHV-8 vGPCR. The initial analysis of the RRV vGPCR in a NIH3T3 model system revealed that the RRV vGPCR possesses transforming properties *in vitro* and *in vivo*, and induces cells to secrete increased levels of vascular endothelial growth factor (VEGF), an angiogenic factor involved in tumorigenesis. Further, the RRV vGPCR displays signaling abilities in NIH3T3 cells, and can activate the extracellular signal-regulated kinase (ERK)1/2 signaling pathway in both constitutive and ligand-dependent manners. Additional studies examining both the HHV-8 and RRV vGPCRs in human B cells were also performed,

and indicated that these receptors are both functional in a cell type relevant to viral infection and disease development *in vivo*. In this cell type, both vGPCRs similarly activate the ERK1/2 and Akt/glycogen synthase kinase-3(GSK-3) pathways in a constitutive manner, utilizing $G\alpha_i$-independent but phosphatidylinositol-3-kinase (PI3K)-dependent mechanisms. However, the constitutive signaling displayed by both vGPCRs in B cells is also responsive to the inhibitory chemokine IP-10. Expression of either receptor in B cells was also found to have anti-apoptotic effects, suggesting that this may be a mechanism of vGPCR mediated transformation in this cell type. Transcriptional analysis of RRV ORF74 revealed that like HHV-8 ORF74, RRV ORF74 is a lytic gene that is transcribed as part of a bi-cistronic transcript with an upstream ORF encoding the viral CD200 homologue (vCD200). Despite these similarities, major variations were found to exist between these transcripts, with splicing events in the RRV message resulting in the production of a soluble form of vCD200, a finding that could have major implications for a role for this protein in viral pathogenesis. Overall, these data suggest that the RRV vGPCR is highly homologous to the HHV-8 vGPCR, and therefore that RRV provides an excellent system to study the contributions of the HHV-8 vGPCR to the viral life cycle and viral pathogenesis.

Chapter 1

INTRODUCTION

1. Human Herpesviruses

a. *Classification*

Herpesviruses are a common cause of disease in both animals and humans, and are ubiquitous, with at least one virus having been associated with most animal species examined (53). Herpesviruses have the unique capability of persisting in a latent stage in infected hosts, with occasional reactivation and shedding of virus. Thus, infection with a herpesvirus results in lifelong presence of the virus in the host. Currently there are eight known human herpesviruses, all of which represent a potential health risk to infected individuals, with some displaying more severe pathogenic properties than others.

Herpesviruses are members of the *Herpesviridae* family, and are further classified into three subfamilies based on biological properties such as host range, cellular tropism, and growth characteristics (53). The *Alphaherpesvirinae* subfamily contains the *Simplexvirus* genus, which includes herpes simplex virus type 1 and type 2 (HSV-1 and HSV-2), and the *Varicellovirus* genus, containing varicella zoster virus (VZV). All alphaherpesviruses are characterized by their neurotropism and relatively short replication cycle. HSV-1, HSV-2, and VZV are known as human herpesvirus (HHV) -1, 2, and 3, respectively, all of which are common in most human populations. The *Betaherpesvirinae* subfamily includes the *Cytomegalovirus* genus, typified in humans by cytomegalovirus (CMV), or HHV-5, whose seroprevalence is around 60% in developed

countries, and often higher in undeveloped countries and among certain socio-economic groups (49). Also in this subfamily is the *Roseolovirus* genus, whose members include HHV-6 and 7, viruses that infect ~85% of the world's population (93). Betaherpesviruses have a longer replication cycle than alphaherpesviruses, and tend to have a more restricted host range. Members of the third subfamily, the *Gammaherpesvirinae*, are lymphotropic viruses that infect and replicate mainly in lymphoid cells. This subfamily contains the *Lymphocryptovirus* (or gamma-1) genus, which includes Epstein-Barr Virus (EBV), or HHV-4, a virus that infects roughly 90% of the world's population. Also in this subfamily is the *Rhadinovirus* (or gamma-2) genus, whose members include Kaposi's sarcoma-associated herpesvirus (KSHV), or human herpesvirus 8 (HHV-8). HHV-8 will be discussed in detail in a later section of this chapter.

b. *Herpesvirus Structure*

Herpesviruses vary widely in genomic sequence, but the general structure of the genome is a common character shared by all family members. Herpesviruses are double-stranded DNA viruses whose genomes range from ~120 to ~250 kb in size, and generally contain terminal repeats of DNA sequence, and in some cases regions of internal repeats (54). Despite similarities in genomic organization, the complete array of proteins encoded differs greatly among the different types of herpesviruses, however, all encode a wide array of proteins involved in nucleic acid metabolism and DNA replication, including a DNA polymerase.

Another commonality of herpesviruses is the general structure of the virion, all of which have been found to be quite similar for all herpesviruses examined thus far (53, 54,

164). The schematic in figure 1.1A depicts the structural components of a typical herpesvirus virion, and an actual electron microscopy image of HHV-8 virions is shown in figure 1.1B. A prototypical herpesvirus virion consists of the core, containing the double-stranded DNA genome, encapsidated by a proteinaceous shell, or capsid. Together the core and capsid are known as the nucleocapsid. The capsid is icosahedral in structure, and generally ~1250 Å in diameter. Also, all herpesvirus capsids have a T number of 16, a unique characteristic among all known viruses (164). The capsid is enclosed in a lipid bilayer envelope, which is derived from cellular membranes obtained during release, or egress, of the virus from an infected cell. An amorphous protein-containing layer between the envelope and capsid is termed the tegument. The envelope contains numerous protrusions that appear as spikes on the surface of the virus when examined by electron microscopy. These protrusions represent viral glycoproteins that have been shown to be important for viral attachment and entry into host cells. In general, the overall size of herpesvirus virions ranges from 120 nm to 300 nm, depending on the identity of the particular herpesvirus under examination.

Figure 1.1 Herpesvirus structure. (A) Cross-section diagram of the structure of a typical herpesvirus virion. The spikes on the surface of the envelope represent viral glycoproteins. (B) Electron microscopy image of HHV-8 virions produced from the HHV-8 positive PEL cell line KS-1 (arrows indicate mature virions). *The image in B was adapted from reference (1).*

A.

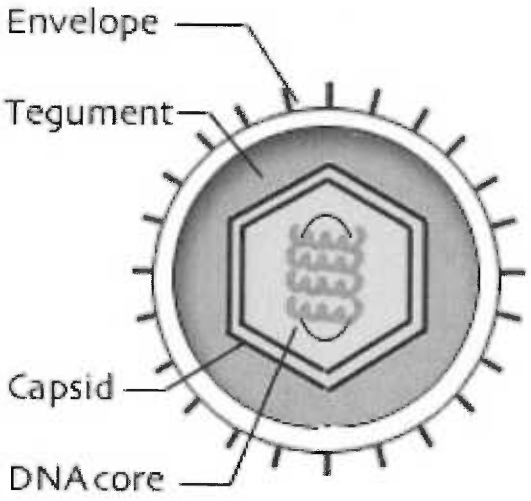

B.

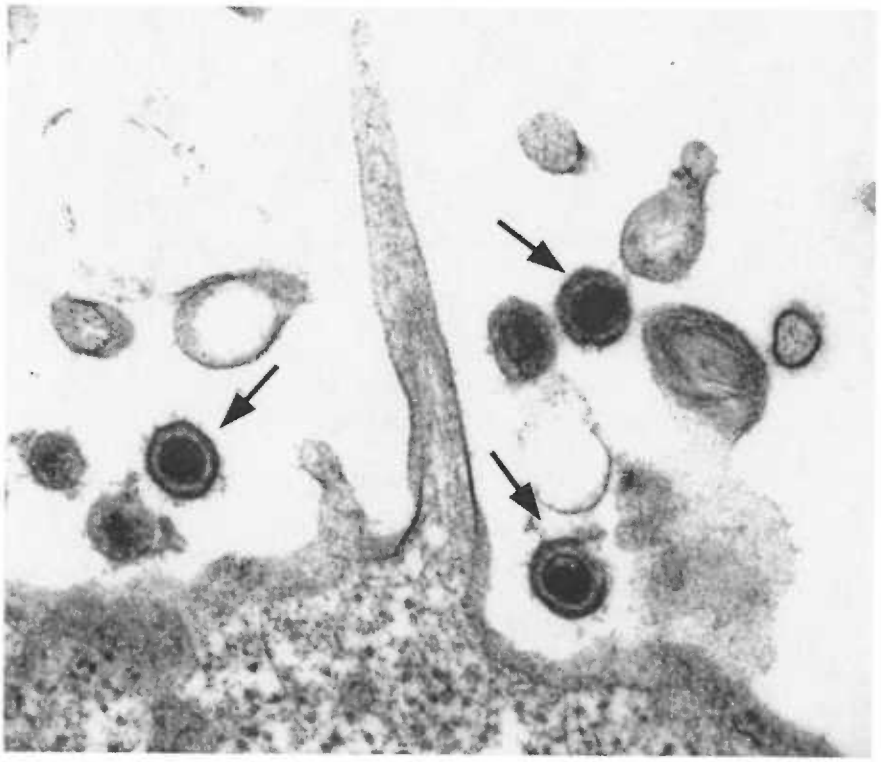

c. *General Herpesvirus Life Cycle*

The general mechanism of herpesvirus infection and replication has been well studied. In a typical infection, viral gylcoproteins on the surface of the virion interact with cellular receptors on host cells, allowing for the initial attachment of the viral particle. The viral receptor involved in attachment in the case of HSV-1 is thought to mainly be gC, however, other proteins such as gB and gD may also be involved (156). The entire array of cellular receptors utilized by all herpesviruses is not completely defined, although heparin sulfate appears play a major role in the attachment of several herpesviruses to target cells (157). After the initial binding of the virus to a cell, other cellular receptors, or co-receptors, mediate fusion of the viral envelope with the cellular membrane via further interactions with viral glycoproteins.

The fusion of the viral envelope with the cellular membrane results in the release of the nucleocapsid into the cytoplasm, followed by the active transport of the nucleocapsid to nuclear pores through interactions with microtubules (153). Once at a nuclear pore, viral DNA is released into the nucleoplasm, where the DNA takes on a circularized form. Transcription of viral genes is conducted by cellular RNA polymerase II, while viral DNA replication occurs via a rolling circle mechanism utilizing a virally-encoded DNA polymerase (54).

Transcription of herpesvirus lytic genes occurs in a cascade fashion, with three classes of genes being expressed at different temporal intervals (53). The first set of genes to be expressed are of the immediate-early class (or α class), which are transcribed immediately after viral DNA enters the nucleus. These genes encode proteins that are necessary for the further transcription of other viral genes. The second group of genes to

be expressed belong to the early class (or β class), and include genes involved in replication of viral DNA. Lastly, the late genes (or γ class) are transcribed only after viral DNA replication has taken place, and tend to encode structural components of the virion. Early and late genes are each dependent on the expression of the class before to be expressed. Thus, in addition to time of expression, the assignment of genes into a particular class is largely dependent on their sensitivity to inhibitors of DNA replication and protein synthesis. For example, genes whose expression is not inhibited by cycloheximide (CHX), a protein synthesis inhibitor, are considered immediate-early (α) genes, which can be transcribed without any prior viral protein synthesis. Those genes whose transcription is not prevented by inhibitors of DNA replication, such as phosphonoacetic acid (PAA), are classified as either immediate-early (α) or early (β) genes, depending on their sensitivity to CHX. Finally, late (γ) genes are those inhibited by either protein synthesis or DNA replication inhibitors.

After DNA replication and generation of viral structural proteins, viral DNA is packaged into preformed capsids. Assembly of viral particles is thought to occur in the nucleus, with subsequent egress of the viral capsid through the nuclear membrane and the vesicles of the trans-Golgi network (106). Finally, enveloped virus is released from the cell, either by budding through the plasma membrane, or lysis of the infected cell.

In addition to lytic replication, herpesviruses all possess the ability to establish latent infections in infected host cells. In this scenario, the virus does not complete the lytic replication cycle, but rather represses the normal cascade of lytic gene expression, essentially becoming quiescent, and preventing production of infectious virus. During latency, a limited subset of latency-associated genes are expressed, and the viral genome

is maintained in the host cell as a viral episome, thus allowing the viral genome to be carried indefinitely in that cell until a lytic replication cycle is initiated. The exact mechanisms involved in initiation and reactivation from latency are not fully understood, and show significant variations depending on the identity of the herpesvirus in question (169). Nevertheless, latency is frequently associated with herpesvirus infections, essentially providing a permanent reservoir of infectious virus that remains hidden in an infected host until favorable conditions arise for further propagation.

d. ***Human Herpesviruses and Disease***

All alphaherpesviruses display the propensity to infect neurons, where once an infection is established, the virus is able to remain latent until reactivation. HSV-1 is the cause of oral herpes, while HSV-2 is associated with the genital form of herpes. Both HSV-1 and HSV-2 are common throughout the world. These viruses initially infect and replicate in epithelial cells, ultimately infecting neurons near the site of infection, then traveling by retrograde transport through these neurons, and establishing latent infections in sensory nerve ganglia (171). The other known human alpha herpesvirus, VZV, is the causative agent of chicken pox (varicella), a common childhood disease characterized by disseminated body lesions. After this initial infection, VZV can establish a latent infection in trigeminal and dorsal root ganglia, and later may reactivate to cause shingles (herpes zoster) (12, 83).

The betaherpesvirus CMV is common in the general population, and is usually asymptomatic, with no apparent disease associated with infection in healthy individuals. However, among immunosuppressed individuals, CMV is commonly associated with

potentially harmful diseases such as pneumonitis, atherosclerosis, and retinitis, while in newborns CMV infection can occur through perinatal transmission from an infected mother, resulting in the development of birth defects (68, 90). HHV-6 and HHV-7 are closely related viruses, and are believed to be the causative agents of roseola infantum (exanthem subitum) and febrile illness in infants and young children (93).

The gammaherpesvirus EBV is a ubiquitous virus capable of infecting B cells, where the virus can establish a life-long latent infection. EBV is generally spread asymptomatically among children, however, when primary infection occurs at later stages of life, infectious mononucleosis occurs in about 50% of cases (99). In addition, EBV has oncogenic properties, and is associated with the development of several malignancies, including nasopharyngeal carcinoma and Burkitt's lymphoma (64). KSHV, or HHV-8, is the most recently identified human herpesvirus, and is associated with the development of Kaposi's sarcoma (KS), as well as the B cell disorders primary effusion lymphoma (PEL) and multicentric Castleman's disease (MCD) (30, 34, 155). HHV-8 is unusual in that the prevalence of the virus in the human population is generally much lower than that of other herpesviruses, and that the virus has a somewhat varied distribution throughout the world. Epidemiological studies have suggested that approximately 2 to 5% of people are positive for HHV-8 throughout most of the world, while in Mediterranean countries anywhere from 4 to 35% can test positive for the virus, depending on the region under examination. These numbers range from 30% to 60% in some regions of sub-Saharan Africa, where HHV-8 is endemic (1, 145, 147). In Western countries, homosexual men appear to be at a much higher risk than the heterosexual population for becoming infected with HHV-8, potentially due to a route of transmission related to sexual behavior (19, 82,

102). In general, HHV-8 infection has recently become much more common, as well as more of a threat to human health, for reasons that will be discussed in the next section.

2.Kaposi's Sarcoma-Associated Herpesvirus(KSHV)/Human Herpesvirus 8(HHV-8)

a. *Identification and Classification of a Kaposi's Sarcoma-Associated Virus*

KSHV/HHV-8 was first identified in 1994 by Chang *et al.*, using representational difference analysis (RDA) of genomic DNA from a Kaposi's sarcoma (KS) lesion obtained from a patient with acquired immunodeficiency syndrome (AIDS) (34). Sequence analysis revealed that this agent was a member of the *Herpesviridae* family, and specifically that the virus belongs to the gamma-2 or *Rhadinovirus* genus of the *Gammaherpesvirinae* subfamily (113). The viral genome consists of a long unique region (LUR) of ~140.5 kb, which contains sequences for 66 conserved herpesvirus genes, and is flanked on both ends by terminal repeat units with a high G+C content of 84.5% (141). Recent data has also shown that the overall structure of the HHV-8 virion is typical of all herpesviruses (142), and examination of the capsid structure of HHV-8 reveals a high similarity to the capsids of HSV-1 and CMV (164, 175). This virus is the first identified gamma-2 herpesvirus known to infect humans, and is the eighth identified human herpesvirus. The virus has the common name of Kaposi's sarcoma-associated herpesvirus (KSHV), and the formal name of human herpesvirus 8 (HHV-8).

The classification of HHV-8 as a rhadinovirus is based on similarities of the virus in genomic sequence and cellular tropism to herpesvirus saimiri (HVS), the prototypical

rhadinovirus, which naturally infects squirrel monkeys (*Saimiri sciureus*) (104). Although HVS infects squirrel monkeys without any apparent development of disease, the virus can cause fatal T cell lymphomas in other new world primates, as well as transform human T cells *in vitro* (52). Other rhadinoviruses that have been identified include murine gammaherpesvirus 68 (MHV-68), as well as several primate viruses found to infect chimpanzees, spider monkeys, African green monkeys, gorillas, mandrill and drill monkeys, pig tail macaques, and rhesus macaques (42, 67, 87, 89, 151). Rhesus macaque rhadinovirus (RRV) will be discussed in greater detail later as the main focus of this thesis.

b. *HHV-8 Associated Diseases*

i. *Kaposi's Sarcoma (KS)*

KS was first identified by the Hungarian dermatologist Moritz Kaposi in 1872. KS is commonly characterized by lesions of the skin, visceral organs, and lymph nodes, containing slit-like vascular spaces and infiltrating inflammatory cells (e.g. T cells, monocytes, macrophages, and dendritic cells), with the dominant cell type of the lesions being proliferating spindle-shaped cells believed to be of endothelial origin (Fig. 1.2A) (50, 116, 143). Neoangiogenesis is a hallmark of KS lesions, and angiogenic cytokines such as vascular endothelial growth factor (VEGF) have been suggested to be involved in spindle cell proliferation and development of lesions (38, 55, 103). In general, an inflammatory component is thought to play a major role in the development of the disease, with cytokines, chemokines, and growth factors such as IFN-γ, TNF-α, IL-1β,

IL-6, IL-8, basic fibroblast growth factor (bFGF), and VEGF, all having been found to be upregulated in KS lesions (50). Most cells in KS lesions appear to be normally diploid, suggesting that KS may be a hyperplastic proliferative lesion, rather than an actual neoplasm (116). Overall, the formation of KS lesions appears to be a complex process, and the exact mechanism of development and identity of all components involved in is not currently known, and continues to be the subject of intense study.

KS is most commonly found in human immunodeficiency virus (HIV) –infected patients with acquired immunodeficiency syndrome (AIDS), which is referred to as AIDS-associated KS (AIDS-KS), although the disease also occurs in several non-AIDS associated forms (50). Both classic and post-transplant KS are milder forms of the disease. Classic KS is most commonly found in elderly men of Eastern European and Mediterranean descent, in which lesions typically form on lower extremities. Post-transplant, or iatrogenic KS, occurs in transplant patients that have received immunosuppressive agents, with lesions appearing mainly on the skin and oral mucosa (116). African KS is another more aggressive form of KS that is found in sub-equatorial Africa, where the disease occurs most frequently in young black men, and is often fatal (162). Before the AIDS epidemic, KS was seen as a relatively rare disease, and was particularly uncommon in North America and Northern Europe. However, since the onset of the AIDS epidemic, KS has become much more prevalent, and is now one of the leading causes of mortality among AIDS patients (166).

Extensive studies have suggested that HHV-8 is the causative agent of Kaposi's sarcoma (KS) in humans. HHV-8 has been associated with all forms of KS (20, 34, 112), and a definitive role for HHV-8 in the development of the disease has been suggested

based on numerous serological data that indicate HHV-8 infection precedes the onset of KS (59, 136, 143). Also, the frequency of KS in various groups throughout the world parallels closely the rates of HHV-8 infection detected in these populations (1). In the case of AIDS-KS, HIV-1 infection appears to be a major co-factor in the development of disease, and may account for the increased frequency and severity of KS in HIV-1 positive individuals compared to those infected with HHV-8 alone. This is most likely due to impairment of the immune system by HIV-1, although direct contributions of HIV-1 proteins such as Tat have also been suggested (72, 80, 116).

The exact mechanisms involved in KS development due to HHV-8 infection are unknown. However, some of the ideas set forth include the direct transformation of infected cells by HHV-8, and the increased production of cytokines by infected cells that act in a paracrine or autocrine fashion to induce changes in cellular components of the lesions (31, 123). In a typical KS lesion, spindle cells have been found to harbor the virus in a latent state, with around 90% of spindle cells in a mature lesion being infected (48). Interestingly, KS spindle cells can be cultured *in vitro*, although upon passage, the viral genome is lost by most cells, with only a small percentage remaining positive for the virus (5, 46, 91). Infection of primary endothelial cell cultures with HHV-8 results in production of a KS-like phenotype and an increased life span of these cells, although only 1-6% of the cells in the culture are positive for the virus (55). This phenotype mimics what is seen *in vivo*, in which only a small percentage (<10%) of cells in early KS lesions are positive for the virus (48), and may suggest that the development of a KS phenotype does not require a cell to be directly infected, and rather that paracrine factors released from infected cells may play a role in transforming uninfected neighboring cells.

Alternatively, some have suggested a possible "hit-and-run" mechanism of HHV-8 transformation, in which viral infection causes irreversible genetic changes in an infected cell leading to transformation, before the viral genome is ultimately lost (7). However, multiple mechanisms may be involved in the development of KS, and lesion formation is likely due to a complex interplay between various events.

ii. *B Cell Abnormalities (PEL and MCD)*

In addition to KS, HHV-8 has also been associated with B cell malignancies, including primary effusion lymphoma (PEL), and multicentric Castleman's disease (MCD) (30, 155). PEL is commonly fatal, and is characterized by pleural or pericardial effusion, with localization of the neoplasm to body cavities, and without the formation of solid tumors or the development of any peripheral lymphadenopathy (56, 166). PEL cells possess characteristics of post-germinal center B cells, and are consistently found to be infected with HHV-8, which is thought to drive development of the lymphoma (Fig. 1.2B) (1, 30, 166). In addition to HHV-8, EBV infection is also common in PEL cells, and is associated with 70% of cases (56). However, any role of EBV in the development of PEL is uncertain, since HHV-8 infection alone appears capable of inducing PEL (11).

Castleman's disease (CD) is a lymphoproliferative disorder characterized by increased B cell and vascular proliferation in germinal centers of lymph nodes, and is thought to result at least partially from over-expression of cytokines such as IL-6 (1). Studies have confirmed that HHV-8 infection is tightly associated with the development of CD, in particular the plasma cell variant of the disease, also known as multicentric Castleman's disease (MCD) (47, 155). MCD involves multiple lymph node sites, and is

characterized by evident plasma cell infiltration and proliferation in these nodes (Fig. 1.2C) (1, 146). The initial examination of HHV-8 in MCD revealed that HHV-8 DNA was associated with all cases of HIV-associated MCD, and 7 of 17 cases of MCD in HIV negative patients (155). Further, the presence of MCD is often associated with the development of other immunological abnormalities, including KS and non-Hodgkin lymphoma (NHL) (1, 125). Unlike the situation in PEL, EBV co-infection does not seem to be associated with MCD (143).

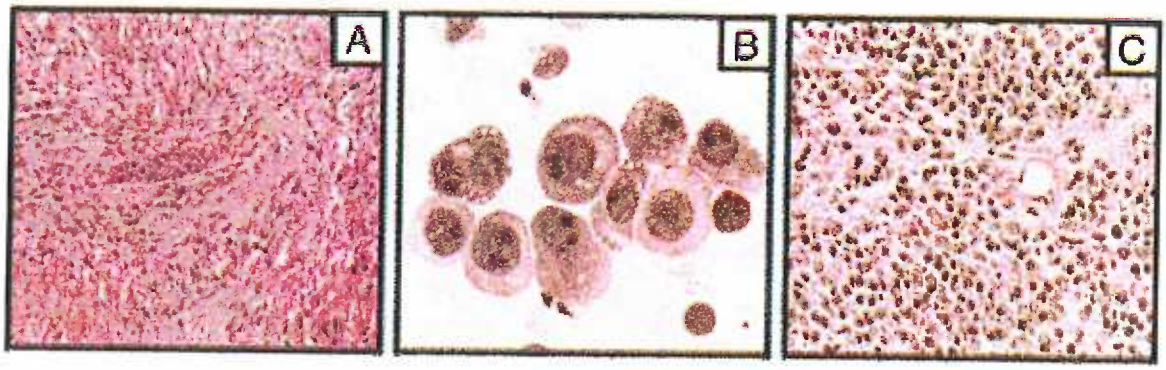

Figure 1.2 Histopathology of KS, PELs and MCDs. (A) Histological section of nodular tumor stage KS lesion stained with hematoxylin and eosin showing infiltrating spindle cells and disorganized vascular lumen filled with red blood cells. (B) Hematoxylin and eosin-stained PEL cells from needle aspirate showing large plasmacytoid tumor cells. (C) Hematoxylin and eosin-stained section of HIV-associated MCDs showing characteristic histopathology including plasmacytoid domination of node architecture. *Figure and legend adapted from reference (166).*

c. *The Role of Viral Genes in Pathogenesis*

Numerous ORFs in HHV-8 have been implicated in the pathogenesis of the virus. Interestingly, a majority of these ORFs have been found to be homologous to cellular genes, and are believed to have been pirated from host cell genes during the evolution of the virus. These include homologues for IL-6 (vIL-6), macrophage inflammatory protein (vMIPs I-III), Bcl-2 (vBcl-2), interferon regulatory factor (vIRFs), FLICE-inhibitory protein (vFLIP), cyclinD (v-cyclin), CD200 (vCD200), and a G protein-coupled receptor (vGPCR). Studies on many of these ORFs have revealed that they retain similar properties to their cellular counterparts, although significant variations also exist. The vBcl-2 and vFLIP homologues have been found to inhibit apoptosis *in vitro* (144, 163), and v-cyclin is a functional protein capable of deregulating cellular proliferation (160). In the case of HHV-8 viral cytokine and chemokine homologues, vIL-6 has been shown to have IL-6-like properties (111, 126), while vMIPs I-III appear to be functional chemokine homologues capable of binding to cellular chemokine receptors to regulate signaling pathways and chemotaxis (121, 158). Also, HHV-8 vIRF has been shown to inhibit IFN-induced signal transduction, and cause cellular transformation (58). The HHV-8 vGPCR is similar to the cellular chemokine receptors for IL-8 (CXCR1 and CXCR2), and has been found to be a functional receptor that possesses transforming properties. A detailed discussion of this receptor follows later. Importantly, all of these HHV-8-encoded cellular homologues are thought to play a role in the transforming and disease causing potential of the virus, due to subversion of cellular pathways involved in cell growth and survival, and through modulation of the host immune system. However, these viral genes likely provide some critical functions required by the virus for efficient

infection, replication, spread, or persistence, and their pathogenic properties may just be a side effect of their expression.

d. *in vitro and in vivo Models of HHV-8*

One major drawback to the analysis of HHV-8 is the lack of a good *in vitro* cell culture system for propagation of the virus. HHV-8 has been found to infect several cell types *in vitro* (e.g. B cells, endothelial cells, fibroblasts, macrophages, and epithelial cells), but in all the systems analyzed thus far, the virus undergoes limited lytic replication, and thus cannot be propagated to high titers for efficient serial passage (16, 134). In most studies of HHV-8 infection *in vitro*, a majority of cells become latently infected with HHV-8, and only a small percentage (~1-5%) of cells support any lytic viral replication (16, 114). This lack of lytic growth has been suggested to be due to a propensity of HHV-8 to establish a latent infection, versus inducing lytic replication after an initial infection (16). Lack of sufficient lytic replication *in vitro* is an enormous hurdle to examining properties of HHV-8 during a *de novo* infection, including lytic gene transcription, viral replication, and viral assembly. Further, without a dependable *in vitro* system of lytic replication, accurate studies of individual genes in the context of HHV-8 are not possible, given that production of modified viruses (e.g. gene "knock-out" and mutant viruses) is not accomplished easily.

Currently, the most reproducible source of infectious virus entails the use of latently infected PEL cell lines induced to undergo lytic replication with phorbol esters or sodium butyrate (11, 108, 135). After treatment, these cells produce infectious virus, but otherwise retain the viral genome in a latent state, with only a small percentage of cells

(~2%) undergoing spontaneous lytic replication (108). Although invaluable to studies on HHV-8, these cells do not provide an ideal system to study properties associated with a *de novo* infection, such as viral replication and lytic gene transcription, due to the constant presence of latently infected cells in these cultures.

Despite the lack of sufficient lytic growth *in vitro*, infection of some endothelial cell cultures with HHV-8 appears to closely mimic what is seen in HHV-8 infected KS lesions *in vivo*, and may provide suitable models for the analysis of HHV-8 in KS development. For example, infection of immortalized dermal microvascular endothelial cells with HHV-8 results in a majority of these cells becoming latently infected, followed by the transformation and ultimate development of a KS-like spindle cell phenotype in these cultures (114). In addition, HHV-8 infection of primary endothelial cell cultures has been associated with increased proliferation and cell survival, acquisition of a transformed phenotype, and upregulation of the VEGF receptor KDR (55). Importantly, this implies that VEGF may play a role in the increased survival and growth of these cultures. Regardless of the obvious drawbacks to these systems, they currently appear to be the best available for *in vitro* analysis of the effects of HHV-8 infection.

In addition to the difficulties associated with lytic HHV-8 growth in culture, there is not an available *in vivo* animal model for infection with HHV-8, thus limiting the knowledge on early stages of HHV-8 infection, establishment of latency, and pathogenic effects in a newly infected host. Taken together, this information suggests that the most attractive choice for bypassing the problems associated with the analysis of HHV-8 *in vitro* and *in vivo* is the use of a closely related herpesvirus with an established cell culture system for lytic replication, and a readily available animal model of *in vivo* infection.

3. Chemokine Receptors and Their Viral Homologues

a. *Chemokines*

Chemokines (*chemo*tactic cyto*kines*) are small molecular weight proteins ranging from 8-12 kDa, which are involved in chemotaxis and activation of target cells. Generally, the cells regulated by chemokines are involved in immune function, and indeed a majority of chemokines are involved in attracting leukocytes to sites of inflammation. So far, approximately 40 chemokines have been identified, which are grouped into categories based on the identity of conserved cysteine residues in the N terminus of the protein. The four categories are the C, CC, CXC (where X is any amino acid), and CX3C chemokines, with the largest groups being the CC and CXC chemokines (13). All chemokines have an original name, as well as an official name as designated by a recently adapted nomenclature system for chemokines based on their receptor binding abilities (e.g. GROα is equivalent to CXC-ligand 1, or CXCL1) (180).

b. *Chemokine Receptors*

Chemokines act on their target cells by binding to and regulating the signaling of their cognate cell surface receptors. Chemokine receptors are expressed on a variety of cell types, including leukocytes, endothelial cells, and neurons, and signaling through these receptors can result in varied effects such as degranulation, mitogenesis, chemotaxis, and lymphocyte homing (131). They are mainly thought to be involved in chemoattraction and activation of leukocytes during a variety of immune responses, but more recently they have also been found to be involved in several stages of cancer

development, including tumor formation, angiogenesis, and metastasis (13). The chemokine receptors are classified into four classes based on the types of ligands they bind, and thus far, eighteen human receptors have been isolated: eleven CC receptors (CCRs), five CXC receptors (CXCRs), one C receptor (XCR), and one CX3C receptor (CX3CR). Chemokine receptors are all members of the seven transmembrane G protein-coupled receptor family (GPCR), which transduce signals through interactions with heterotrimeric G proteins associated with intracellular regions of the receptors. GPCRs represent the largest known family of cell surface receptors, with around 1,000 encoded in the human genome, and are involved in the detection of a wide variety of ligands, including odorants, photons, lipids, proteins, and amino acids (101, 172).

The G proteins associated with seven transmembrane receptors consist of an α, β, and γ subunit. Upon ligand binding, GPCRs undergo conformational changes that result in the associated Gα protein subunit releasing bound GDP, and binding to GTP. In the GTP bound state, the Gα protein subunit dissociates from the βγ subunits, which remain associated as a dimer, and signals are transduced via interactions of the α or βγ subunits with downstream effectors (Fig. 1.3) (122). Upon GTP hydrolysis, the α subunit re-associates with the βγ subunits, and G protein signaling is thus terminated. There are currently 18 different types of identified α subunits, which are divided into four subfamilies: $G\alpha_s$, $G\alpha_{i/o}$, $G\alpha_{q/11}$, and $G\alpha_{12/13}$. These four subfamilies of Gα subunits are capable of regulating a variety of signaling pathways. For example, $G\alpha_s$ members can regulate ion channels and activate adenylyl cyclase, $G\alpha_{i/o}$ can regulate ion channels, inhibit adenylyl cyclase, and activate phopshoplipases and phosphodiesterases, while $G\alpha_{q/11}$ can activate phospholipase C, and $G\alpha_{12/13}$ can activate small GTPases such as Rho

(101, 122). In addition to the various types of α subunits, five subtypes of β and eleven subtypes of γ subunits are currently known, increasing the potential number of combinations of heterotrimeric G proteins that can interact with GPCRs. Further, in addition to signaling by dissociated α subunits, free βγ heterodimers are also capable of transducing signals to downstream molecules, such as phosphatidylinositol-3-kinase (PI3K), and phospholipase C (PLC), extending the signaling capabilities of heterotrimeric G proteins associated with a particular receptor (71, 118). Recent data has also shown that GPCRs can signal through a diverse and complex array of mechanisms, including G protein-independent mechanisms, to activate signaling pathways such as the mitogen-activated protein kinase (MAPK) pathway, a major pathway involved in cellular growth and proliferation (71, 97). Overall, the array of signaling pathways regulated by GPCRs appears to be complex, and numerous other pathways yet to be examined are also likely affected by these receptors in some manner.

The expression patterns of G protein subunits can vary widely between cell types, potentially making the signaling properties of a particular GPCR differ depending upon the cell type in which the receptor is being expressed, and the receptors G protein coupling preferences (74). This idea becomes especially important when examining a GPCR's signaling properties in model cell systems *in vitro*, given that the presence or absence of particular signaling responses or activities may not fully represent the behavior of a receptor in other cell types, such as those in which the receptor is naturally expressed *in vivo*. In the case of chemokine receptors, the G protein coupling patterns of this family has been suggested to be highly cell type-dependent (9), stressing the importance of examining their function in relevant cell types *in vitro*. In addition to

variability in G protein coupling, recent evidence indicates that many GPCRs are able to form multi-receptor complexes in the plasma membrane, including homo- and hetero-oligomers (23). Hetero-oligomers could further increase the range of responses generated by a particular receptor, due to alterations in properties such as G protein coupling and ligand binding, resulting from the association of GPCRs with different properties.

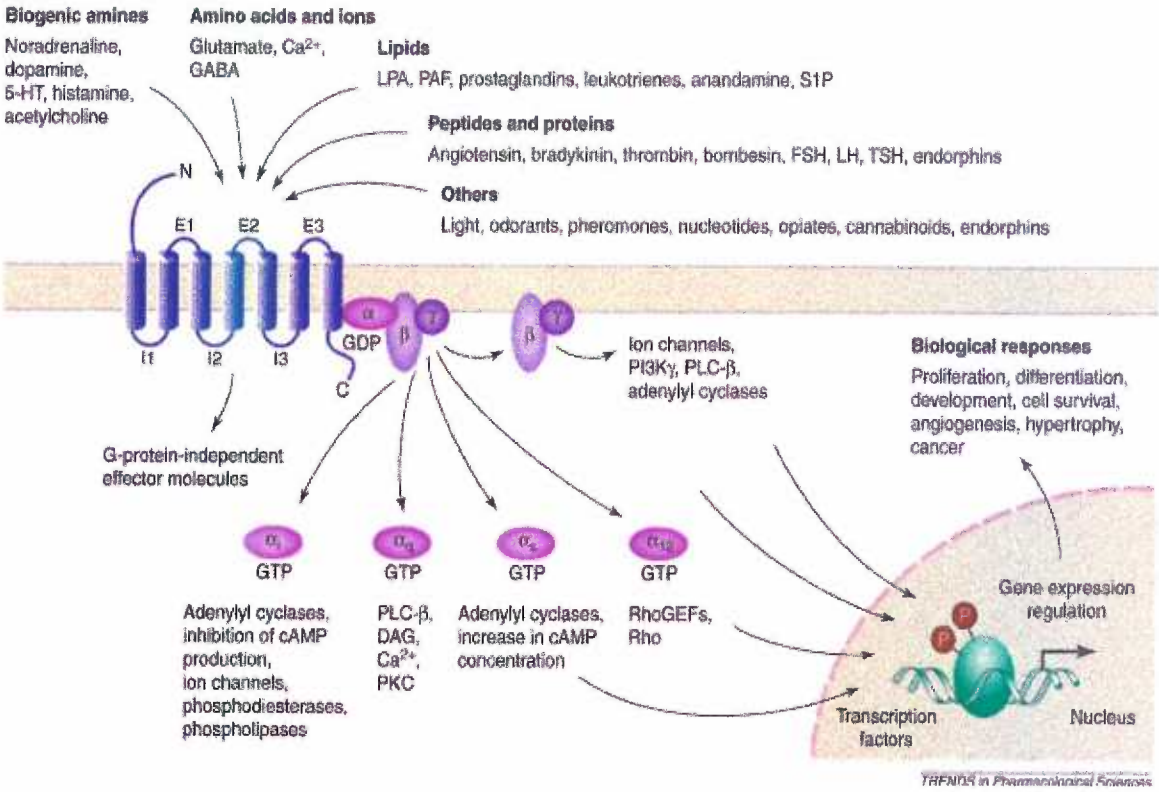

Figure 1.3 Diversity of G protein-coupled receptors (GPCRs). A wide variety of ligands, including biogenic amines, amino acids, ions, lipids, peptides and proteins, use GPCRs to stimulate cytoplasmic and nuclear targets through heterotrimeric G-protein-dependent and -independent pathways. Such signaling pathways regulate key biological functions such as cell proliferation, cell survival and angiogenesis. Abbreviations: DAG, diacylglycerol; FSH, follicle-stimulating hormone; GEF, guanine nucleotide exchange factor; LH, leuteinizing hormone; LPA, lysophosphatidic acid; PAF, platelet-activating factor; PI3K, phosphoinositide 3-kinase; PKC, protein kinase C; PLC, phospholipase C; S1P, sphingosine-1-phosphate; TSH, thyroid-stimulating hormone. *Figure and legend adapted from reference (101).*

c. *Viral Chemokine Receptor Homologues*

Viral homologues of chemokine receptors have been identified in several viruses, including, CMV (human, rat, and mouse), HHV-6, HHV-7, animal poxviruses (Swinepox and Capripox), herpesvirus saimiri, MHV-68, and HHV-8 (131). Several of these viral G protein-coupled receptors (vGPCRs) appear to play a role in the development of viral associated diseases. Also, those viruses that do not encode homologues of GPCRs often tend to upregulate cellular GPCRs upon infection. For example, EBV does not encode any chemokine receptor-like proteins, however, in infected B cells, EBV upregulates the expression of CCR7 (18). This information suggests that GPCRs, either virally encoded or cellular, may play an important role in the life cycle of some viruses. However, the exact functions that these GPCRs may provide to these viruses are not fully understood, nor are their potential contributions to viral disease and pathogenesis.

HCMV encodes four seven transmembrane receptors, US27, US28, UL33, and UL78. US28 has been the most extensively studied, and has been found to be a chemokine receptor homologue which can bind to several CC chemokines, as well as membrane bound fractalkine (CX3CL1) (57, 86). In addition to signaling in response to chemokines, US28 has been found to possess constitutive signaling properties (28), and a role for US28 in the development of CMV-associated vascular diseases has been suggested, due to the ability of the receptor to cause smooth muscle cell migration in response to chemokines (159). Although less is known about CMV UL33, this receptor has also been found to possess constitutive signaling abilities (29). In the case of HHV-6 and 7, both viruses induce the expression of CCR7 in infected cells (73), while also

encoding two chemokine receptor homologues, U12 and U51 (65). Of these, only U12 has been found to be a functional chemokine receptor (79).

Some of the most extensively studied viral GPCRs are those encoded by open reading frame (ORF) 74 of the gammaherpesviruses HVS, MHV-68, and HHV-8. These vGPCRs are all similar receptors, most closely related to the cellular IL-8 receptor CXCR2 (3, 32, 170). HVS ORF74, also known as ECRF3, has been shown to encode an IL-8-like receptor that can signal in response to the CXC chemokines IL-8, GRO/MGSA, and NAP-2 (3). The MHV-68 ORF74 encoded vGPCR has been shown to be similar to CXCR2, and transduces signals in response to chemokines (167). Further, the MHV-68 vGPCR possesses transforming potential (170), and recently has been suggested to be important for replication and reactivation of latent MHV-68 (92). The HHV-8 ORF74 encoded vGPCR has been the focus of a large amount of work since the first description of the receptor in 1996 (32), due to a potential role for this protein in the development of HHV-8-associated diseases. The HHV-8 vGPCR will be discussed in greater detail in the following section.

4. The HHV-8 ORF74 Encoded Viral G Protein-Coupled Receptor (vGPCR)

a. *ORF74 Encodes a GPCR Homologue*

One of the most intensely studied HHV-8 genes has been ORF74, which encodes the viral GPCR (vGPCR). Upon initial examination of the HHV-8 genome, ORF74 was found to encode a protein with high sequence similarity to cellular chemokine receptors

CXCR1 and CXCR2, the cellular receptors for IL-8 (69). Specifically, the HHV-8 vGPCR is most similar to CXCR2, sharing ~74% similarity and ~27% identity with this receptor at the protein level (32). The HHV-8 ORF74 encoded protein has typical properties of a GPCR, containing seven transmembrane domains, as well as predicted glycosylation sites and conserved cysteine residues found in all GPCRs (32). However, some significant differences are also present in the sequence of the HHV-8 vGPCR when compared to the receptors cellular counterpart, suggesting that variations in the properties of the vGPCR are likely to exist.

b. ***Signaling Properties of the HHV-8 vGPCR***

The initial analysis of the activities of the HHV-8 vGPCR revealed some major differences between this viral receptor and cellular CXCR2. Arvanitakis *et al.* demonstrated that the HHV-8 vGPCR could signal in a constitutive, or ligand-independent manner, given that the cellular phospholipase-C (PLC) signaling pathway was activated by the receptor in the absence of exogenous ligand (10). Numerous studies have continued to demonstrate that the HHV-8 vGPCR is capable of activating several cellular pathways, including the PLC, phosphatidylinositol-3-kinase (PI3K)/Akt, and the mitogen-activated protein kinase (MAPK)/extracellular signal-regulated kinase (ERK)1/2 pathways, and in most cases, addition of exogenous ligand appears unnecessary to induce receptor signaling (14, 39, 110, 152, 154). In addition, constitutive signaling by the vGPCR is also capable of activating several cellular transcription factors, such as NF-κB, AP-1, and NF-AT (26, 129, 130, 148, 150).

Unlike cellular chemokine receptors that tend to bind one or only a few chemokines, the HHV-8 vGPCR has been found to bind numerous cellular chemokines

of both the CXC and CC families, including IL-8, GROα, NAP-2, RANTES, and SDF-1α (10, 61, 139), as well as the HHV-8 encoded chemokine homologue vMIP-II (60). Binding of some chemokines by the vGPCR can alter the constitutive signaling of the receptor, and can either activate the receptor above basal levels, or inhibit constitutive signaling. Chemokines found to activate the receptor include IL-8 and GROα, while inhibitory chemokines include IP-10, SDF-1α, and HHV-8 vMIP-II (60-62, 139). Of the chemokines that have been shown to regulate the activity of the HHV-8 vGPCR, those that activate the receptor all contain an N-terminal ELR motif (ELR+ chemokines), while those that inhibit signaling of the receptor lack this motif (ELR- chemokines) (62). Interestingly, ELR+ chemokines are known to have angiogenic properties, while ELR- chemokines tend to be angiostatic (13), which may have implications for a role of the vGPCR in angiogenesis and KS development. An important note to make is that because of the ability of the HHV-8 vGPCR to be modulated by chemokines, the true constitutive signaling properties of the receptor have not been definitively proven, due to the potential presence of exogenous ligands in most assay systems that could unknowingly affect receptor signaling.

The HHV-8 vGPCR has been found to couple to multiple G proteins to regulate varying signaling pathways. Depending on the pathway in question, and the cell type in which the vGPCR is being examined, the receptor has been suggested to couple to $G\alpha_i$, $G\alpha_q$, and $G\alpha_{13}$ (26, 39, 110, 150, 152). For example, ERK1/2 signaling induced by the vGPCR has been suggested to be either $G\alpha_i$-dependent or independent, depending on the cell type in question (26, 95, 152), while PLC signaling appears to be $G\alpha_i$-independent (39), and PI3K/Akt signaling may be either $G\alpha_i$-dependent or independent (39, 110, 152).

Much of the data on exactly which G proteins are involved in signaling by the vGPCR is conflicting, and again is likely due to variations in cell types used to examine G protein coupling. Nevertheless, the HHV-8 vGPCR appears to couple to multiple G proteins to activate a wide variety of signaling pathways. Further, other G protein-independent mechanisms of GPCR signaling may also be utilized by the HHV-8 vGPCR to transduce signals, although this possibility remains to be investigated

Some variations in the protein sequence of the HHV-8 vGPCR have been implicated in the constitutive signaling ability of the receptor. For example, in most GPCRs, a conserved DRY motif is located in the second intracellular loop near the third transmembrane domain. However, in the HHV-8 vGPCR, a D to V amino acid substitution changes this motif to VRY. Initially, this single amino acid substitution was suggested to be responsible for the transforming and constitutive signaling abilities of the receptor (24), although later this was found not be the case (76, 129, 140, 148). Further studies have revealed that mutation of various residues in the vGPCR sequence can alter the signaling properties and chemokine responsiveness of the receptor (76, 129, 140), and that the N-terminus of the receptor, although required for ligand binding, is dispensable for constitutive signaling (75, 140). Taken together these studies suggest that multiple residues and regions of the vGPCR likely contribute to the overall properties of the receptor, and that one specific amino acid does not account for the overall constitutive signaling, chemokine responsiveness, and transforming abilities of the receptor.

c. *Consequences of HHV-8 vGPCR Expression*

The initial examination of the biological effects of HHV-8 vGPCR signaling indicated that this receptor possesses oncogenic properties, given that expression of the

receptor resulted in the transformation of mouse fibroblasts *in vitro*, and since these same cells also had tumorigenic potential *in vivo* (14). Also, vGPCR expression in these cells was shown to induce the secretion of VEGF, a major factor involved in neovascularization and tumor angiogenesis (165), and a known growth factor for KS spindle cells (38, 103). This initial work has been further strengthened by several *in vivo* studies in which the HHV-8 vGPCR was expressed in transgenic mice, with the results in all cases being the formation of lesions in these mice that closely resembling KS lesions (70, 78, 109, 176). The first transgenic mouse model described expressed the vGPCR under the CD2 promoter, limiting expression of the receptor to T cells and NK cells (176). These mice developed angioproliferative lesions in various tissues and organs, which contained spindle-like cells, inflammatory cells, and increased VEGF levels. This finding suggests that vGPCR expression strictly in hematopoietic cells could potentially result in the production of KS, likely via paracrine mechanisms involving secreted growth factors such as VEGF. In another transgenic mouse model in which the vGPCR was expressed preferentially in endothelial cells, the development of vascular lesions resembling KS also occurred, indicating that the vGPCR may cause KS development when expressed in this cell type (109).

Expression of the vGPCR in primary endothelial cells *in vitro* causes cell spindling, reminiscent of what occurs in a KS lesion *in vivo* (129). These cells also show increased production of cytokines such as IL-6, RANTES, and VEGF, which could play a role in the development of KS lesions in either a paracrine or autocrine manner. In addition, the vGPCR has been shown to induce the secretion of several cytokines when expressed in T cells and human embryonic kidney cells *in vitro* (148). The expression of

the vGPCR can also result in the immortalization of primary endothelial cells *in vitro*, and is accompanied in this situation by an upregulation of the VEGF receptor KDR (15). This observation closely parallels what is seen with HHV-8 infection of endothelial cells *in vivo* (55), and suggests that VEGF induced by the vGPCR may indeed play a significant role in promoting endothelial cell growth and KS lesion development. The HHV-8 vGPCR has also been shown to induce anti-apoptotic signaling pathways in endothelial cells, and thus promote survival of these cells in the face of an apoptotic stimulus (110). Interestingly, expression of the vGPCR in these endothelial cells does not appear to have any effects on proliferation.

d. *Transcription and Expression of HHV-8 ORF74*

Detailed analysis of HHV-8 ORF74 transcription has revealed some interesting features of the expression patterns of this ORF. Using RNA obtained from latently HHV-8 infected PEL cell lines induced to undergo lytic replication with phorbol esters, Northern blot analysis demonstrates that this ORF is expressed as an early-lytic gene, and is encoded on a ~2.8 kb bi-cistronic message with the upstream ORF K14, which encodes the viral homologue of the cellular immuno-regulatory protein CD200/OX-2 (35, 85, 120, 161). Further analysis indicates that a splicing event removes 149 bp of the intergenic region between these ORFs, but does not delete any K14 or ORF74 sequence (85, 120). Translation of the vGPCR from this bi-cistronic message has been suggested to occur via an internal ribosomal entry site (IRES) mechanism, translational reinitiation, or leaky ribosomal scanning, although the actual production of protein from these transcripts has not been examined in any manner. The significance, if any, of ORF74 being encoded as

the second ORF on a bi-cistronic message with an immuno-modulatory protein (vCD200) is currently unknown.

Importantly, transcripts for ORF74 can also be detected in uninduced PEL cells, and in KS lesions, in which a small percentage (~1-3%) of cells spontaneously undergo lytic replication (69, 85). Further, using anti-sera to the vGPCR, expression of the receptor can be detected in B cells in PEL and MCD tumor samples, as well as in spindle cells in KS lesion biopsies (35). Taken together, these data imply that the vGPCR is expressed in HHV-8 infected cells *in vivo*, and therefore that the receptor may be directly involved in the development of KS and B cell abnormalities associated with HHV-8 infection.

e. *Putative Roles of the vGPCR in the Life Cycle and Pathogenesis of HHV-8*

Due to the various properties associated with the HHV-8 vGPCR, the receptor could be envisioned to have significant effects on cells in which the protein is expressed. Therefore, the vGPCR is thought to play a major role in the development of HHV-8 associated malignancies when expressed in infected cells. For example, the ability of the vGPCR to induce cytokine secretion suggests that this viral protein is involved in the increased production of inflammatory and growth factors important for KS lesion development (e.g. VEGF), as well as various chemokines that could be involved in stimulating immune cell infiltration. Also, the ability of the vGPCR to directly transform cells may suggest that in infected endothelial or B cells *in vivo*, expression of the receptor could lead to the development of diseases such as KS, PEL, or MCD, due to the

activation of growth promoting signaling pathways such as ERK1/2, and pro-survival pathways such as PI3K/Akt.

The major question surrounding the role of the HHV-8 vGPCR in the development of KS and B cell disorders stems from the fact that the receptor is expressed only during lytic replication. Specifically, if the vGPCR is only expressed lytically in cells destined to be destroyed by viral replication, how could an infected cell possibly become transformed by the vGPCR, and therefore, how could this protein ever contribute to disease development? Some possible explanations might include aberrant expression of the vGPCR in latently infected cells, as well as expression during an abortive viral replication cycle. In either instance, the vGPCR could be produced in cells in which viral replication is not occurring or is not completed, and thus could have direct transforming effects on these cells. Interestingly, some evidence suggests that expression of HHV-8 ORF74 is induced by HIV-1 Tat, which could thus result in abnormal vGPCR expression in the context of a concurrent HIV-1 infection (177). This finding could be of significance to the development of HHV-8-induced KS and B cell abnormalities in the AIDS setting. Another possibility is that the small percentage of latently HHV-8 infected cells that spontaneously enter the lytic cycle express the vGPCR, resulting in the producion of soluble factors (e.g. cytokines and growth factors) before a cell is ultimately destroyed. These factors might then act in a paracrine fashion to cause abnormal cell growth and transformation of surrounding cells, resulting in disease development.

The exact roles that the HHV-8 vGPCR may play in the viral life cycle are also unknown, although some speculations can be made based on current knowledge about the receptor. Since ORF74 is a lytic gene, the suggestion has been made that the vGPCR may

be involved in inducing a favorable environment in lytically infected cells for increased viral replication, perhaps by activating signaling pathways that induce cellular proliferation, such as ERK. Along this same line, activation of anti-apoptotic pathways such as PI3K/Akt by the vGPCR could be envisioned to keep a cell alive in the face of apoptotic stimuli induced by lytic viral replication, allowing for increased survival of these cells, and thus, enhanced viral replication. In addition, the increased production of cytokines due to vGPCR expression in infected cells may provide an environment conducive to increased viral replication in these cells. vGPCR-induced cytokine production may also be involved in other aspects of the viral life cycle, such as viral spread, perhaps by recruiting target cells to sites of infection. Further, an idea which has not been explored in detail, is that the vGPCR may be directly involved in chemotaxis of infected cells, and might allow infected cells expressing the receptor to home to target sites containing the proper array of chemoattracting cytokines. This chemotactic activity could also be involved in promoting spread of the virus in an infected host.

Despite these speculations, the only way to accurately address many of the questions concerning the roles of the vGPCR in the viral life cycle and pathogenesis is through analysis of the vGPCR in the context of HHV-8 infection. Specifically, the ability to inhibit or manipulate vGPCR expression during an infection would be invaluable for answering many of these questions. However, as noted earlier, an *in vivo* model for HHV-8 infection and pathogenesis does not exist, and the production of altered forms of HHV-8 *in vitro* are currently not possible.

5. Rhesus Rhadinovirus (RRV); a Rhesus Macaque Model for HHV-8

a. *Identification and Classification of RRV*

Rhesus rhadinovirus (RRV) is a recently identified γ-herpesvirus of rhesus macaques (*Macacca mulatta*), which has been shown to be the homologue of human herpesvirus 8 (HHV-8)/Kaposi's sarcoma-associated herpesvirus (KSHV). The particular isolate that is the focus of this thesis, RRV strain 17577 (RRV_{17577}), was obtained from a simian immunodeficiency virus (SIV)-infected macaque that had developed B cell hyperplasia. Upon isolation and characterization of this herpesvirus isolate, the RRV_{17577} genome was found to be essentially co-linear with HHV-8, retaining many of the ORFs believed to be involved in the pathogenesis of HHV-8 (149). Specifically, 67 of 79 ORFs are similar to those in HHV-8. The general structure of the RRV_{17577} genome is similar to other herpesviruses, and consists of a long unique region (LUR) of ~131 kb in length, flanked on both ends by regions of terminal repeats (Fig. 1.4). Further, phylogenetic analysis of several RRV_{17577} genes compared to those from other gammaherpesviruses reveals that RRV and HHV-8 are the most closely related (Fig. 1.5). A second independent RRV isolate (H26-95) has also been described (4, 44), and appears to be very similar to RRV_{17577}, although some differences between these isolates do exist. RRV_{17577} was utilized in all of the work described in this thesis, and therefore, this strain will be referred to throughout only as RRV, unless noted otherwise for purposes of clarity.

Figure 1.4 Alignment of the RRV and HHV-8 genomes. The figure depicts a sequence alignment of the DNA sequences of RRV and HHV-8, indicating all putative ORFs for both viruses, as well as terminal repeat regions (TR). Numbers represent kilobases of nucleotide sequence, and the color scheme demonstrates the distribution of viral ORFs among various herpesviruses. The ORFs are not drawn to scale. *The alignment is a modified version of a figure from reference (4).*

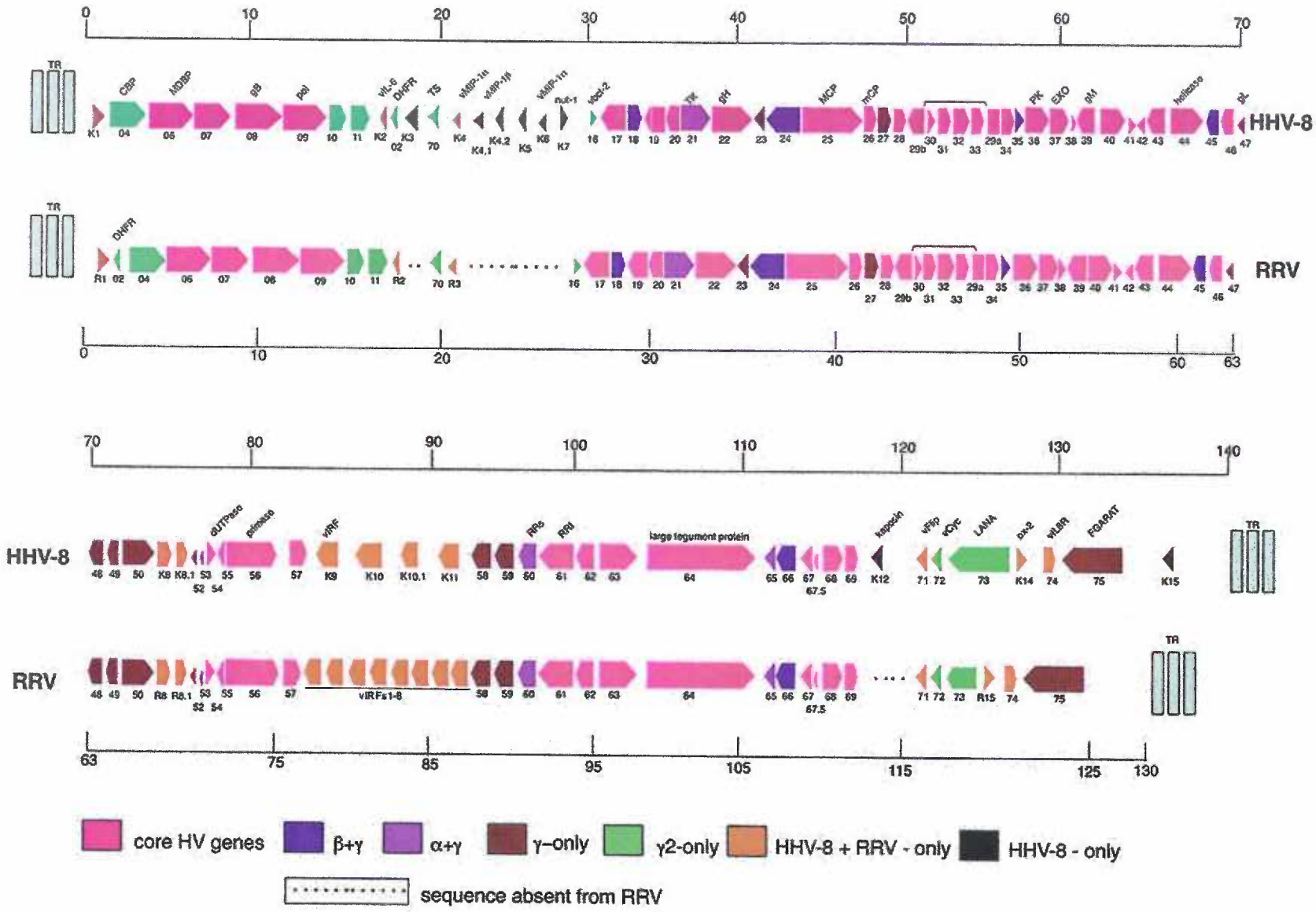
HHV-8
RRV
HHV-8
RRV
core HV genes
β+γ
α+γ
γ–only
γ2-only
HHV-8 + RRV - only
HHV-8 - only
sequence absent from RRV

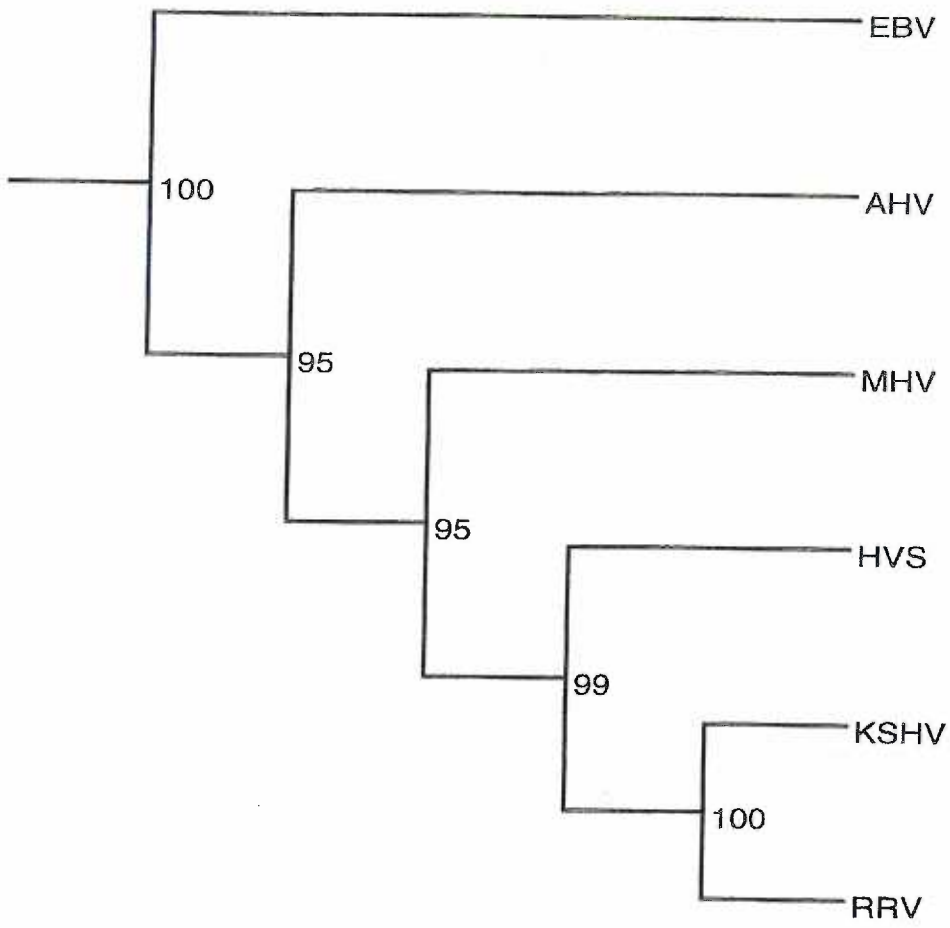

FIGURE 1.5 Phylogenetic relationship between RRV and other gammaherpesviruses. The diagram depicts the consensus tree constructed from the phylogenetic analysis of six gammaherpesvirus genes (ssDBP, gB, Pol, MCP, Hel, and UDG). The numbers represent the number of Protpars trees out of 100 that contained the same sequences to the right of the branch point as in the consensus tree. EBV= Epstein-Barr virus, AHV= alcelaphine herpesvirus, MHV= murine herpesvirus 68, HVS= herpesvirus saimiri, KSHV= Kaposi's sarcoma-associated herpesvirus/human herpesvirus 8 (HHV-8), RRV= rhesus rhadinovirus. *Figure adapted from reference (149).*

b. *RRV-Associated Disease*

Importantly, experimental inoculation of SIV-infected macaques with RRV results in the development of a B cell hyperplasia that shares similar characteristics to MCD in humans (173). Specifically, these animals develop multicentric and persistent angiofollicular lymphadenopathy, hepatomegaly, splenomegaly, hypergammaglobulinemia, and display an increase in B cell proliferation. Further, RRV DNA can be detected in all lymphoid tissues associated with disease development in these animals. RRV has also been found to be capable of establishing a latent infection in B lymphocytes in rhesus macaques, suggesting this cell type may be a site of viral persistence in naturally infected animals (17). However, RRV infection alone does not appear to result in the development of lymphoproliferative disease, and indeed, >90% of captive immunocompetent rhesus macaques are positive for RRV, but never develop signs of disease. This information suggests that SIV co-infection, and the accompanying immunosuppression, may play a major role in disease development associated with RRV infection in rhesus macaques. In addition to B cell hyperplasia, recent data suggests that RRV infection of SIV-infected macaques may be associated with the development of a non-Hodgkin lymphoma in these animals, and in at least one instance, has been associated with the development of retroperitoneal fibromatosis (RF), a vascular fibroproliferative malignancy with histomorphological features similar to KS (63). Taken together, this information suggests that infection of SIV-infected rhesus macaques with RRV may result in the manifestation of similar diseases as seen in humans co-infected with HHV-8 and HIV, making RRV an ideal model system to study the mechanisms of HHV-8 pathogenesis.

c. ***Viral Genes Potentially Involved in Pathogenesis***

Since 67 of 79 ORFs in RRV are similar to those in HHV-8, many of the same viral genes thought to play a role in disease development in HHV-8 are thought to be involved in the pathogenesis of RRV. For example, the R1 protein of RRV, which is similar to the transforming K1 protein of HHV-8, has been shown to possess transforming abilities *in vitro* (43). Similar to HHV-8, RRV also encodes several cellular homologues, containing ORFs for vIL-6, vFLIP, v-cyclin, vBcl-2, vIRFs, vMIP, vCD200, and a vGPCR. RRV vIL-6 has been shown to possess IL-6-like activity *in vitro*, suggesting this protein functions similarly to HHV-8 vIL-6 (81). However, besides the analysis of RRV vIL-6, the remaining cellular homologues in RRV have not been examined. Therefore, work in our laboratory aims to characterize these ORFs in detail, in order to determine their similarity to their counterparts in HHV-8, and to decipher their potential roles in RRV-associated disease development.

d. ***Utility of RRV as a Model for HHV-8***

Unlike HHV-8, RRV grows well in culture and can be passaged to high titers. Thus, given the many problems associated with growth of HHV-8 in culture, RRV provides an ideal model system for the analysis of *in vitro* infection of an HHV-8-like virus. In particular, the ability for consistent *de novo* lytic infection makes RRV extremely suitable for the analysis of lytic gene transcription, as well as other aspects of infection such as replication and assembly.

RRV is also currently the most attractive virus identified that is suitable for development as a model for HHV-8 infection *in vivo*. Although MHV-68 is currently

utilized in mice as an animal model for HHV-8, the diseases associated with infection do not appear to mimic HHV-8-associated diseases as closely as does RRV infection of rhesus macaques (151). In addition, MHV-68 is not as closely related to HHV-8 as RRV (149) (see also figure 1.5), and contains some significant differences in sequence and genomic organization, as well as encoded ORFs, when compared to these viruses (168). Also, a non-human primate model for HHV-8 is much more attractive than a murine model, given that humans and non-human primates are genetically more closely related.

RRV-like viruses have also been identified in rhesus and pig-tail macaques, and are associated with retroperitoneal fibromatosis (RF) development in these animals (138). These viruses are known as retroperitoneal fibromatosis-associated herpesviruses (RFHV), and partial sequencing of these viral genomes has suggested they are both similar to RRV and HHV-8, although significant differences appear to exist between these viruses and RRV/HHV-8 (137). Rhadinovirus sequences have also been detected in chimpanzees, gorillas, and African green monkeys, however, these viruses have not been successfully cultured, and thus remain incompletely characterized (67, 87, 88). In addition, infection with these rhadinoviruses does not appear to be associated with any disease development in their natural hosts. On the other hand, the diseases associated with RRV infection of SIV-infected macaques closely resembles diseases seen in individuals co-infected with HHV-8 and HIV (173), suggesting that the pathogenesis of RRV infection may mimic closely that of HHV-8 infection in humans. Importantly, although the related RRV isolate H26-95 is highly similar to RRV_{17577}, H26-95 has not been found to be pathogenic *in vivo* (100), thus making RRV_{17577} the closest primate

virus to HHV-8 identified to date with a suitable and readily available animal model for HHV-8-associated disease development.

6. RRV ORF74 as a Model System for HHV-8 vGPCR Pathogenesis

a. *Preliminary Analysis of RRV ORF74*

Examination of the genome of RRV reveals that like HHV-8, RRV ORF74 appears to encode a putative vGPCR. This ORF is located in a similar position of the RRV genome as in HHV-8, and the genomic structure surrounding this ORF is nearly identical to HHV-8 (Fig. 1.4). HHV-8 ORF74 and RRV ORF74 are both 1029 nucleotides in size, encoding predicted proteins of 342 amino acids. Based on this preliminary examination, the idea that these two viral ORFs could likely produce very similar proteins became apparent. Therefore, we wished to address the similarities and potential differences of RRV and HHV-8 ORF74, to determine if these ORFs are expressed in a similar fashion, and if they encode homologous proteins.

b. *Overview of Thesis Project*

To address the question of whether or not RRV ORF74 is similar to ORF74 of HHV-8, we initially undertook studies examining the RRV vGPCR in an NIH3T3 model system, based on the preexisting knowledge of the properties of the HHV-8 vGPCR in this cell type. This work is presented in chapter 2, and describes the preliminary characterization of the vGPCR encoded by RRV ORF74. We also wished to address the

activities of the RRV and HHV-8 vGPCRs in a cell type relevant to *in vivo* RRV and HHV-8 infection, and thus, studies examining the effects of both receptors in B cells were performed, the results of which are presented in chapter 3. Important to the analysis of any viral ORF is the determination of how the ORF is transcribed from the viral genome, since production of the transcript plays a defining role in how and when a particular viral protein is made, and may dictate an ORF's role(s) in the viral life cycle and viral pathogenesis. Therefore, studies investigating the transcriptional patterns of RRV ORF74 were undertaken, and are described in chapter 4.

c. *Significance of this Work*

Although RRV is highly similar to HHV-8 in sequence and biological properties, the analysis of individual RRV ORFs similar to those thought to be involved in pathogenesis of HHV-8 in humans is extremely important. These types of studies will help to determine whether particular RRV genes can be studied in the context of RRV infection, and ultimately determine their potential contributions to HHV-8-like diseases in RRV-infected macaques. The studies described in this thesis present novel findings about a gammaherpesvirus vGPCR, and demonstrate that this receptor is similar to a potentially pathogenic vGPCR of a related human virus, HHV-8. The information described here not only provides further knowledge about vGPCRs in general, but also implicates RRV as an excellent model system to determine the contributions of the HHV-8 vGPCR to viral pathogenesis. This work also suggests that RRV may prove beneficial for the analysis of vGPCRs as potential therapeutic targets to treat viral-associated diseases, including HHV-8-associated malignancies such as KS, PEL, and MCD.

d. ***Author's Contributions***

All work presented in chapter 2 was performed by the author of this thesis, with the exception of figure 2.3C (M.K.A). All work described in chapter 3 was performed solely by the author. In chapter 4, the author contributed 50% effort to each figure (figures 4.1-4.6).

Chapter 2

A G Protein-Coupled Receptor Encoded by Rhesus Rhadinovirus is Similar to ORF74 of Kaposi's Sarcoma-Associated Herpesvirus

Ryan D. Estep[1,2,3], Michael K. Axthelm[1,2] and Scott W. Wong[1,2,3,*]

Vaccine and Gene Therapy Institute[1], Oregon Health & Science University West Campus, Division of Pathobiology and Immunology[2], Oregon National Primate Research Center, Beaverton, Oregon 97006;
Department of Molecular Microbiology and Immunology[3], Oregon Health & Science University, Portland, Oregon 97201.

* Corresponding author:

Vaccine and Gene Therapy Institute
Oregon Health & Science University West Campus
505 N.W. 185th Avenue
Beaverton, Oregon 97006
Tel: (503)-690-5285
Fax: (503)-418-2719
e-mail: wongs@ohsu.edu

Running title: Rhesus rhadinovirus ORF74

*** Manuscript published in *Journal of Virology*, Feb 2003;77(3):1738-46.**

ABSTRACT

Rhesus rhadinovirus (RRV) is a gamma-2 herpesvirus, and is the rhesus macaque homologue of human herpesvirus 8 (HHV-8), also known as Kaposi's sarcoma-associated herpesvirus. DNA sequence analysis of RRV indicates that it shares numerous open reading frames (ORFs) with HHV-8, including one (ORF74) encoding a seven transmembrane G protein-coupled receptor (GPCR) with similarity to cellular chemokine receptors. Examination of the predicted amino acid sequence of RRV ORF74 reveals that it encodes a seven-transmembrane-spanning GPCR sharing 40.8% amino acid sequence identity with HHV-8 ORF74, and 24.1% amino acid sequence identity with rhesus macaque CXCR2. In addition, immunofluorescence studies indicate that an epitope-tagged version of RRV ORF74 is expressed on the surface of transfected cells, suggesting this protein is in fact a membrane receptor. In *in vitro* cell culture assays, RRV ORF74 possesses transforming potential, as NIH3T3 clones stably expressing the receptor demonstrate an increased ability to grow in soft agarose and to induce tumor formation in nude mice. Further analysis of RRV ORF74 indicates that expression of the receptor in NIH3T3 cells causes an increased secretion of vascular endothelial growth factor (VEGF), and activation of the ERK1/2 (p44/42) mitogen-activated protein kinase signaling pathway. The results of these studies suggest that RRV ORF74 encodes a GPCR with similar properties to its homologue in HHV-8 and that this gene may play a role in RRV-associated pathogenesis.

INTRODUCTION

Human herpesvirus 8 (HHV-8), also known as Kaposi's sarcoma(KS)-associated herpesvirus, is a recently identified herpesvirus associated with several AIDS- and non-AIDS-related malignancies. In particular, HHV-8 is the etiological agent of Kaposi's sarcoma (KS), the most common AIDS-associated neoplasm, as well as primary effusion lymphoma (PEL) and multicentric Castleman's disease (MCD) (30, 34, 119, 155). The genome of HHV-8 has been sequenced and has been found to contain several unique open reading frames (ORFs) postulated to play a role in the transforming potential of the virus (141). Several of these ORFs appear to be viral homologues of cellular genes involved in cell cycle control (v-cyclinD), chemokines (vMIP-I, II, and III), cytokines (vIL-6), apoptotic regulators (vBcl2 and vFLIP), interferon regulators (vIRFs), and a G protein-coupled receptor (vGPCR).

The HHV-8 viral GPCR, encoded by ORF74, has been the focus of numerous studies. HHV-8 ORF74 appears to be similar to CXCR2, the cellular chemokine receptor for IL-8, and has been demonstrated to be a constitutively active receptor, which can activate numerous signaling pathways in different cell types (10, 14, 39, 110, 152, 154). Although the GPCR seems to possess constitutive signaling abilities in the absence of exogenous ligand, it has been found that chemokines can modulate this activity. Chemokines containing an N-terminal ELR motif, such as IL-8, appear to activate the receptor above basal levels, while chemokines lacking this motif, such as IP-10, appear to inhibit constitutive signaling (60-62). The exact reason for the constitutive activity of ORF74 is not known, although it has been postulated that the presence of a VRY motif

instead of a highly conserved DRY motif often found in the second intracellular loop of many GPCRs may play a role (24). However, despite this finding, more recent evidence suggests that this single base substitution is likely not responsible for the receptors constitutive activity (140).

The signaling pathways activated by ORF74 appear to be extremely diverse, and numerous other pathways not yet examined are also likely affected by this receptor. One of the signaling pathways initially shown to be activated by this receptor is the phospholipase C pathway (10), which results in the production of soluble inositol-1,4,5-triphosphate (IP3) and membrane-associated 1,2-diacylglycerol (DAG), and causes the activation of various downstream signaling events. In addition to PLC, signaling through this GPCR appears to activate members of the mitogen-activated protein kinase (MAPK) family, although the data on exactly which members of this family are being activated by the receptor is somewhat conflicting, and activation appears to be cell type dependent (14, 115, 152, 154). Recently, it has been shown that ORF74 can also activate the pro-survival kinase Akt (also known as PKB) in endothelial cells in a PI3K dependent manner, resulting in their increased resistance to apoptosis (110). The receptor also appears capable of activating transcription of NF-κB- and AP-1- responsive promoters, resulting in the increased production of several cytokines and chemokines in transfected cells of epithelial, monocytic, endothelial, and T cell origin (129, 148). Moreover, there is likely a significant amount of cross talk between signaling pathways which are directly activated by the receptor, and other cellular signaling pathways, further extending the signaling capabilities of the protein.

The signaling activities of HHV-8 ORF74 appear to confer oncogenic properties on the protein. NIH3T3 mouse fibroblasts expressing ORF74 form foci in *in vitro* assays, exhibit growth in soft agar, and form tumors in nude mice (14, 24), indicating the transforming potential of this protein. In addition, cells expressing this receptor secrete increased levels of vascular endothelial growth factor (VEGF), an angiogenic cytokine, which has been suggested to play a role in the development of KS (14). The increased secretion of VEGF by ORF74 expressing cells has been partially attributed to the activation of the VEGF promoter by MAPK family members p38 and ERK1/2 (154). It also appears that ORF74 expression may play a direct role in the development of KS, since expression of the receptor has been demonstrated to induce endothelial cells to become spindle-shaped cells, a characteristic cell type found in KS lesions, and it is expressed in KS, primary effusion lymphoma, and MCD (85). Further, studies conducted with transgenic mice expressing ORF74 in hematopoietic cells have shown that these animals develop angioproliferative lesions resembling KS in various tissues, suggesting that vGPCR expression alone may be able to promote the development of KS-like disease (176).

Despite the abundance of information on HHV-8 ORF74, the role this protein has in HHV-8 pathogenesis is difficult to elucidate without an appropriate animal model for HHV-8. An alternative approach is to utilize a closely related animal model, such as rhesus macaques, that can be infected with a closely related herpesvirus, referred to as rhesus rhadinovirus (RRV) (44). Our laboratory independently isolated a related strain, RRV_{17577}, from a rhesus macaque that was infected with the simian immunodeficiency virus (SIV) and developed widespread lymphoproliferative disorder (173). Analysis of

the entire genome of RRV_{17577}, and the related isolate H26-95 (4), revealed that RRV shares high sequence similarity with HHV-8, and phylogenetic analysis of several ORFs indicated that RRV is the rhesus macaque homologue of HHV-8 (4, 149). More importantly, experimental inoculation of SIV-infected rhesus macaques with RRV_{17577} resulted in the induction B-cell hyperplasia and persistent lymphadenopathy resembling MCD in the macaques (173). Recently, some SIV and RRV_{17577}-infected macaques have developed B cell lymphoma, or a proliferative mesenchymal lesion referred to as retroperitoneal fibromatosis that possesses histomorphological features resembling KS (unpublished data). The utility of this animal model is intriguing, given the fact that RRV shares several unique genes with HHV-8, including homologues of HHV-8 genes potentially involved in pathogenesis, such as those for vIL-6, vFLIP, vIRF, vMIP and a vGPCR. Like HHV-8 vIL-6, RRV vIL-6 has been shown to be a functional homologue of cellular IL-6 (81); however, the functions of many of the other HHV-8-like genes in RRV have not yet been examined. In an attempt to further characterize more of these genes, we decided to examine the activities of the putative GPCR of RRV, also encoded by ORF74. Our studies with RRV ORF74 aim to characterize the activities of this protein to determine if it in fact behaves like ORF74 of HHV-8. If so, this may allow RRV to be used as an animal model to study the contributions of the viral GPCR to HHV-8-associated disease.

MATERIALS AND METHODS

Protein Alignments. Protein alignment was performed using ClustalW with MacVector 6.5.3 software (Accelrys, Inc. Madison, WI). The Blosum 30 scoring matrix was used in pairwise alignment of each sequence, with a gap introduction penalty of 10 and gap extension penalty of 0.1.

Cell lines and transfections. NIH3T3 mouse fibroblasts were maintained in Dulbecco's modified Eagle's medium (Mediatech, Herndon, VA) containing 5% bovine calf serum (Hyclone, Logan, UT). The DNA sequence encoding ORF74 was isolated from RRV_{17577} by PCR with primers specific for ORF74, which also contained restriction sites for *Xho*I (primer 1: 5′-CCGCTCGAGA ACAACATGGACGCC-3′) and *Eco*RI (primer 2: 5′-CGGAATTCCTATAAACTACC TGAAGTGGA-3′). The resulting product of the PCR was sequenced to confirm its identity. Stable ORF74 cell lines were produced by cloning the ORF74 sequence into the retroviral vector plasmid pLNCX (Clontech, Palo Alto, CA), and using this vector to transfect the amphotropic retrovirus packaging cell line PA317 (107) using Lipofectin reagent (Invitrogen, San Diego, CA). Retroviral particles containing the inserted gene were then collected from the PA317 cell supernatants, and used to infect NIH3T3 cells. Stable cells which had integrated the retrovirus were then selected for Neomycin resistance using G418 at 1mg/ml, and individual cell clones were isolated using cloning cylinders and maintained in medium with G418 at 750 μg/ml. Cells transduced by the pLNCX vector only were created in a similar manner. ORF74 clones were tested for ORF74 gene expression by reverse transcription-PCR (RT-PCR)

analysis of total RNA utilizing the Titan One Tube RT-PCR System (Roche, Indianapolis, IN) and ORF74 specific primers. RNA was isolated from cells with a High Pure RNA Isolation Kit (Roche). For transient transfection assays, the ORF74 sequence was cloned into the expression vector pcDNA3.1(-) (Invitrogen), and NIH3T3 cells were transfected in 35mm 6-well dishes using Transit-LT1 reagent (Mirus, Madison, WI) following the manufacturer's protocol.

HA Tagged RRV-ORF74 Protein Expression. A hemagglutinin (HA) tag was introduced to the N-terminus of RRV-ORF74 by performing PCR with primers specific for the full-length ORF74 sequence as described above, using a primer containing the sequence for the HA epitope inserted after the initiating methionine (5′-CCGCTCGAGATGTACCCAT ACGACGTCCCAGACTACGCTGACGCCTTGAA CAATAACCTT-3′) in place of primer 1. The product of this reaction was purified and sequenced to confirm the presence of the HA epitope sequence in the correct reading frame, as well as the absence of mutations in the ORF74 sequence. The tagged sequence was then cloned into the expression vector pcDNA3.1(-), and used to transfect NIH3T3 cells plated on chambered slides (Nunc, Inc., Naperville, IL) for use in immunofluorescence analysis. Empty pcDNA3.1(-) vector was used as a control. Briefly, cells were transfected with 1μg DNA per chamber using Transit-LT1 reagent, and 48 hours post-transfection cells were fixed with either 2% paraformaldehyde (non-permeabilized) to detect only surface expressed receptor, or with 100% cold methanol (permeabilized) to detect both surface and total cellular expression. The fixed cells were then probed with mouse anti-HA antibody (Sigma, St. Louis, MO) in TBS-1% bovine

serum albumin overnight at 4 °C. The following day cells were washed with TBS and probed with anti-mouse FITC antibody (Sigma) in TBS-1% bovine serum albumin for 30 minutes at room temperature. Visualization of FITC staining of nonpermeabilized cells was performed using a Zeiss Axiovert 25 microscope, and confocal images of permeabilized cells were acquired using a TCS SP confocal system (Leica Microsystems, Heidelberg, Germany) with a Plan Apo 40x NA 1.25 objective.

Soft-Agarose Assays. Five thousand stably transfected NIH3T3 cells were plated in 1.5 ml Dulbecco's modified Eagle's medium with 5% bovine calf serum and 0.3% melted agarose, onto a 1.5-ml bottom layer of 0.6% agarose medium in a well of a 6-well dish. Each clone tested was plated in triplicate wells. Cells were fed every 3 days with several drops of medium, and foci were photographed after 2 to 3 weeks.

Nude Mouse Tumor Formation. Four- to 5-week old athymic nude (*nu/nu*) mice were obtained from Harlan (Indianapolis, IN), and were maintained according to Division of Animal Resources Standard Operating Procedures at the Oregon National Primate Research Center. Stable cell clones were resuspended in sterile phosphate-buffered saline (PBS) to 10^6/100 µl, and 100 µl of the suspension was injected subcutaneously into the right flank of individual nude mice. The mice were observed daily for signs of tumor formation at the sight of injection. The mice were euthanized once tumors had reached ~1 cm in diameter or when the tumors appeared to stop growing rapidly. The mice were also euthanized if they appeared unhealthy or injured. The tumors were measured, photographed, and then excised from the mice, and samples of each tumor were saved for

further analysis. Total RNA was extracted from tumor samples using Tri-Reagent (Sigma), according to the manufacturer's protocol. Tumor samples were analyzed for ORF74 expression using 500 ng of total RNA for RT-PCR with the Titan One Tube RT-PCR system and primers specific for ORF74. Reactions with GAPDH (glyceraldehydes-3-phosphate dehydrogenase)-specific primers with and without reverse transcription served as positive and negative controls, respectively.

VEGF ELISA. Enzyme-linked immunosorbent assay (ELISA) analysis was performed with a commercial mouse VEGF ELISA kit (Oncogene Research Products, San Diego, CA), following the manufacturer's protocol. Supernatants were obtained from transiently transfected NIH3T3 cells. The cells were transfected in 35 mm wells in triplicate with 2 μg of DNA/well and serum starved at 24 h post-transfection, and the supernatants from individual wells were collected at 48 h for analysis of VEGF levels. The VEGF levels of individual wells were measured, and an average level of VEGF was then calculated from triplicate samples. Statistical significance was determined using a t test analysis program available from http://www.graphpad.com, and the unpaired two-tail P values are reported.

Western Blot Analysis. For transient transfections, cells were transfected in 35-mm-diameter wells in triplicates with 2 μg of DNA per well, serum starved at 24 h post-transfection for an additional 24hrs, and then lysed at 48 h for analysis. For stable clones, cells were plated in 35-mm-diameter wells and serum starved the day following plating for 24 h before lysis. Where appropriate, stimulation with GROα (Peprotech, Rocky Hill, N.J.) was done for exactly 5 min prior to lysis by adding it to designated wells. For cell

lysis, media was removed from wells and cells were rinsed with 1X PBS; RIPA buffer (1X PBS, 1%NP-40, 0.1% SDS, 0.5% sodium deoxycholate) containing a mixture of 1X protease and phosphatase inhibitors (Sigma) was added to each well, and the cells were removed from dishes by scraping. Lysates were cleared of cellular debris by centrifugation, and protein concentration was measured by Bradford analysis. Equivalent amounts of each protein sample were loaded and run on a 10% polyacrylamide gel, transferred to a nitrocellulose membrane, probed with antibody against phospho-ERK (Cell Signaling Technology, Inc., Beverly, MA), and detected by chemiluminescence. To control for total ERK levels, the membranes were then stripped and reprobed in a similar manner using antibody recognizing total ERK protein (Cell Signaling Technology, Inc.). Quantitation was performed by using a Kodak Image Station 440 CF to obtain images of exposed films and using relative band intensities obtained from the accompanying Kodak 1D Image Analysis Software to calculate relative phospho-ERK induction versus total ERK levels.

RESULTS

Alignment of RRV ORF74, HHV-8 ORF74, and rhesus CXCR2. The amino acid sequences of RRV ORF74 and HHV-8 ORF74 were aligned with that of rhesus macaque CXCR2, and analyzed with the ClustalW analysis program to determine the degree of amino acid sequence identity. Alignment of RRV ORF74 with HHV-8 ORF74 reveals high similarity between the two ORFs (Fig. 2.1). At the protein level, the two ORFs show ~62% similarity and ~40% identity. These sequence similarities suggest that RRV ORF74 encodes a GPCR, and that this receptor may in fact function in a manner similar to that of ORF74 of HHV-8. Moreover, alignment of RRV ORF74 with the published rhesus macaque sequence for CXCR2 shows that these proteins are ~41% similar and ~24% identical, suggesting that RRV ORF74 may be a viral homologue of the cellular macaque receptor for IL-8. Further examination of the sequences reveals that a DRY motif located in the second intracellular loop of many GPCRs is conserved in CXCR2, but is converted to VRY in HHV-8 ORF74 and IRC in RRV ORF74. The constitutive activity of HHV-8 ORF74 has previously been attributed to the presence of this VRY motif, suggesting that there may in fact be significant differences in the sequences of the two viral receptors, which could potentially affect their functions.

Cell surface expression of RRV ORF74. NIH3T3 cells were chosen as the cell type to address the transforming potential of RRV ORF74. First, ORF74 protein expression was evaluated to determine whether the protein could be detected on the surfaces of these cells. Unfortunately, initial attempts to generate polyclonal antisera to RRV ORF74 were

unsuccessful. Therefore, to facilitate detection of the protein, an HA epitope tag sequence was attached to the N-terminus, which is a predicted extracellular region of the protein. Transient transfection of NIH3T3 cells with HA-ORF74 expressing vector, followed by immunofluorescence analysis of nonpermeabilized cells using anti-HA antibody and a FITC labeled secondary antibody, revealed that the protein is expressed on the surfaces of these cells, and that the receptor displays a clustered pattern of expression on the surfaces of these cells (Fig. 2.2A and 2.2B). In addition, confocal analysis of permeabilized cells transfected with HA-ORF74 revealed that, as expected, the protein could be detected throughout the cytoplasm, as well as on the cell surface (Fig. 2.2C and 2.2D). In both cases, similar staining done on vector only transfected cells did not show any significant signal above background (data not shown), indicating that the observed staining patterns are specific for cells expressing the HA-tagged receptor. These data demonstrate that NIH3T3 cells transfected with RRV ORF74 do in fact express this protein, and that like HHV-8 ORF74, RRV ORF74 is also a membrane receptor.

Transforming potential of RRV ORF74. To initiate studies on the function of RRV ORF74, individual clones of NIH3T3 mouse fibroblasts that stably express this gene were created, and used to assess the ability of ORF74 to cause transformation of these cells. Control clones which contained empty pLNCX vector or HHV-8 ORF74 were also created. Stable clones were initially tested for anchorage-independent growth in soft agarose medium, a common property of transformed cells. Cells were seeded in soft agarose medium, and after ~3 weeks in culture, both pLNCX clones tested exhibited no significant growth, while both pLNCX-RRV ORF74 clones proliferated well in the soft

agarose and had formed numerous foci (Fig. 2.3A). An HHV-8 ORF74 expressing clone was capable of growth in soft agarose as expected, and grew in a fashion similar to that of RRV ORF74 clones (data not shown).

The results of the soft-agarose assays suggest that RRV ORF74 has transforming potential similar to that of HHV-8 ORF74. To test the transforming ability of RRV ORF74 *in vivo*, stable NIH3T3 clones were injected into nude mice to assess their ability to form tumors. The results of this experiment are summarized in Table 1, and a representative mouse is shown in Figure 2.3B. In this case, all of the mice injected with ORF74-expressing clones developed tumors after only 11 weeks, while only two of five mice injected with one vector clone had developed tumors at this same time point. All of the tumors were collected and analyzed for ORF74 mRNA expression by RT-PCR, and as expected, only the tumors from mice initially injected with ORF74-expressing cells were positive for the transcript (data not shown). The development of tumors in mice injected with a vector-only clone is not uncommon in these types of experiments, and has been reported by numerous others performing similar studies in nude mice (8). In addition, the fact that ORF74-expressing cells could induce tumor formation in all injected mice, and that these tumors appeared more rapidly than the vector clone tumors, suggests that ORF74 expression promotes the transforming potential of stably transfected NIH3T3 cells *in vivo*. Analysis of tissue samples taken from tumors induced in mice injected with stable clones expressing ORF74 revealed that they possess histomorphological features of mesenchymal tumors, and are comprised of pleomorphic spindle-shaped cells, with mitotic cells evident throughout the tissue section (Fig. 2.3C).

RRV ORF74 can induce VEGF Secretion. HHV-8 ORF74 has been shown to induce the secretion of VEGF in transfected cells (14, 148, 154). To determine if RRV ORF74 expression was also capable of up-regulating the production of VEGF in NIH3T3 cells, stable NIH3T3 clones expressing RRV ORF74 were analyzed and found to have various levels of VEGF, but consistently higher levels of VEGF production than vector clones (data not shown). In an attempt to eliminate some of the variability of these results, and to directly compare HHV-8 ORF74 with RRV ORF74, the abilities of both of these genes to induce VEGF secretion were examined in transiently transfected NIH3T3 cells. Since each transfection is done identically for all vectors in each experiment, transient transfections eliminate some of the variability seen with stable clones, and allow a better comparison of the activities of these two viral genes. In these experiments, cells were transfected in triplicate, and individual wells were measured for VEGF levels. Figure 2.4 shows that cells transiently transfected with either RRV ORF74 or HHV-8 ORF74 secrete 159.1 pg/mL (standard deviation [SD] $\pm$ 10.75) and 143.8 pg/mL (SD $\pm$ 10.56), respectively, versus 120.6 pg/mL (SD $\pm$ 9.67) for the cells transfected with vector alone. These values correlate to 31.9% and 19.2% mean higher levels of VEGF than in cells transfected with vector alone. Although small, the differences compared to vector are statistically significant (RRV ORF74 p=0.01, HHV-8 ORF74 p= 0.0486), and similar results were obtained in three independent experiments. Thus, like its HHV-8 counterpart, RRV ORF74 is capable of inducing the increased secretion of VEGF in cells in which it is expressed.

RRV ORF74 activates ERK Signaling. The increased activation of the MAPK pathway family member ERK1/2 (p44/p42) is often involved in cellular transformation, and has been implicated in various cancers, including KS (6). More importantly, data from various studies reports that ERK1/2 is activated by HHV-8 ORF74 in different types of transfected cells (152, 154); however, there seems to be no consensus on exactly which other MAPK family members (i.e. p38 and JNK) might also be activated by the receptor, although evidence for both exists (14, 115, 154). To elucidate the potential signaling capabilities of RRV ORF74, NIH3T3 cells expressing the receptor that grew in soft agarose assays and formed tumors in nude-mouse studies were examined for increased ERK activation. Lysates from these stable clones possess higher levels of activated ERK than a vector-only clone or wild-type cells, as measured by an increased level of phosphorylation of ERK1/2 in Western blot analysis (Fig. 2.5A). The activation seen in these experiments appears to be constitutive in that the addition of no exogenous ligand was needed to stimulate ERK activity, although the presence in the culture medium of stimulating ligand(s) that activates receptor signaling cannot be ruled out.

To determine if receptor signaling was in fact responsive to the presence of exogenous ligand, a stable RRV ORF74-expressing clone, which demonstrated growth in soft-agarose, was treated with GROα prior to lysis and examination by Western analysis for ERK activation (Fig. 2.5B). GROα was chosen as a potential ligand, since it is known to bind to HHV-8 ORF74 and further stimulate its constitutive signaling abilities (62), including signaling through the ERK pathway (152). Although the constitutive ERK activation of the particular RRV ORF74 clone examined in these experiments seemed lower than those of some clones tested in previous assays, it did demonstrate slightly

elevated basal ERK activation (~1.23-fold above vector), and the addition of exogenous GROα stimulated the ERK activating abilities of this clone above basal levels (~1.95-fold induction versus untreated vector) and to a much greater extent than a similarly treated vector clone (~1.57-fold induction versus untreated vector). This demonstrates that RRV ORF74 expressing NIH3T3 cells are more responsive to GROα than cells not expressing the receptor. Therefore, like HHV-8 ORF74, RRV ORF74 is capable of interacting with a stimulating exogenous ligand, and signaling by the receptor, at least through the ERK pathway, appears to be responsive to these interactions.

Since the RRV and HHV-8 GPCRs can signal through ERK, the ERK signaling properties of RRV ORF74 were directly compared with HHV-8 ORF74, to determine whether these receptors displayed similar constitutive signaling capabilities. To achieve this, NIH3T3 cells were transiently transfected with equivalent amounts of plasmid DNA, and lysates were then collected and analyzed for ERK activation by Western blot analysis. In these experiments, both RRV ORF74 and HHV-8 ORF74 are capable of constitutively activating ERK signaling when compared to a vector control (Fig. 2.5C). Quantitation of ERK activation revealed that on average, the levels of phospho-ERK in RRV ORF74 transfected cells were 1.49-fold higher than in vector-transfected cells (SD, +/- 0.325), while HHV8 ORF74 transfected cells displayed a 2.3-fold-higher level (SD+/-1.19) than vector-transfected cells. Interestingly, from these experiments it appears that RRV ORF74 is not as potent a stimulator of the ERK pathway as the HHV-8 receptor, since the levels of phospho-ERK tended to be somewhat less elevated in RRV ORF74-expressing cells than in those expressing HHV-8 ORF74. These observations were made in multiple experiments, and similar patterns were observed. Although the differences in

activation did vary between transfections, the trend consistently demonstrated a slightly stronger activation of ERK by HHV-8 ORF74 than by RRV ORF74. This demonstrates that despite a similar constitutive activation of ERK signaling, variations in the signaling abilities of these two receptors are also likely to exist.

DISCUSSION

Several herpesviruses are known to carry GPCRs with sequence similarity to cellular chemokine receptors, including cytomegalovirus (US27, US28, UL33, and UL78), *Herpesvirus saimiri* (ECRF3), and HHV-8 (ORF74). Here we have demonstrated that RRV ORF74 encodes a protein with high sequence similarity to ORF74 of HHV-8, and that these receptors display some similar activities *in vitro*. Like its HHV-8 counterpart, RRV ORF74 possesses transforming potential, given that RRV ORF74 expressing cells can grow in soft-agarose and can induce tumor formation in nude mice. Also, we have examined the ability of ORF74 of RRV to induce the up-regulation of VEGF production in transfected NIH3T3 cells, and in transient transfection assays we have found that RRV ORF74 is capable of inducing a slight increase in VEGF secretion, similar to that seen with HHV-8 ORF74. Despite these similarities, we have only been able to detect constitutive activation of the ERK signaling pathway in NIH3T3 cells, and this activation appears to be somewhat less potent than what is observed with HHV-8 ORF74. Due to a lack of antibodies against these receptors, the levels of RRV and HHV-8 ORF74 protein expression in transfected cells could not be examined, and indeed, variations in expression could affect the levels of ERK activation seen in these experiments. Alternatively, it is also very likely that the observed differences in ERK signaling are in fact due to the sequence variations between these two viral receptors, which may ultimately result in differences in their abilities to activate certain signaling pathways. In addition to ERK, we have also examined several other signaling pathways known to be activated by HHV-8 ORF74 in various cell types (i.e. PLC/PKC, JNK, p38,

AKT/PKB), and have found no evidence that these pathways are similarly activated by RRV ORF74, at least in NIH3T3 cells. However, further studies, possibly using other cell types, would be necessary to completely rule out the involvement of any of these pathways in RRV ORF74 signaling and activities. Nevertheless, our data seem to indicate that the signaling abilities of these two receptors may actually vary, even though they display similar activities in other assays.

Since cells expressing RRV ORF74 possesses transforming ability and can induce VEGF secretion, it is likely that the receptor retains some of the signaling properties found in the HHV-8 receptor, which are responsible for these activities. For example, the induction of ERK1/2 activity by RRV ORF74 appears to correlate with its ability to increase VEGF secretion in transfected cells. In fact, cells that were transiently transfected with RRV ORF74 and found to secrete increased levels of VEGF, also demonstrated increased phospho-ERK levels. The same was true with cells transfected with HHV-8 ORF74. This observation is not surprising since induction of VEGF secretion by HHV-8 ORF74 has been partially attributed to the ability of this receptor to activate MAPK members ERK1/2 and p38, resulting in the activation of the VEGF promoter (154). However, all of the signaling pathways RRV ORF74 may be activating to produce its various activities are unknown, as is the case for HHV-8 ORF74. Many of these pathways could be the same as or differ from those activated by the HHV-8 receptor, but may still ultimately result in similar activities, such as cellular transformation.

As mentioned previously, it is highly possible that sequence variations in the receptor carried by RRV could result in differences in activity from the HHV-8 receptor,

due to alterations in the signaling capabilities of the protein. Of particular interest is the presence of an IRC motif in the second intracellular loop instead of the VRY motif found in the HHV-8 GPCR, a motif that has been speculated to be responsible for the constitutive activity of this receptor. In mutagenesis studies with RRV ORF74, we have found that alterations in this motif which more closely resemble CXCR2 (DRY) and HHV-8 ORF74 (VRY), specifically 143I/D and 145C/Y, do not appear to alter the transforming or ERK signaling abilities of the receptor (data not shown; see appendix 1). Interestingly, the CXCR2-like receptor encoded by ECRF3 of *Herpesvirus saimiri* contains an LRC motif at this same position, which is structurally quite similar to the IRC motif. This receptor does not appear to be constitutively active, although it is responsive to chemokines (3).

Another reason for the potential differences in signaling between these receptors may be that HHV-8 ORF74 is not truly a constitutively active receptor, and that it may in fact require the presence of exogenous ligand(s) to become fully stimulated. These ligands could be factors that are present in cell culture media, that is normally secreted by cells used to analyze the receptor, or whose expression is up-regulated by cells expressing the receptor (i.e. an autocrine signaling mechanism). If this were the case for HHV-8 ORF74, it could be that RRV ORF74 is either less responsive to similar ligands, or is less capable of inducing their expression to stimulate the receptor in an autocrine fashion, thus resulting in weaker constitutive activity of the receptor. We have shown that when GROα is added to cells expressing RRV ORF74, the constitutive ERK activation of the receptor is elevated, suggesting responsiveness to exogenous ligand(s). Although we have not determined whether the RRV and HHV-8 receptors respond identically to GROα, or

whether other ligands might also alter signaling of the RRV receptor, it appears that both of these receptors are capable of being regulated by exogenous ligands.

Despite the differences mentioned above, it appears that RRV ORF74 encodes a protein that demonstrates activities similar to those of HHV-8 ORF74. It should be noted, however, that this receptor likely does not function in mouse fibroblasts as it might in other more relevant cell types. Indeed, studies recently done with HHV-8 ORF74 in endothelial cells have shown that some of the constitutive signaling properties and activation of pathways seen in cells such as NIH3T3 and COS cells do not occur in endothelial cells (39). Therefore, it will be extremely important to test the activities of the RRV GPCR in different cell types as well, particularly in those cell types that may be naturally infected by RRV, such as B cells and endothelial cells.

The fact that RRV ORF74 has similar activities to HHV-8 ORF74 suggests that this gene may be involved in the development of HHV-8-like diseases seen in RRV infected macaques. Although the RRV receptor may in fact have some activities that differ from those of the HHV-8 GPCR, it is likely that these viral proteins both provide some similar functions that are crucial to the survival and replication of these two highly homologous viruses. The exact functions that these receptors may provide to the virus are unknown; however, possibilities include homing of virally infected cells and regulation of cellular activities that affect viral growth and replication. In addition, the fact that these viral receptors possess transforming activity is likely not reflective of the true function they provide for the virus, but rather may be an unintended side effect of GPCR expression in infected cells. Further analysis of RRV ORF74 should provide greater

insight into the contributions of herpesvirus GPCRs to virus-induced disease, and the role they may play in the viral life cycle.

Table 1. Tumorigenic activity of RRV ORF74

Transduced cells[a]	Mice developing Tumors[b]	Average time (weeks)	ORF74 positive[c]
pLNCX-6	2/5	10.4	0/2
pLNCX-8	0/1	NA[d]	NA
ORF74-3	5/5	5.8	5/5
ORF74-7	5/5	8.7	5/5

[a] NIH3T3 cells transduced with retroviral vector were grown in the presence of 1.0 mg/mL G418 and individual colonies were isolated.

[b] Number with tumors/total. Athymic nu/nu mice were inoculated with 1 x 10^6 cells as described in the Materials and Methods and observed for the formation of tumors.

[c] Number positive/total. ORF74 expressing tumors were determined by RT-PCR as described in the Materials and Methods.

[d] NA, not applicable.

Figure 2.1 Amino acid alignment of RRV ORF74 with HHV-8 ORF74, and macaque CXCR2. Alignment was performed with ClustalW using the Blosum scoring matrix. Darker boxes indicate identical residues, and lighter colored boxes indicate residues with similarity. Dashes represent regions not shared between proteins, and the underlined regions are putative transmembrane domains.

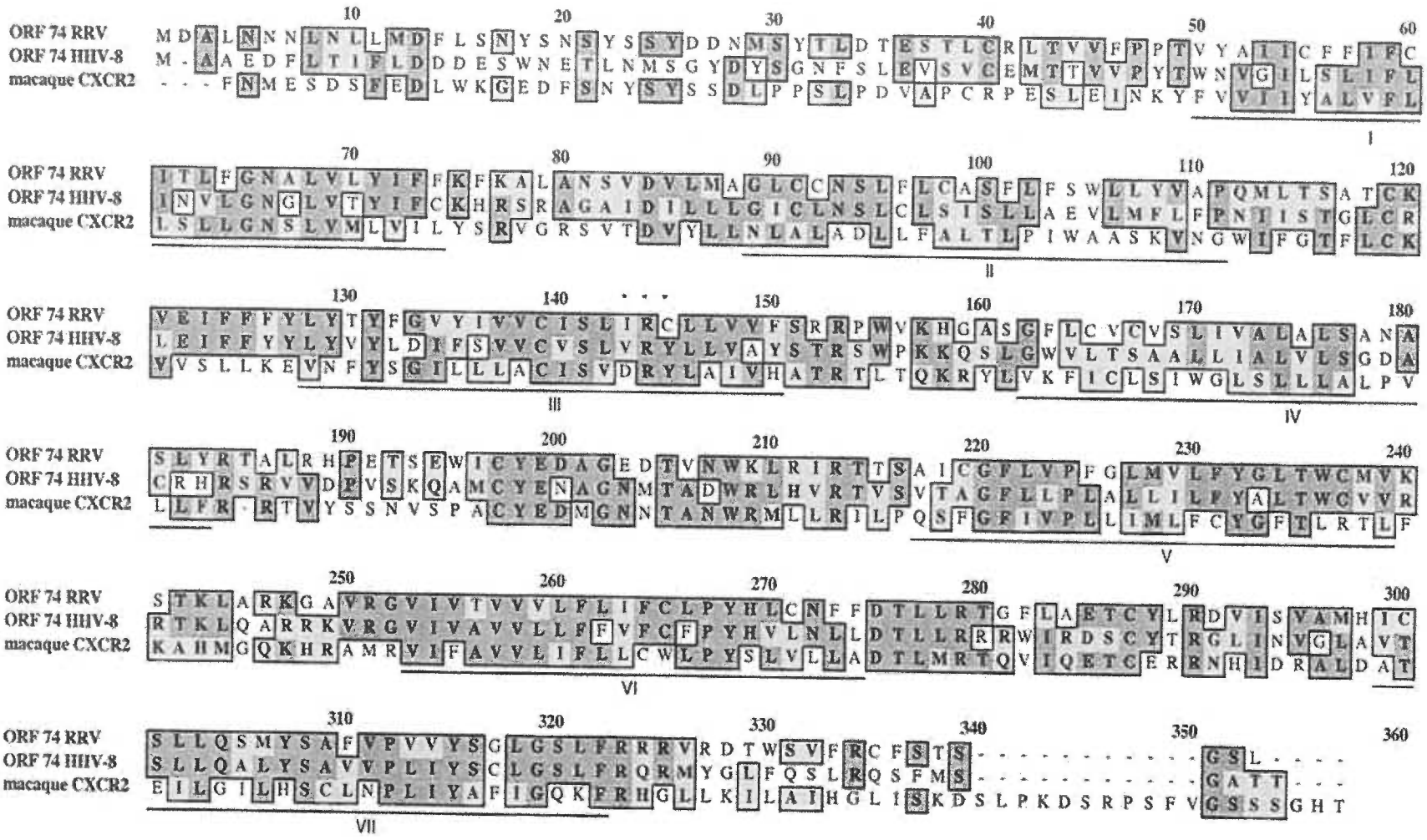
ORF 74 RRV
ORF 74 HHV-8
macaque CXCR2
I
II
III
IV
V
VI
VII

Figure 2.2 Immuno-fluorescence analysis of transfected NIH3T3 cells. NIH3T3 cells were transfected with an expression vector encoding N-terminally HA-tagged RRV ORF74, and stained with primary anti-HA antibody and FITC labelled secondary. (A and B) Non-permeabilized cells (magnification, x317). (C and D) Permeabilized cells visualized by confocal microscopy. The field shown in C is 250 by 250 μm. Panel D is a enlarged image (x3.5) of the same field shown in C, and is 74.1 by 74.1 μm.

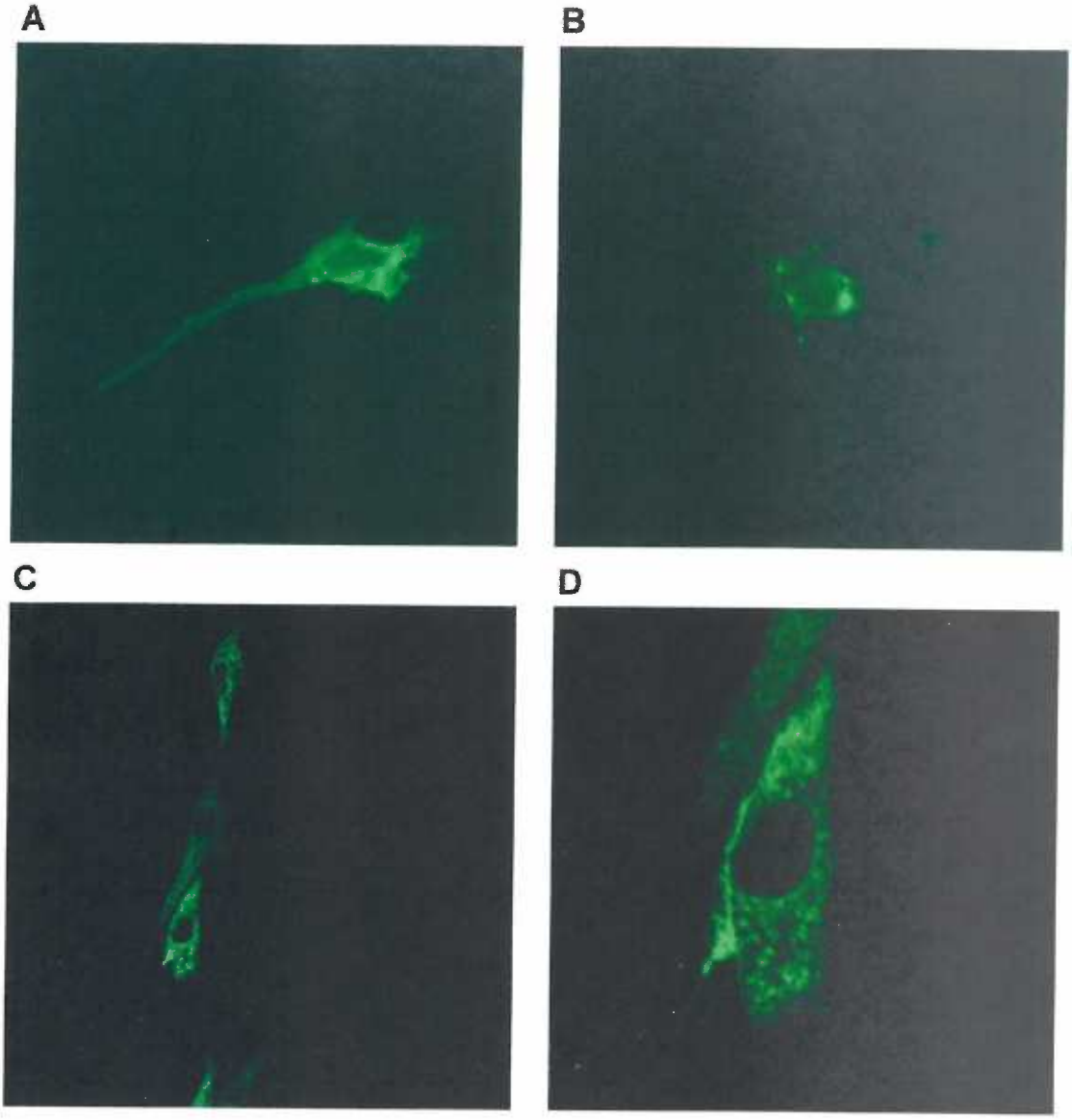
A
B
C
D

Figure 2.3 RRV ORF74-transduced cells exhibit transformation potential. (A) Cell growth in soft-agarose (magnification, x40). (B) RRV ORF74-transformed NIH3T3 cells induce tumor formation in nude mice. (C) Histological analysis of tumor stained with hematoxylin and Lee stain. Arrows indicate endothelial-cell-lined blood vessels. Bar = 20 μm.

A.

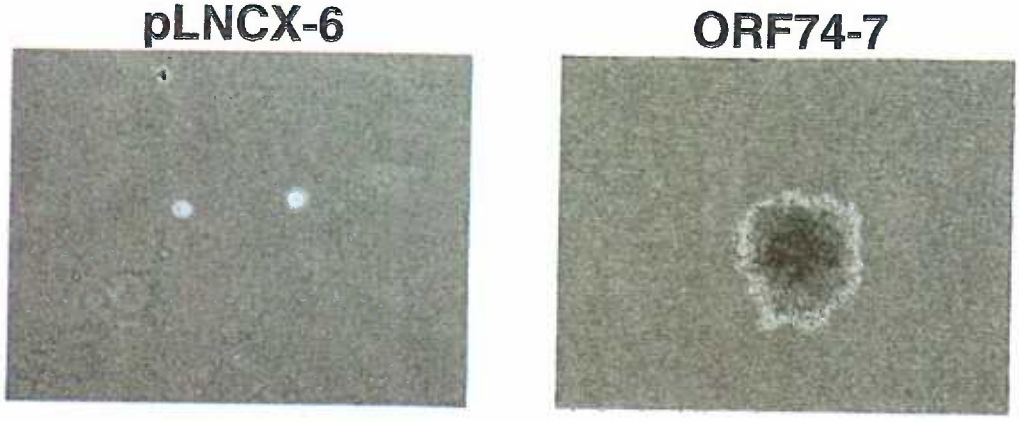

B.

C.

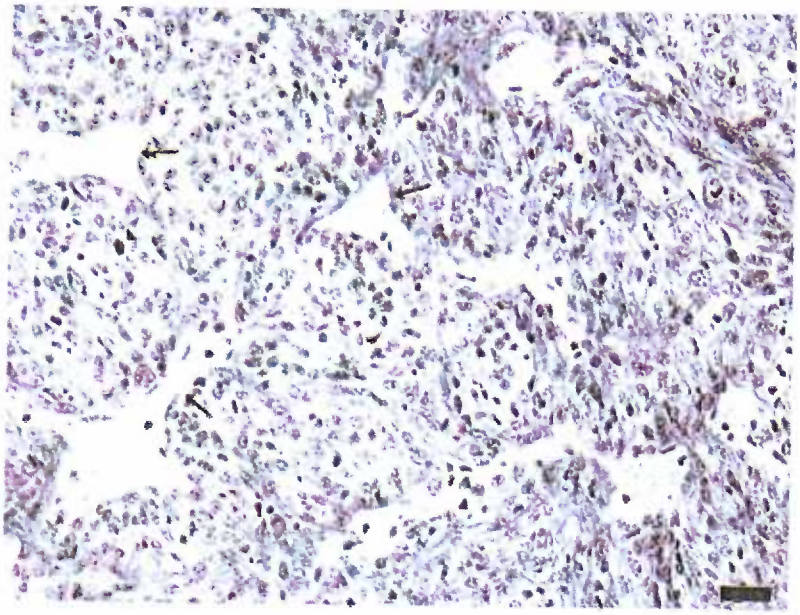

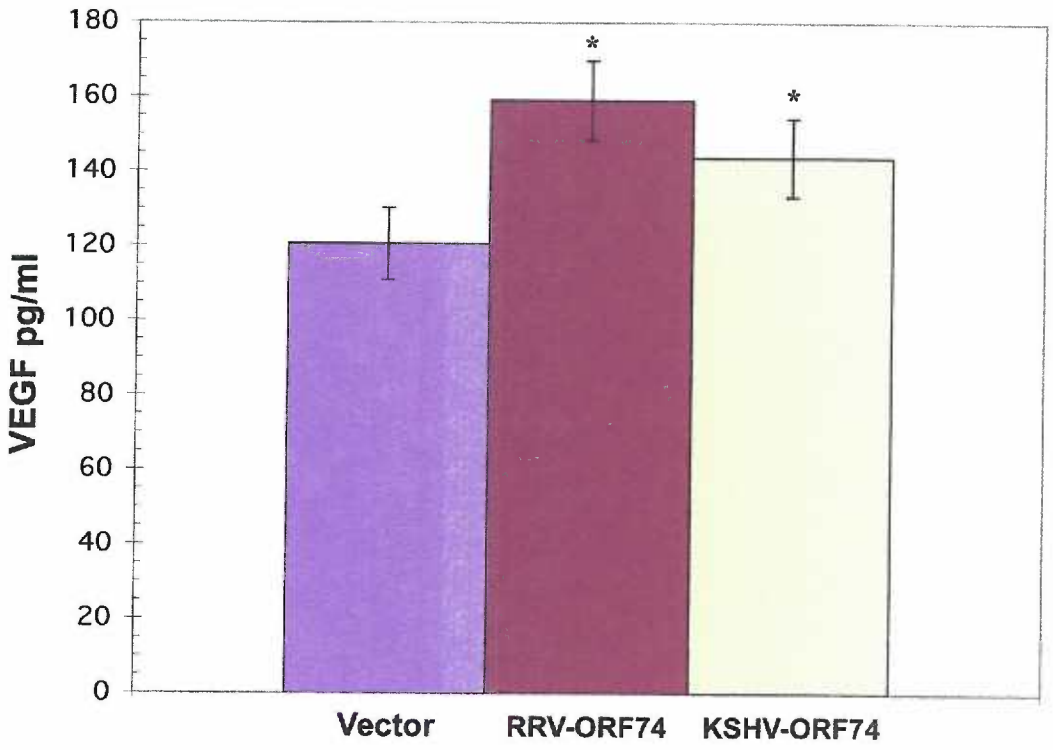

Figure 2.4 RRV ORF74 induces VEGF secretion. Supernatants were collected from transiently transfected NIH3T3 cells and subjected to ELISA using a commercial kit. * statistically significant difference from vector control as measured by t test. RRV-ORF74 p=0.01, KSHV-ORF74 p=0.0486. The error bars indicate SDs. One representative experiment of three is shown.

Figure 2.5 Analysis of RRV ORF74 induced ERK1/2 activation in NIH3T3 cells. The blots were probed with phospho-ERK (p-ERK) antibody, and then stripped and re-probed with antibody recognizing total ERK protein. (A) Lysates from wild-type NIH3T3 cells and stable clones (pLNCX-6, RRV ORF74-3, and RRV ORF74-7). (B) Lysates from stable clones (pLNCX-A and RRV ORF74-I) either untreated (-), or stimulated with 30nM GROα 5 minutes prior to lysis (+). A single blot with quantitation is shown, and is representative of two independent experiments with similar results. (C) Lysates from cells transiently transfected with equivalent amounts of empty vector (Vector), RRV ORF74, or HHV-8 ORF74. Representative blots from two independent transfections are shown, and the quantitation represents the average of three independent experiments +/- SD.

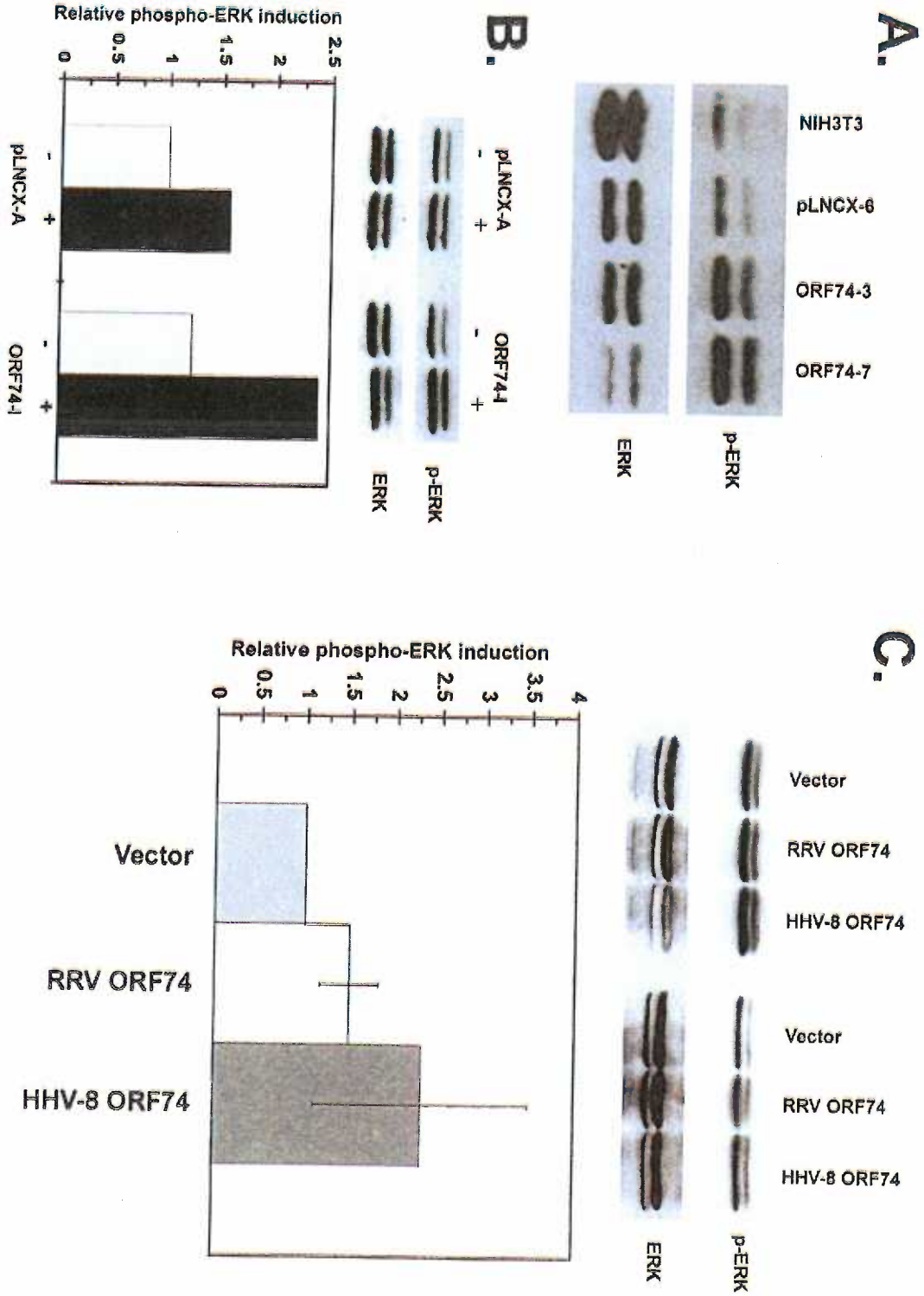
A.
NIH3T3
pLNCX-6
ORF74-3
ORF74-7
ERK
p-ERK
B.
Relative phospho-ERK induction
0
0.5
1
1.5
2
2.5
pLNCX-A
ORF74-I
-
+
-
+
pLNCX-A
ORF74-I
-
+
-
+
ERK
p-ERK
C.
Relative phospho-ERK induction
0
0.5
1
1.5
2
2.5
3
3.5
4
Vector
RRV ORF74
HHV-8 ORF74
Vector
RRV ORF74
HHV-8 ORF74
Vector
RRV ORF74
HHV-8 ORF74
ERK
p-ERK

Chapter 3

Rhesus Rhadinovirus and Human Herpesvirus 8/Kaposi's Sarcoma-Associated Herpesvirus vGPCRs Regulate Signaling Pathways and Apoptosis in B cells

Ryan D. Estep[1,3] and Scott W. Wong[1,2,3,*]

Vaccine and Gene Therapy Institute[1], Oregon Health & Science University West Campus, Division of Pathobiology and Immunology[2], Oregon National Primate Research Center, Beaverton, Oregon 97006;

Department of Molecular Microbiology and Immunology[3], Oregon Health & Science University, Portland, Oregon 97201.

[*] Corresponding author:
Vaccine and Gene Therapy Institute
Oregon Health & Science University West Campus
505 N.W. 185th Avenue
Beaverton, Oregon 97006
Tel: (503)-690-5285
Fax: (503)-418-2719
e-mail: wongs@ohsu.edu

Running title: Activity of the RRV and HHV-8 vGPCRs in B cells

Keywords: rhesus rhadinovirus (RRV); Kaposi's sarcoma-associated herpesvirus (KSHV); human herpesvirus-8 (HHV-8); viral G protein-coupled receptor (vGPCR)

*** This manuscript in preparation for submission to *Journal of Virology***

ABSTRACT

Human herpesvirus 8 (HHV-8)/ Kaposi's sarcoma-associated herpesvirus (KSHV) is the causative agent of Kaposi's sarcoma (KS), as well as B cell lymphoproliferative disorders primary effusion lymphoma (PEL) and multicentric Castleman's disease (MCD). Rhesus rhadinovirus (RRV) is the rhesus macaque homologue of HHV-8/KSHV, and is associated with several HHV-8-like diseases in infected monkeys, including a B cell hyperplasia similar to MCD. RRV encodes a viral G protein-coupled receptor (vGPCR) homologous to the HHV-8 encoded vGPCR, a viral protein implicated in the development of HHV-8 associated malignancies. Importantly, neither vGPCR has been examined in detail in B cells, a relevant cell type to HHV-8 and RRV infection *in vivo*. Our findings indicate that both receptors possess similar signaling abilities in B cells, and specifically, that they are capable of constitutively activating the ERK1/2 and PI3K/Akt/GSK-3 signaling pathways utilizing $G\alpha_i$-independent and PI3K-dependent mechanisms, while also displaying responsiveness to cellular chemokine IP-10. Finally, we demonstrate that expression of either vGPCR can inhibit the induction of apoptosis in B cells. Overall, this indicates that the RRV and HHV-8 vGPCRs possess similar activities in B cells, making RRV an attractive model for the analysis of the role of the HHV-8 vGPCR in B cell malignancies.

INTRODUCTION

Rhesus rhadinovirus (RRV) is the rhesus macaque homologue of human herpesvirus 8 (HHV-8)/Kaposi's sarcoma-associated herpesvirus (KSHV) (4, 149). HHV-8 is the causative agent of Kaposi's sarcoma (KS) in humans, the most common AIDS associated neoplasm, and a common cause of mortality in AIDS patients (34, 113). KS is characterized by multifocal lesions of the skin and visceral organs, consisting mainly of spindle-shaped cells, presumably of endothelial origin, with a high amount of vascularization. The lesions also contain large amounts of infiltrating inflammatory cells, and an inflammatory component appears to play a major role in the development of KS (50). In addition to KS, HHV-8 infection of B cells is associated with the development of B cell lymphoproliferative disorders, including primary effusion lymphoma (PEL) and multicentric Castleman's disease (MCD) (30, 155).

Experimental infection of SIV-infected rhesus macaques with RRV strain 17577 (RRV_{17577}) results in the development of a B cell hyperplasia in these animals reminiscent of MCD in humans (173). This suggests that like HHV-8, RRV also plays a role in the development of B cell lymphoproliferative disorders in immuno-suppressed hosts. Further studies have also shown that RRV_{17577} is capable of establishing a persistent infection in B lymphocytes in infected rhesus macaques (17). Taken together these data suggest that HHV-8 and RRV_{17577} share similar properties in B cells *in vivo*, making RRV an attractive model system to study the potential contributions of these viruses to B cell abnormalities.

HHV-8 Open Reading Frame (ORF) 74 encodes a viral G protein-coupled receptor homologue (vGPCR), which shares sequence similarity to the cellular chemokine receptor CXCR2 (32). The HHV-8 vGPCR has been shown to be a constitutively signaling receptor capable of activating multiple cellular signaling pathways, including the phospholipase C (PLC), mitogen-activated protein kinase (MAPK), and phosphatidylinositol-3 kinase (PI3K) pathways, in the absence of exogenous ligand (10, 39, 110, 152, 154). In addition, signaling by this receptor results in the activation of several transcription factors, such as NF-κB, AP-1, and NF-AT (129, 130, 148). Despite its constitutive signaling abilities, the HHV-8 vGPCR has been found to be a promiscuous receptor capable of binding several cellular chemokines, which can act either as agonists (e.g. GROα), or antagonists (e.g. IP-10) of receptor signaling (61, 62, 139). A role for the vGPCR in HHV-8 induced disease has been suggested, since expression of the receptor can cause cellular transformation in NIH3T3 cells (14, 148), induce the secretion of cellular cytokines such as vascular endothelial growth factor (VEGF) (110, 129, 148, 154), and promote the formation of KS-like lesions in ORF74 transgenic mice (176).

HHV-8 infects both endothelial and B cells *in vivo*, which is believed to result in the development of KS and HHV-8 related B cell malignancies, respectively. The HHV-8 vGPCR may contribute to disease development when expressed in infected cells, and indeed, examination of the function of the HHV-8 vGPCR in endothelial cells has shown that expression of this viral protein alone can alter several cellular signaling pathways, inhibit apoptosis, and cause cell spindling (39, 110, 129). In the case of lymphocytes, some properties of HHV-8 vGPCR have been examined in T cells (130, 148), while its

effects in B cells are currently limited to only microarray analysis (132). The effects of the expression of the HHV-8 vGPCR in PEL cells has also recently been examined, where it has been found that the receptor activates cellular signaling, as well as cellular and viral gene transcription (25, 26). However, PEL cells are HHV-8 positive, and the use of a non-HHV-8 positive B cell line to examine vGPCR activity would be more desirable, eliminating the possibility of any potential background interference of HHV-8 gene expression.

We have previously shown that RRV ORF74 encodes a vGPCR that appears homologous to the HHV-8 ORF74 vGPCR (51). Specifically, we demonstrated that when expressed in NIH3T3 mouse fibroblasts, the RRV vGPCR is capable of causing cellular transformation, activating cellular signaling pathways, and inducing the secretion of VEGF. Importantly, the activities of the RRV vGPCR have never been examined in any cell types relevant to RRV infection *in vivo*, including B cells. Given that a potential role for both the HHV-8 and RRV vGPCRs in viral induced B cell abnormalities exists, we sought to examine the activities of both viral receptors in B cells to determine what effects both receptors have in this cell type. Studies comparing these vGPCRs are extremely important in order to gain a full understanding of their potential similarities and differences, and to determine the utility of RRV as an animal model to study the role of the HHV-8 vGPCR in viral pathogenesis.

In the work presented here, we show that the RRV and HHV-8 vGPCRs are both functional in B cells, and can constitutively activate signaling through the ERK1/2 MAPK pathway, as well as the phosphatidylinositol 3-kinase (PI3K)/Akt/Glycogen Synthase Kinase-3 (GSK-3) pathway. In addition, signaling of both receptors in these

cells is responsive to the addition of an inhibitory cellular chemokine (IP-10). We also show that the signaling mechanisms utilized by these receptors in B cells are similar, with both utilizing $G\alpha_i$-independent but PI3K-dependent pathways to activate ERK1/2 and Akt/GSK-3, findings that differ somewhat from some studies analyzing HHV-8 vGPCR signaling in other cell types. Finally, we demonstrate that the HHV-8 and RRV vGPCRs can provide a survival signal in B cells, resulting in protection from an apoptotic stimulus. This could have major implications for the roles that these receptors play in the viral life cycle in infected B cells, and in the development of viral-associated B cell malignancies.

MATERIALS AND METHODS

Cells and generation of stable populations. Human BJAB B cells were grown in RPMI media (Mediatech, Herndon, VA) containing 10% Fetal Bovine Serum (Hyclone, Logan, UT). For generation of stable cells, $2x10^6$ BJAB cells were electroporated using a BioRad Genepulser (250 V/975 μF) with 10 μg of empty pcDNA3.1(-) vector (Invitrogen life technologies, Carlsbad, CA), or pcDNA3.1(-) expressing N-terminally HA epitope tagged versions of RRV or HHV-8 ORF74 created as described previously (51). 48 hrs post-transfection, cells were placed in media containing 1mg/ml G418 (Invitrogen life technologies), and media was changed every 2-3 days until resistant cell populations emerged. To confirm expression of the correct receptors, RNA was isolated from stable populations using a High Pure RNA Isolation Kit (Roche, Indianapolis, IN), and RT-PCR was performed with gene specific primers using the Titan™One Tube RT-PCR System (Roche). Cells were maintained in the presence of G418 at 1 mg/ml.

Chemokines and inhibitors. Human IP-10 was obtained from Peprotech (Peprotech Inc., Rocky Hill, NJ), LY294002 was obtained from Cell Signaling (Cell Signaling Technology, Inc., Beverly, MA), and pertussis toxin (PTX) was obtained from Calbiochem (Calbiochem/EMD Biosciences, La Jolla, CA).

FACS analysis for surface expression of tagged receptors. $1x10^6$ of each stable BJAB population were resuspended in ice-cold PBS, and incubated for 10 minutes on ice. Next, 1 μg of mouse anti-HA antibody (Sigma, St. Louis, MO) was added to the cells, along

with 1 μg of an anti-mouse FITC conjugated secondary antibody (Sigma), and the cells were incubated for an additional 30 minutes on ice. After incubation, cells were washed and resuspended in ice-cold PBS, and live cells were analyzed for FITC surface staining using a FACScalibur flow cytometer (BD Biosciences). An isotype-matched antibody was also used as a control.

Western blot analysis. For Western analysis of phosphorylated proteins, cells were starved for 24 hrs in serum-free RPMI before preparation of lysates. For PARP Westerns, cells were incubated in serum-free RPMI for 48 hrs, or in serum containing media as a control. Where indicated, cells were incubated in the presence or absence of the noted inhibitors. To prepare lysates, cells were lysed in RIPA buffer (1X PBS, 1%NP-40, 0.1% SDS, 0.5% Sodium Deoxycholate) containing a mixture of 1X protease and phosphatase inhibitors (Sigma). Protein concentration was determined by Bradford analysis, and equivalent amounts of each sample were run on a 10% polyacrylamide gel, transferred to a nitrocellulose membrane, and probed with antibodies against phospho-ERK, phospho-Akt, phospho-GSK-3β (Cell Signaling Technology, Inc., Beverly, MA), or anti-PARP (Santa Cruz Biotechnology, Inc., Santa Cruz, CA). To control for total protein levels in phospho Westerns, membranes were stripped and re-probed with antibody recognizing total ERK, Akt, or GSK-3β proteins (Cell Signaling Technology, Inc.). Quantitation was performed by using a Kodak Image Station 440 CF to obtain images of exposed films, then using band intensities obtained from Kodak 1D Image Analysis Software to calculate relative phospho-protein levels versus total levels, or the percentage of cleaved PARP. Percent inhibition of PARP cleavage was determined by subtracting the

percentage of cleaved PARP detected in cells expressing either the RRV or HHV-8 vGPCRs from the value obtained with vector control cells.

RESULTS

Generation of stable vGPCR expressing BJAB cells. To address the activities of the RRV and HHV-8 vGPCRs in B cells, we utilized BJAB cells, a human B cell lymphoma cell line negative for EBV and HHV-8. Stable BJAB populations expressing N-terminally HA epitope tagged RRV or HHV-8 vGPCRs were generated as described in materials and methods, and initially tested for expression by RT-PCR with gene specific primers (data not shown). Stable populations containing empty vector were also created as a control for all experiments. Since the N termini of both receptors are extracellular, surface expression of HA tagged receptors was assessed by FACS analysis of live cells stained with anti-HA antibody. When compared to vector control cells, a shift in the intensity of the peaks detected by FACS for the RRV and HHV-8 vGPCR expressing populations indicates that these cells do indeed express the HA tagged receptors at the cell surface (Fig. 3.1). Given that a variable range of receptor expression is anticipated for a population of cells, many cells appear to express the receptors at low to moderate levels, while only a small percentage of each population express the receptors to high levels at the cell surface. In the experiment shown, ~ 4.8% of the RRV vGPCR population, and ~4.4% of the HHV-8 vGPCR population showed significantly higher surface HA staining over the highest levels detected with vector control cells. The levels of surface expression did vary slightly between experiments, however, these cells consistently stained positive for their respective receptors, usually in the range of 3 to 5%. This indicates that the RRV and HHV-8 vGPCRs are expressed at the cell surface in stable BJAB B cell populations.

RRV and HHV-8 vGPCRs constitutively activate ERK1/2 signaling and are responsive to chemokines in B cells. Signaling of GPCRs can vary significantly depending on the cell type in which they are expressed. Thus, we wished to address the signaling abilities of the receptors in BJAB cells, to determine if both are capable of activating signaling pathways in a similar fashion in B cells, as in other cell types. We initially decided to examine the activation of ERK1/2, since both receptors have been shown previously to activate this pathway in other cell types (51, 152, 154). To assess levels of activated ERK1/2 in the stable BJAB populations, lysates of these cells were prepared and used in Western blot analysis to detect levels of phosphorylated ERK1/2 (pERK). Compared to vector control cells, BJAB cells expressing either the RRV or HHV-8 vGPCR did indeed contain increased levels of pERK (Fig. 3.2A), indicating that both the RRV and HHV-8 receptors are capable of constitutively activating the ERK1/2 signaling pathway in B cells.

Next, we wanted to address the ability of cellular chemokines to modulate the signaling abilities of the RRV and HHV-8 receptors in B cells. IP-10 (CXCL10) is a CXC chemokine known to bind to and inhibit signaling of the HHV-8 vGPCR through PLC, ERK1/2, and Akt (39, 110, 139, 152). The potential inhibitory effects of IP-10 on signaling of the RRV vGPCR have never been examined, although we anticipated that its effect on this receptor would mimic those seen with the HHV-8 vGPCR in other cell types, since we have shown previously that the RRV vGPCR is responsive to GROα, an agonist for the HHV-8 vGPCR (51). Indeed, treatment of stable BJAB cells expressing either receptor with IP-10 essentially blocked their ability to activate ERK1/2 signaling, while cells not treated with IP-10 showed the typical constitutive activation pattern of

ERK1/2 (Fig. 3.2B). This result demonstrates that IP-10 is capable of inhibiting the constitutive signaling abilities of either the RRV or HHV-8 vGPCRs in B cells, and further shows that the RRV vGPCR is responsive to multiple cellular chemokines, similar to its HHV-8 counterpart.

RRV and HHV-8 vGPCRs activate PI3K/Akt/GSK-3 signaling in B cells. PI3K is activated via $G\alpha_i$ and $G\alpha_q$ coupled GPCRs, resulting in the phosphorylation and activation of the downstream serine/threonine kinase Akt (117, 118). The HHV-8 vGPCR has been shown to constitutively activate PI3K/Akt in several cell types (110, 129, 152), and in endothelial cells, activation of Akt by the receptor is believed to result in protection from apoptosis (110). To examine activation of PI3K/Akt in stable BJAB B cell populations, lysates of these cells were analyzed for increased levels of phosphorylated Akt by Western blot analysis. Compared to vector control cells, those expressing either the RRV or HHV-8 vGPCRs contained increased levels of phosphorylated Akt (pAkt), indicating that both receptors constitutively activate the PI3K/Akt pathway in B cells (Fig. 3.3A).

In the PI3K/Akt pathway, a major downstream target of Akt is the protein Glycogen Synthase Kinase-3 (GSK-3), an enzyme first identified for its ability to regulate glycogen metabolism (40), but which more recently has been found to play a direct and significant role in the induction of apoptosis (127). In its active form, GSK-3 is unphosphorylated, with the phosphorylation of a key serine residue by Akt resulting in its inactivation. Thus, to examine the activation state of GSK-3 in stable BJAB cells, lysates were examined by Western blot analysis for increased levels of phosphorylated GSK-3β

(pGSK-3β), one of two isoforms of GSK-3. As expected, both the HHV-8 and RRV vGPCR expressing populations displayed increased levels of phosphorylated GSK-3β (Fig. 3.3B), closely paralleling the ability of both receptors to activate the upstream kinase Akt. This finding confirms the activation of Akt, and demonstrates that Akt activated by either receptor in B cells can have effects on downstream targets involved in the regulation of apoptosis. Therefore, expression of the RRV or HHV-8 vGPCR in B cells is likely to protect these cells from apoptosis.

RRV and HHV-8 vGPCRs signal via $G\alpha_i$-independent and PI3K-dependent mechanisms to activate ERK1/2 and Akt/GSK-3. Despite the finding that the RRV and HHV-8 vGPCRs similarly activate the ERK1/2 and PI3K/Akt/GSK-3 signaling pathways in BJAB cells, the possibility of variations in the exact mechanism of activation of these pathways by these receptors exists. The G protein coupling pattern of the HHV-8 vGPCR appears to display wide diversity, with $G\alpha_i$, $G\alpha_q$, and $G\alpha_{13}$ all having been implicated in receptor signaling (39, 95, 110, 150, 152). Signaling of the HHV-8 vGPCR to ERK1/2 has been suggested to be $G\alpha_i$-dependent (152), and $G\alpha_q$-dependent (26, 95), while signaling to the PI3K/Akt pathway has been suggested to be $G\alpha_i$-dependent (26, 152), as well as both $G\alpha_i$ and $G\alpha_q$-dependent (110). In the case of Akt, activation of this pathway by the HHV-8 vGPCR has been shown to be PI3K dependent (110, 129, 152), as expected, although it may also be capable of being activated by ERK1/2 (152).

To decipher the modes by which these receptors interact with the ERK1/2 and Akt/GSK-3 pathways in B cells, we utilized known inhibitors of PI3K signaling (LY294002) and $G\alpha_i$ G protein signaling (pertussis toxin) to determine what mechanisms

each vGPCR may utilize to activate signaling. Cells were prepared as in previous assays, and either left untreated, or treated with pertussis toxin or LY294002. Examination of pERK and pGSK-3β levels indicates that treatment of cells expressing either vGPCR with pertussis toxin has no significant effect on the activation of the ERK1/2 or PI3K/Akt/GSK-3 pathways (Fig. 3.4A and 3.4B). Although we cannot rule out some minor involvement of $G\alpha_i$ proteins in regulation of ERK1/2 or PI3K/Akt/GSK-3 signaling, this seems to suggest that neither the RRV or HHV-8 vGPCRs significantly utilize $G\alpha_i$ proteins to activate the these pathway in B cells, and further indicates that both receptors likely couple to similar G proteins in B cells.

As expected, treatment of cells with the PI3K inhibitor LY294002 reduced the amounts of pGSK-3β in cells expressing either the RRV or HHV-8 vGPCR, confirming that both receptors regulate the Akt/GSK-3 pathway via PI3K (Fig. 3.4B). Interestingly, examination of pERK levels revealed that treatment of cells with LY294002 also reduced the activation of ERK1/2 by either vGPCR, suggesting that ERK1/2 signaling by both the RRV and HHV-8 vGPCRs in B cells is at least partially dependent on PI3K (Fig. 3.4A). This data is similar to what has been seen in studies on the HHV-8 vGPCR in COS-7 cells (152), but differs from recent data examining this receptor in PEL cells, in which it was found that PI3K inhibition did not have any effects on its ability to activate ERK1/2 (26). This may suggest that there are indeed cell type specific differences in vGPCR signaling to ERK1/2 in BJAB and PEL cells, or that the presence of other viral factors could be influencing signaling patterns in PEL cells.

The RRV and HHV-8 vGPCRs inhibit apoptosis in B cells. Given that the RRV and HHV-8 vGPCRs were found to activate the anti-apoptotic kinase Akt, and inhibit the pro-apoptotic kinase GSK3-β in BJAB cells, we wished to address whether signaling by these receptors could provide a protection signal to B cells induced to undergo apoptosis. A major hallmark of apoptosis is the activation of cellular caspases (aspartate-specific cysteine proteases), which are critical regulators of cell death (179). Effector caspases (caspases-3, -6, and –7) are involved in actual proteolysis events leading to cell death, and are activated by upstream caspases such as caspase-9. Importantly, Akt phosphorylation of caspase-9 has been shown to inhibit its activity, and thus protect cells from apoptosis induced through this pathway (27). Given this information, we speculated that signaling by either the RRV or HHV-8 vGPCR could inhibit caspase activation, and more specifically, inhibit the induction of apoptosis in cells expressing these receptors. Poly (ADP-ribose) polymerase (PARP) is a protein involved in DNA repair, and is a major target of effector caspases (21). Upon activation of effector caspases, PARP, a 112 kDa protein, becomes cleaved to produce an 89 kDa product, which is indicative of the induction of apoptosis within a cell. Thus, to address the ability of the RRV and HHV-8 vGPCRs to inhibit apoptosis in BJAB cells, PARP cleavage was analyzed in cells induced to undergo apoptosis by serum deprivation, a treatment known to induce apoptosis in this cell type (37). Stable BJAB populations were grown in serum-free media for 48 hrs, and lysates were then collected and analyzed by Western blot for the presence of uncleaved and cleaved forms of PARP. In cells expressing either the RRV or HHV-8 vGPCR, the level of serum-starvation induced PARP cleavage was consistently reduced compared to vector cells treated in an identical fashion (Fig. 3.5A), indicating that both

receptors provide a protection signal in response to an apoptotic stimulus. Cells grown in serum-containing media contained no cleaved PARP, demonstrating a lack of apoptosis induction. These experiments were repeated multiple times with similar results, and quantitation revealed a consistent average level of protection by both receptors of approximately 20% compared to vector control cells (Fig. 3.5B). Thus, expression of either the RRV or HHV-8 vGPCR in B cells appears to protect these cells from apoptosis, likely due to activation of anti-apoptotic proteins such as Akt, which can in turn inhibit the function of pro-apoptotic proteins such as caspase-9 and GSK-3.

DISCUSSSION

The rhesus rhadinovirus (RRV) viral G protein-coupled receptor (vGPCR) is homologous to the ORF74 encoded vGPCR of HHV-8/KSHV, and shares similar activities with this receptor *in vitro* (51). Examination of the activities of the HHV-8 vGPCR in relevant cell types to HHV-8 infection have been generally restricted to endothelial cells (39, 110, 129, 130), with a limited report of its function in B cells (132). Further, the RRV vGPCR has never been examined in any cell types relevant to viral infection. Thus, assessing the properties of these vGPCRs in B cells would provide insight into their potential roles in the development of B cell abnormalities associated with RRV infection in rhesus macaques (173), and HHV-8 infection in humans (30, 155), and further help determine the utility of RRV as an animal model to study the contributions of the HHV-8 vGPCR in viral pathogenesis.

Utilizing the EBV and HHV-8 negative human BJAB B cell line, we report for the first time that the RRV and HHV-8 vGPCRs possess similar signaling abilities in B cells, and specifically that they are capable of constitutively activating the ERK1/2 and PI3K/Akt/GSK-3 signaling pathways in this cell type. Also, we demonstrate that the RRV vGPCR is responsive to the cellular chemokine IP-10, a known inhibitor of HHV-8 vGPCR signaling, extending the known chemokine responsiveness of the RRV vGPCR, and indicating that both the RRV and HHV-8 vGPCRs can be regulated by chemokines when expressed in B cells.

Examination of the exact mechanisms of signaling reveals that both receptors utilize $G\alpha_i$-independent and PI3K-dependent pathways to activate ERK1/2 and

Akt/GSK-3. Treatment of cells with pertussis toxin, a $G\alpha_i$ inhibitor, had no noticeable effects on the phosphorylation of ERK1/2 or GSK-3β by either vGPCR, suggesting that both receptors may utilize mainly non-$G\alpha_i$ G proteins to activate these pathways. Our finding that both RRV and HHV-8 vGPCR induced PI3K/Akt/GSK-3 signaling is pertussis toxin insensitive varies from some previously published reports on the activity of the HHV-8 vGPCR in COS-7 cells (110, 152), and PEL cells (26), in which activation of this pathway appears to be at least partly $G\alpha_i$ -dependent. However, in the case of ERK1/2 signaling, our findings are similar to those obtained in PEL cells and HEK293 cells expressing the HHV-8 vGPCR, in which pertussis toxin does not inhibit ERK1/2 activation induced by the receptor (26, 95). We also found that treatment of cells expressing either vGPCR with the PI3K inhibitor LY294002 resulted in a reduction in pGSK-3β levels, as expected for a PI3K dependent pathway. In addition, PI3K inhibition also caused a reduction in pERK levels, suggesting that ERK1/2 activation is also at least partially PI3K-dependent in B cells. This is similar to what has been seen with HHV-8 vGPCR in COS-7 cells (152), but differs from the reported PI3K-independence of ERK1/2 activation seen in PEL cells expressing the HHV-8 vGPCR (26). These differences in $G\alpha_i$- and PI3K-dependence in activation of these pathways could be due to experimental differences, but more likely represent actual variations in G protein coupling, and divergences in signaling pathways utilized by these receptors in different cell types. Overall, our data demonstrates that in B cells, both the RRV and HHV-8 vGPCRs couple to similar G proteins to activate the ERK1/2 and Akt/GSK-3 pathways. Signaling to these pathways most likely occurs via $G\alpha_q$ G proteins (Fig. 3.6), given that PI3K is thought to be activated by either $G\alpha_q$ or $G\alpha_i$ coupled GPCRs (117, 118).

We have also shown that expression of the RRV or HHV-8 vGPCRs confers resistance to apoptotic stimuli in B cells. Serum-starvation was utilized to induce BJAB cells to undergo apoptosis, as measured by cleavage of PARP, a known target of effector caspases, and it was found that expression of either the RRV or HHV-8 vGPCRs reduced the levels of PARP cleavage in these cells compared to vector control cells. Although the HHV-8 vGPCR has been shown previously to protect endothelial cells from apoptosis (110), this is the first time this receptor has been shown to provide a protection signal in B cells, and the first time the RRV vGPCR has been shown to have any anti-apoptotic properties in any cell type. These findings suggest that when expressed in infected B cells, signaling by these vGPCRs may provide a protection signal, allowing for prolonged survival in the face of apoptotic stimuli. Although we did not demonstrate that inhibition of caspase mediated PARP cleavage was specifically due to Akt activation, the activation of this kinase in cells expressing the RRV or HHV-8 vGPCRs, and its defined role in the regulation of apoptosis, suggests that it likely plays a major role in the protection of cells from apoptosis due to caspase activation (Fig. 3.6). Other signaling pathways may also be involved in the inhibition of apoptosis by both vGPCRs, although this remains unknown.

The questions of what role these vGPCRs play in the viral life cycle, and how they may be involved in transformation and pathogenesis associated with viral infection, is at this point still unclear. Recent data from our laboratory indicates that like HHV-8 ORF74, RRV ORF74 is transcribed during lytic viral replication (manuscript in submission). It seems plausible from the information collected on the HHV-8 vGPCR, as well as the RRV vGPCR, that these viral genes are involved in providing a favorable environment for viral replication in an infected cell. For example, activation of signaling

pathways by these vGPCRs could produce an optimal environment in an infected cell for increased viral DNA replication, or perhaps protect these cells from apoptotic stimuli induced by viral factors. Indeed, viral replication within a cell often induces apoptosis, and this has been shown to be the case with lytic HHV-8 replication *in vitro* (84). Therefore, anti-apoptotic properties of RRV or HHV-8 vGPCR expression could be envisioned to keep the host cell alive for a sufficient period of time to allow the virus to successfully complete replication. Interestingly, murine gamma-herpesvirus 68 (MHV-68) also encodes a vGPCR with some similarities to the HHV-8 vGPCR (170), and recently it was found that deletion of this gene from MHV-68 results in a decreased ability of the virus to reactivate from latency or replicate in response to chemokine (92). Future studies utilizing ORF74-deleted RRV_{17577} could provide further insight into a role for the HHV-8 and RRV vGPCRs in latency and viral replication in a primate model.

How a viral gene can be involved in transformation of an infected cell that is destined for destruction has become a common question associated with studies of several HHV-8 lytic genes that have been found to possess oncogenic properties. These questions could be explained by aberrant expression of viral lytic genes during latency, or perhaps due to expression associated with an abortive or incomplete replication cycle, with either event resulting in unintended expression of potentially oncogenic genes. In any case, expression of these vGPCRs in infected cells could have significant effects on signaling pathways controlling cellular growth, proliferation, or apoptosis, ultimately resulting in the production of a transformed phenotype. Activation of pathways such as PI3K/Akt/GSK-3 might be a major mechanism involved in abnormal B cell growth induced by the RRV and HHV-8 vGPCRs, due to increased survival and resistance to

apoptosis of cells expressing these receptors. Analysis of the RRV vGPCR in the context of viral infections *in vivo* should provide greater insight into the exact roles of this receptor and its HHV-8 counterpart in viral-associated malignancies.

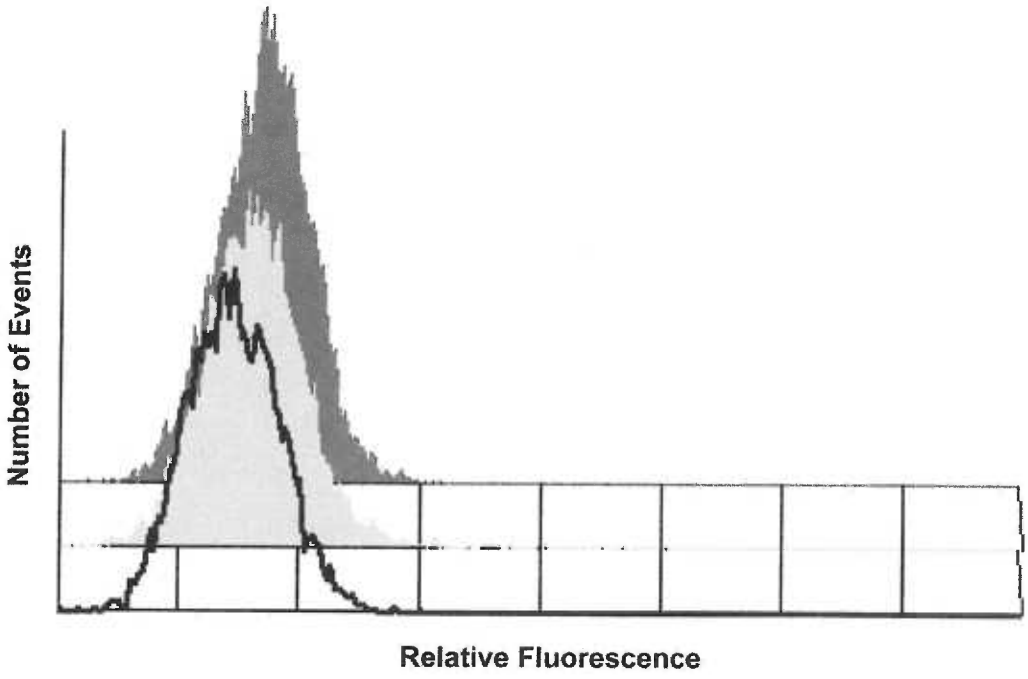

Figure 3.1. Surface expression of RRV and HHV-8 vGPCRs in stable BJAB populations. Fluoresence activate cell sorting (FACS) analysis of live stable BJAB cells expressing N-terminal HA tagged RRV vGPCR (light gray) or HHV-8 vGPCR (dark gray), compared to vector control cells (black line). Cells were stained with mouse anti-HA and anti-mouse-FITC antibodies. The data shown is representative of one experiment.

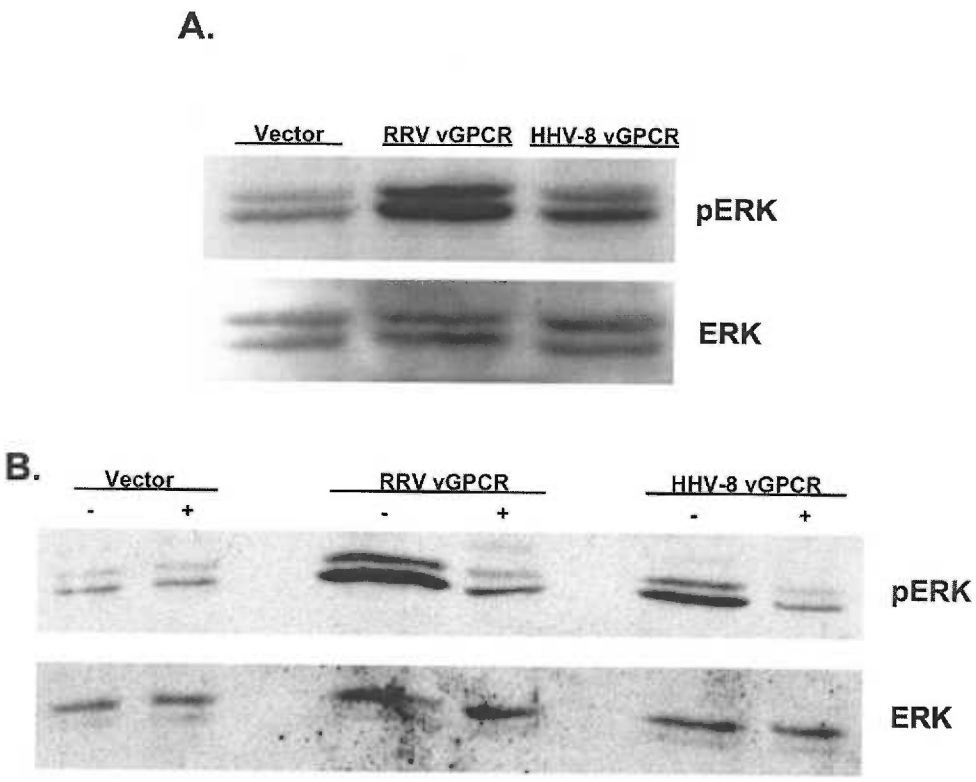

Figure 3.2 RRV and HHV-8 vGPCRs constitutively activate ERK1/2 in B cells and are responsive to IP-10. Western blot analysis of phospho-ERK1/2 (pERK) levels in (A) lysates from stable BJAB populations, or (B) lysates from stable BJAB populations untreated (-) or treated (+) with IP-10 (30nM, 2 hrs). Blots were probed for phospho-ERK1/2, then stripped and reprobed with total ERK antibody.

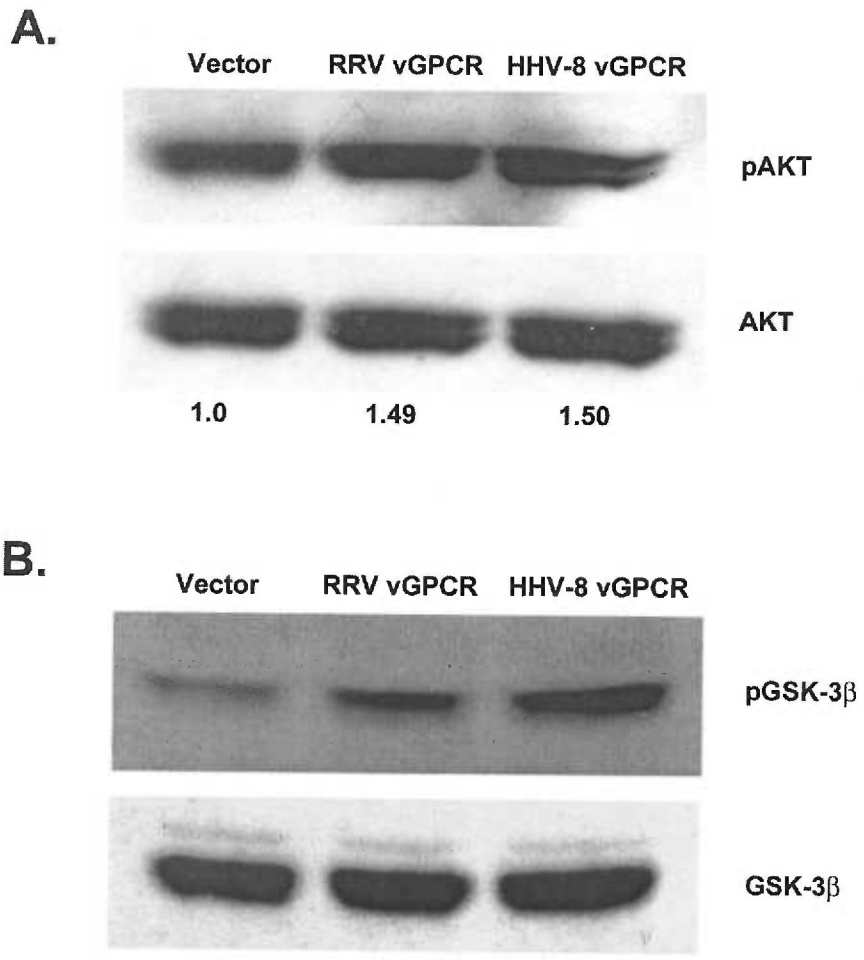

Figure 3.3 Activation of the Akt/GSK-3 pathway in B cells by the RRV and HHV-8 vGPCRs. Western blot analysis was performed on lysates from stable BJAB populations for levels of (A) phospho-Akt (pAkt) or (B) phospho-GSK-3β (pGSK-3β). Blots were probed for phospho-Akt or phospho-GSK-3β, then stripped and reprobed with total Akt or GSK-3β antibody. Numbers represent fold change in activation versus vector cells.

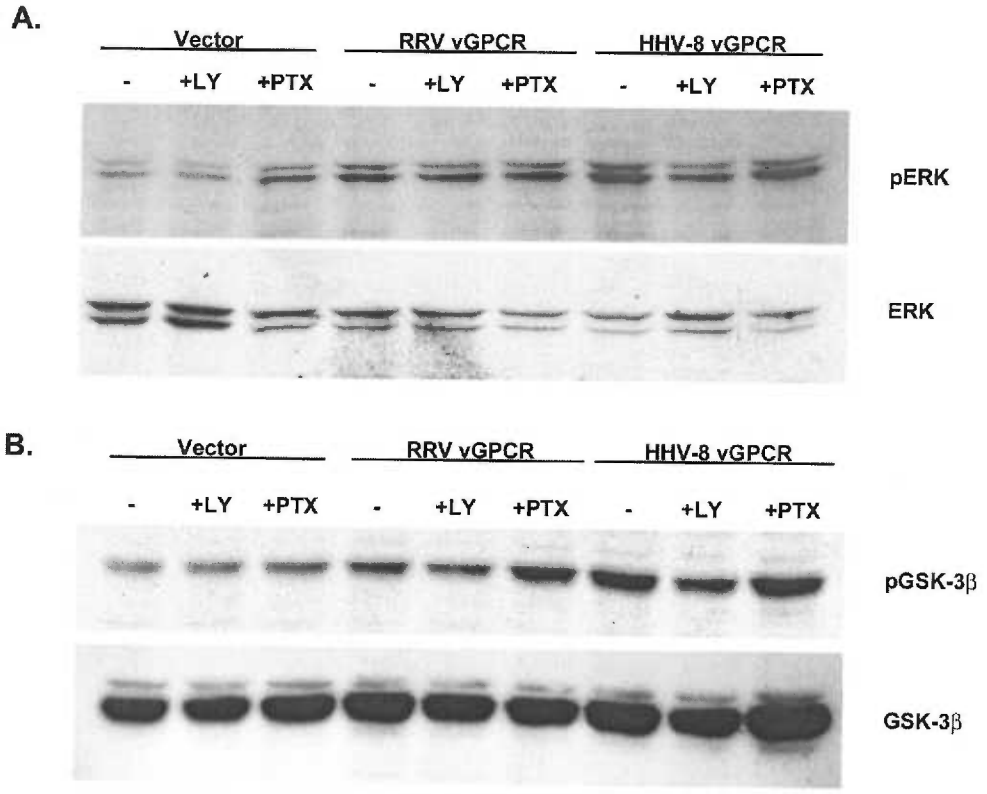

Figure 3.4 Effects of $G\alpha_i$ and PI3K inhibition on the activation of ERK1/2 and GSK-3β by the RRV and HHV-8 vGPCRs. Western blot analysis was performed for (A) phospho-ERK1/2 (pERK), or (B) phospho-GSK-3β (pGSK-3β) in lysates from stable BJAB populations either untreated (-), or treated with the PI3K inhibitor LY294002 (10 μM, 2 hrs) (+LY), or pertussis toxin (100 ng/ml, 24 hrs) (+PTX). Blots were probed for phospho-ERK1/2 or phospho-GSK-3β, then stripped and reprobed with total ERK or GSK-3β antibodies.

Figure 3.5 Inhibition of serum-starvation induced PARP cleavage in B cells by the RRV and HHV-8 vGPCRs. Western blot analysis for levels of PARP cleavage in lysates from stable BJAB B cells expressing RRV or HHV-8 vGPCRs. (A) images of Western blots of lysates from cells grown in the presence (+ serum) or absence (- serum) of serum for 48 hrs. The uncleaved and cleaved forms of PARP are indicated. (B) average percent inhibition of PARP cleavage by the RRV and HHV-8 vGPCRs calculated from three independent experiments. Error bars indicate standard deviation.

A.

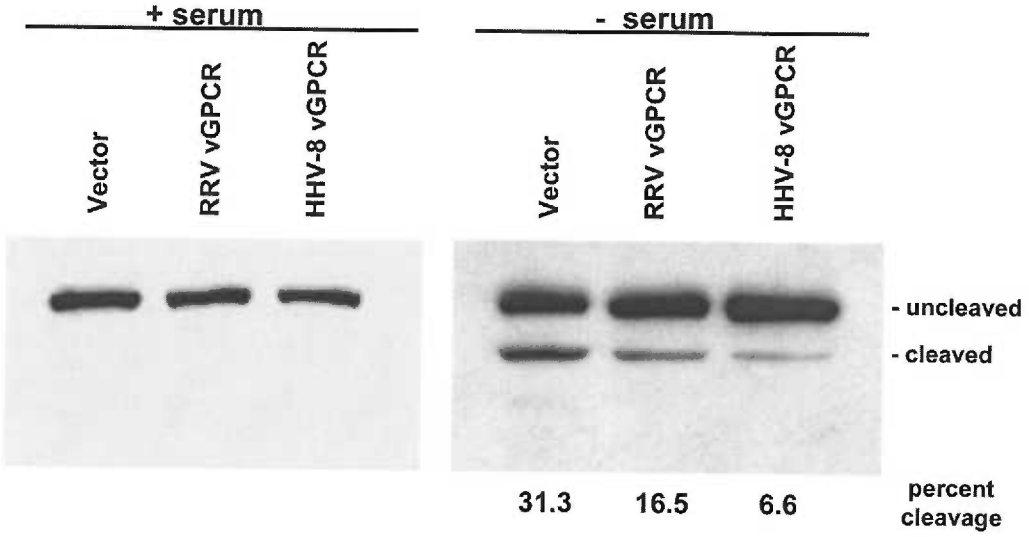
+ serum
- serum
Vector
RRV vGPCR
HHV-8 vGPCR
Vector
RRV vGPCR
HHV-8 vGPCR
- uncleaved
- cleaved
31.3
16.5
6.6
percent cleavage

B.

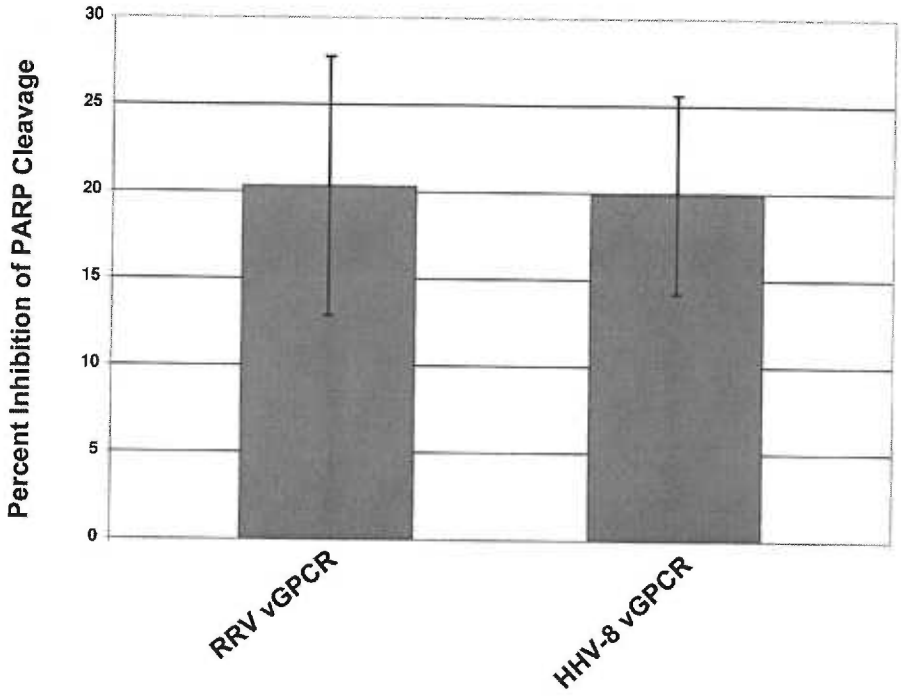
Percent Inhibition of PARP Cleavage
30
25
20
15
10
5
0
RRV vGPCR
HHV-8 vGPCR

Figure 3.6 Model of RRV and HHV-8 vGPCR signaling and regulation of apoptosis in B cells. Based on the data acquired in this study, the image shown depicts a potential model of the signaling and apoptotic pathways regulated by both the RRV and HHV-8 vGPCRs in B cells. Activation of ERK1/2 and GSK-3 appears to occur partially via $G\alpha_q$, due to insensitivity of these pathways to the $G\alpha_i$ inhibitor pertusis toxin (PTX). Signaling to ERK1/2 and Akt/GSK-3 appears to be PI3K-dependent based on sensitivity the receptors to the PI3K inhibitor LY294002. Other pathways may also converge upon ERK1/2 from the vGPCRs, although the pathways potentially utilized are unknown. Due to activation of ERK1/2, these receptors may have effects on proliferation and transformation in B cells. Akt activation by both vGPCRs in B cells results in inhibition of GSK-3, and likely the activity of other downstream targets of Akt such as caspase-9, ultimately inhibiting the induction of apoptosis.

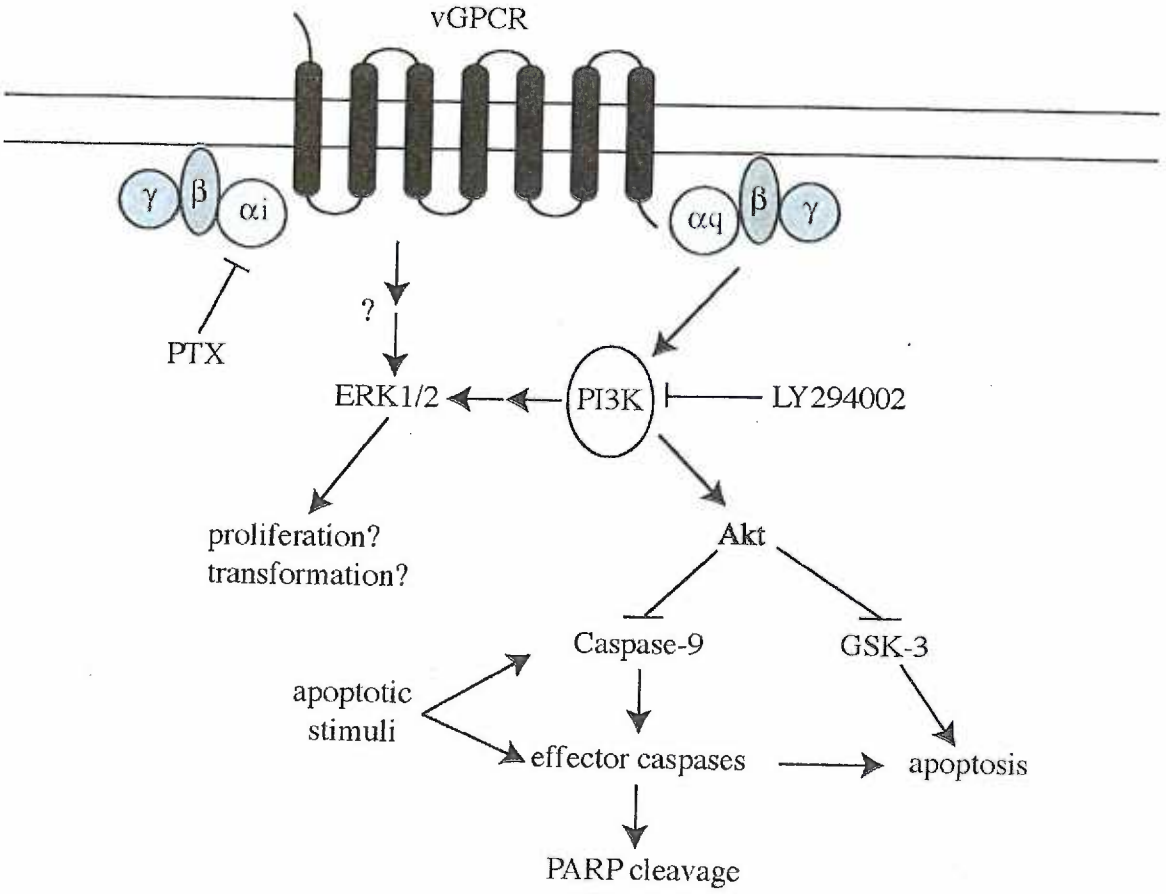
vGPCR
γ
β
αi
αq
β
γ
PTX
?
ERK1/2
PI3K
LY294002
proliferation?
transformation?
Akt
Caspase-9
GSK-3
apoptotic
stimuli
effector caspases
apoptosis
PARP cleavage

Chapter 4

Differential Splicing of Rhesus Rhadinovirus R15 and ORF74 Bi-cistronic Transcripts During Lytic Infection and Analysis of Effects on Production of vCD200 and vGPCR

Carly L. Pratt[1,3,+], Ryan D. Estep[1,3,+] and Scott W. Wong[1,2,3,*]

Vaccine and Gene Therapy Institute[1], Oregon Health & Science University West Campus, Division of Pathobiology and Immunology[2], Oregon National Primate Research Center, Beaverton, Oregon 97006;

Department of Molecular Microbiology and Immunology[3], Oregon Health & Science University, Portland, Oregon 97201.

[+] These authors contributed equally to the study.

[*] Corresponding author:

Vaccine and Gene Therapy Institute
Oregon Health & Science University West Campus
505 N.W. 185th Avenue
Beaverton, Oregon 97006
Tel: (503)-690-5285
Fax: (503)-418-2719
e-mail: wongs@ohsu.edu

Running title: Transcriptional Analysis of RRV R15 and ORF74

*** This manuscript has been submitted for publication in *Journal of Virology***

ABSTRACT

Human herpesvirus 8/ Kaposi's sarcoma-associated herpesvirus (HHV-8/KSHV) is the etiological agent of Kaposi's sarcoma (KS), the most predominant AIDS-associated malignancy, as well as lymphoproliferative disorders including multicentric Castleman's disease (MCD), primary effusion lymphoma (PEL), and some non-Hodgkin lymphomas (NHL). The rhesus macaque homologue of HHV-8, rhesus macaque rhadinovirus (RRV), has been associated with lymphoproliferative disease in simian immunodeficiency virus (SIV)-infected macaques, with the primary display of disease being B cell hyperplasia and MCD. Understanding the roles of pathogenic open reading frames (ORFs) in RRV-associated disease is critical to developing RRV as an animal model to study the contributions of individual viral ORFs to HHV-8 pathogenesis. Here we examine the transcriptional pattern of RRV R15 and ORF74. RRV ORF74 is similar to HHV-8 ORF74, encoding a constitutively active and transforming viral G protein-coupled receptor (vGPCR). R15 is highly similar to K14 of HHV-8, which encodes a putative homologue of a cellular immuno-regulatory protein CD200. As in HHV-8, the message encoding RRV R15 and ORF74 is bi-cistronic. However, unlike what has been suggested for HHV-8, RRV R15 and ORF74 encoding transcripts are expressed late during lytic infection, and undergo unique splicing events that result in the production of multiple species of bi-cistronic transcripts capable of encoding vGPCR, as well as membrane-associated and secreted forms of vCD200. This is a novel finding for any CD200 or CD200-like protein, and could have major implications for a role for this protein in virally-induced disease.

INTRODUCTION

Rhesus macaque rhadinovirus (RRV) has been demonstrated to be the rhesus macaque homologue of human herpesvirus 8 (HHV-8)/Kaposi's sarcoma-associated herpesvirus (KSHV) (44, 149). HHV-8 is the etiological agent of Kaposi's Sarcoma (KS), the most common AIDS-associated neoplasm, as well as B cell malignancies including primary effusion lymphoma (PEL), multicentric Castleman's disease (MCD), and some non-Hodgkin lymphomas (NHL) (22, 30, 34, 125, 155). Our laboratory has previously identified an independent RRV isolate, termed 17577, from an SIV-infected rhesus macaque which had developed lymphoproliferative disorder (LPD) (149). Sequencing of the complete genome of this RRV isolate provided evidence that, indeed, this virus is highly homologous to HHV-8. In addition, further work done in our laboratory has shown that experimental inoculation of SIV-infected macaques results in these animals developing a lymphoproliferative disorder similar to MCD in AIDS patients infected with HHV-8 (173). Also, experimental infection with RRV_{17577} is potentially associated with the development of retroperitonial fibromatosis (RF), a disease that displays cellular characteristics similar to KS (unpublished observation). Therefore, the SIV/RRV_{17577} system provides an excellent animal model to study the contributions of RRV to disease manifestations that are similar to those seen with HIV/HHV-8 infection in humans.

Examination of the RRV genome shows that this virus maintains numerous open reading frames (ORFs) that are found in HHV-8. Specifically, 67 of 79 ORFs encoded by RRV are similar to those in HHV-8. Studies to examine the properties of individual ORFs in RRV will help to decipher exactly how similar and/or different RRV is to HHV-

8, and will ultimately determine the importance of the SIV/RRV model to understanding HHV-8 pathogenesis in HIV infected individuals. Thus far, the examination of several ORFs from RRV has demonstrated that they appear to have similar functions and activities to their counterparts in HHV-8. For example, the RRV IL-6 homologue (vIL-6), encoded by ORF R2, has been shown to be a functional IL-6 homologue, similar to vIL-6 of HHV-8 (81). In addition, the RRV G protein-coupled receptor (GPCR), encoded by ORF74, is a seven-transmembrane receptor that displays similar properties to the homologous protein encoded by ORF74 in HHV-8. Like ORF74 of HHV-8, RRV ORF74 has been shown to encode a constitutively signaling GPCR with transforming potential (51). Work has also been done to characterize the R1 protein from RRV, demonstrating similar transforming potential and lymphocyte signaling abilities as the homologous KSHV K1 protein (41, 43), and to identify the RRV bZIP and Rta homologues (94). Another RRV ORF of interest is R15, which to date has not been examined in detail. R15 appears to be homologous to ORF K14 of HHV-8, which encodes a putative viral CD200 (vCD200) homologue similar in sequence and predicted structure to human CD200 (huCD200). Specifically, these proteins are predicted to be type-I transmembrane proteins with two immunoglobulin domains in the extracellular region. It has been shown that engagement of huCD200 with its corresponding receptor (CD200R) on cells of myeloid lineage results in the production of an anti-inflammatory (TH2) response from these cells (66, 77, 174), while examination of the properties of HHV-8 vCD200 suggest that the extracellular domain of this protein induces an opposite, pro-inflammatory (TH1), response from cells of myeloid lineage (36). Despite apparent differences in the activities of these proteins, it appears that both proteins possess immuno-regulatory

properties. Thus, the possibility exists that vCD200 proteins may play an important role in the modulation of the host immune response during viral infection.

Transcriptional analysis of various ORFs in HHV-8 has demonstrated that the transcriptional patterns of viral ORFs can be intricate and complicated. For example, analysis of HHV-8 ORF74 has revealed that this ORF is transcribed as the second ORF of bi-cistronic messages with ORF K14, the ORF encoding the viral CD200 homologue. The studies examining the transcription of this region of the HHV-8 genome seem to suggest that both the vCD200 and vGPCR proteins are made in full-length from these bi-cistronic transcripts, however this has not been demonstrated. In addition, detection of the K14 and ORF74 transcripts has been reported to occur early during lytic HHV-8 gene expression (35, 85, 120, 161). To date, transcriptional analysis of RRV ORFs have been limited (45). Here we demonstrate that similar to K14 and ORF74 in HHV-8, RRV R15 and ORF74 are also encoded on bi-cistronic transcripts. However, in the case of RRV, the transcripts encoding these ORFs are made late during RRV lytic infection. In addition, further examination of these RRV transcripts reveals that a unique splicing event occurs within the R15-ORF74 coding sequence that allows RRV vCD200 to be produced as a soluble/secreted protein, a novel finding for a viral CD200-like protein that could have major implications in viral-mediated pathogenesis.

MATERIALS AND METHODS

Cells and virus. Primary rhesus fibroblasts were grown in Dulbecco's modification of Eagle's medium (DMEM) (Mediatech, Herndon, VA) supplemented with 10% fetal bovine serum (HyClone, Logan, UT). Viral stocks used were obtained by infection of primary fibroblasts with RRV_{17577} clone #7. For virus infection studies, cell cultures were grown in either the presence or absence of inhibitors (cycloheximide [75 μg/mL] or phosphonoacetic acid [300 μM]) (Sigma) for two hours and then infected with RRV at a multiplicity of infection (MOI) of 5 in the presence of inhibitors. Chinese hamster ovary (CHO) cells were grown in F12K media (Mediatech) containing 5% fetal bovine serum (HyClone). Nucleotide sequence accession number for RRV_{17577} is AF083501.

RNA. Total RNA was obtained from primary rhesus fibroblasts cultures infected with RRV using TRI Reagent (Sigma, St. Louis, MO) according to manufacturer's specifications. RNA used in RT-PCR from transfected CHO cells was isolated using Hi Pure RNA Isolation Kit (Roche, Nutley, NJ) per manufacturer's instructions.

Northern Blot analysis. RNA was run on 1.0% agarose gels containing 1.0% formaldehyde, with 10 μg of total RNA loaded per lane. Gels were then transferred to nitrocellulose membranes, and probed with specific dsDNA or oligo probes using standard protocols. dsDNA probes were generated by random primed labeling with specific cloned DNA fragments for the entire R15 or ORF74 sequence, using [α-^{32}P]dCTP and a random prime labeling kit (Stratagene, La Jolla, CA). R15 oligo probe (5′-GGTCGTTCTGGTCAACTTGTGTTC-3′) and ORF73 oligo probe (5′-

TTCCCATACCGTATCCCTCATCAG-3′) were generated by end-labeling oligos with [γ-^{32}P]ATP using polynucleotide kinase (Fermentas, Hanover, MD). As loading control, blots were stripped using 0.1% boiling SDS, and re-probed with a [α-^{32}P]dCTP labeled dsDNA probe specific for rhesus GAPDH.

RACE reactions. Rapid amplification of cDNA ends (RACE) was performed using a First Choice™ RLM-RACE kit (Ambion, Austin, TX) as per manufacturer's instructions. The RNA utilized was from RRV infected rhesus fibroblasts from 72 hr/untreated time point. Gene specific primers used in 3′ RACE reactions were for ORF74 (5′-GCATTACGCTGTTTGGGAACG-3′) and ORF75 (5′-TGCCAAAACTTTGACTGCCG-3′). For 5′ RACE, primers used were specific for ORF72 (5′-ATGGCTTCTGTTGGCCCAGT-3′), ORF73 (5′-ATGTGGGGCAGCCGGCCACA-3′), R15 (5′-AATGTAATTCCTCCCGACAT-3′), and ORF71 (5′-ATGTTCCCGCATAAGCGG-3′). Products obtained were gel purified and cloned into pCRII-Topo vector (Invitrogen life technologies, Carlsbad, CA) for DNA sequence determination.

RNase protection analysis. Oligonucleotide primers were designed to amplify a DNA fragment containing the sequence between nt 119421 to 119511 of RRV, which was subsequently cloned into pSP73 (Promega, Madison, WI). This plasmid was then linearized with *Hin*dIII, and transcribed in the presence of [α-^{32}P]GTP using the SP6 promoter. The resulting labeled anti-sense probe was then hybridized with RNA and digested with RNase. Approximately 15 μg of total RNA from uninfected and 72 hr

RRV-infected cultures were used for hybridization, and yeast tRNA was used a negative control. Products of these reactions were run on an acrylamide gel along with RNA size standards (Ambion), and subsequently exposed to film.

Reverse Transcription-PCR (RT-PCR) of spliced transcripts. RT-PCR was performed using a Titan One-step RT-PCR kit (Roche), following manufacturer's instructions. 500 ng of RNA was used per reaction, utilizing conditions that were optimized for each specific reaction. Reactions containing Vent DNA polymerase without RT enzyme served as controls to demonstrate the absence of DNA. Primers used to amplify the upstream region of the R15-ORF74 transcript were specific for ORF71 (5′ primer: 5′-ATCGCCCAACGAGAAACA-3′) and R15 (3′ primer: 5′-AATGTAAATCCTCCCGACAT-3′), while those used to amplify the R15-ORF74 region were specific for R15 (5′ primer: 5′-ATGTCGGGAGGAA-3′) and ORF74 (3′ primer: 5′-TCATAAACTACCTGAAGTGGA-3′). Products were analyzed on 1.7% agarose gels, then purified and cloned into pCRII-Topo vector for sequencing.

Protein expression analysis of spliced transcripts. An internal FLAG epitope tag was introduced to R15 coding sequence (at nt 632) by PCR using a R15 specific primer containing the FLAG sequence as the 3′ primer (5′-GCCGCGGCCTTGTCGTCGTCGTCCTTGTAATCCAAACCGCCTATATGAGT-3′), a primer for the exact 5′ end of R15 sequence, and 2.1 kb R15-ORF74 cDNA as template. PCR products were then cloned into 1.7 kb and 2.1 kb R15-ORF74 cDNAs from RT-PCR using a unique *Sac*II site located within R15 sequence. The FLAG coding sequence

of these constructs is in frame with vCD200 protein, and is located upstream of the splice site identified in this region. A C-terminal HA epitope was introduced in frame with vGPCR by performing PCR with either the 1.7 kb or 2.1 kb R15-ORF74 cDNAs as templates, using a 5′ R15 primer and a 3′ ORF74-HA primer (5′-TCAAGCGTAGTCTGGGACGTCGTATGGGTATAAACTACCTGAAGTGGAA-3′). Epitope sequences are underlined. All products were sequenced to confirm their identity and cloned into pcDNA3.1(-) (Invitrogen) for expression analysis. For immunofluorescence analysis, CHO cells were plated the day before transfection on chamber slides (Nunc, Naperville, IL), and transfected using Transit LT-1 reagent (Mirus, Madison, WI) with 0.5 μg of DNA per chamber. Approximately 48 hours post-transfection, cells were fixed with 100% cold methanol, stained for FLAG or HA using the appropriate primary antibodies (Sigma), and a FITC-labeled secondary antibody (Sigma). Fixed cells were then analyzed by confocal microscopy using a TCS SP confocal system (Leica Microsystems, Heidelberg, Germany) with a Plan Apo 40X or 100X objective. For Western blot analysis of vCD200-FLAG expression, CHO cells were plated in 6-well dishes the day before transfection, and were transfected with either empty vector, 1.7 kb R15-FLAG, or 2.1 kb R15-FLAG, using Transit LT-1 reagent with 3 μg DNA per well. Supernatants were then collected at 48 hours post-transfection and concentrated using Amicon ultra centrifugal filter devices (Millipore, Bedford, MA). Lysates from these same cells were prepared by lysing cells in RIPA buffer (1X PBS + 1% NP-40, 0.1% SDS, 0.5% sodium deoxycholate). 50 μl of concentrated supernatant, and 50 μl of lysates were run on 10% acrylamide gels, transferred to nitrocellulose membranes, and probed with anti-FLAG antibody. To detect HA tagged ORF74 protein,

CHO cells were plated in 60 mm dishes the day before transfection, and then transfected with either empty vector, 1.7 kb ORF74-HA, 2.1 kb ORF74-HA, or pcDNA3.1(-) encoding an N-terminally tagged version of RRV ORF74 as a control. Cells were lysed 48 hrs post-transfection with 500 μl RIPA per dish, and HA tagged protein was immunoprecipitated by incubating lysates overnight with anti-HA antibody (Sigma) and protein A beads. The beads were then washed 4X with PBS, and immunoprecipitated protein was then eluted by incubation with 2X SDS-PAGE buffer at 37^0C for 1 hr before loading onto a 10% acrylamide gel. The gel was transferred to a nitrocellulose membrane and probed with anti-HA antibody (Sigma).

Prediction of RNA secondary structure. The program RNA mFOLD was used to predict secondary structure within the R15-ORF74 5.5 kb transcript (98).

Prediction of protein signal sequence. The program SignalP was utilized to predict signal sequences within RRV vCD200 (124).

Spliced cDNA Nucleotide Sequence. The cDNA sequence of the dually-spliced R15-ORF74 transcript has been deposited into GenBank under accession no. AF083501.

RESULTS

Northern Blot Analysis of R15 and ORF74 transcripts. The area of the RRV genome under investigation is depicted in Figure 4.1. To examine the expression pattern of RRV R15 and ORF74, we utilized our *in vitro* system of RRV infection of primary rhesus fibroblasts to obtain total RNA from infected cells. Primary rhesus fibroblasts were infected with RRV_{17577} in the presence of cycloheximide (CHX) to inhibit protein synthesis, phosphonoacetic acid (PAA) to inhibit DNA replication, or left untreated to detect immediate-early, early, or late viral transcripts, respectively. The time points for collection of RNA were 24 hours (CHX), 48 hours (PAA), and 72 hours (untreated), as these three classes of transcripts have been determined to roughly appear at these time points after infection with RRV *in vitro*, even in the absence of inhibitory drugs. As seen in Figure 4.1B and C, both ORF74 and R15 transcripts are only detected in untreated cultures collected 72 hrs post-infection, demonstrating that these ORFs are transcribed as late-lytic genes.

Examination of the RRV transcripts seen by Northern blot analyses indicate that the similar size species of transcripts are detected using either a double-stranded R15 or ORF74 DNA probe, suggesting that as in HHV-8, these two ORFs are encoded together on bi-cistronic messages. Interestingly, there appears to be at least two RNA species present encoding R15 and ORF74, a large transcript of approximately 5.5 kb and a smaller transcript of approximately 3.0 kb. The presence of other transcripts is also possible, since the bands in the Northern blots are somewhat diffuse in both cases. One possible explanation for the larger transcript is that it represents an antisense message that is transcribed from the opposite strand of the viral genome, initiating somewhere near the

right end (3′) of ORF74 and extending through both ORFs. If this were true, this message would be detectable when using double-stranded DNA (dsDNA) probes, but not with an anti-sense oligo probe. To examine this possibility, we used an antisense oligo probe specific for R15 in Northern analysis of 72 hr/untreated RNA. Using this probe we were able to detect two messages of similar size to those obtained when using the dsDNA probes for R15 and ORF74 (Fig. 4.1D), demonstrating that the two bands seen in Northern analysis are indeed specific for transcripts initiating in a region upstream of R15 and extending through ORF74. In addition, bands for any apparent mono-cistronic R15 or ORF74 messages were not detected in Northern analyses.

Interestingly, utilizing a dsDNA probe for ORF71 sequence in Northern analysis of 72 hr/untreated RNA, we detected a pattern of transcripts very similar to those seen with probes for R15 and ORF74 (Fig. 4.1E). Specifically, the ORF71 probe detects a large transcript of approximately 5.5 kb, and to a lesser extent an approximate 3.0 kb transcript. In addition, there appears to be the potential for numerous other transcripts containing sequence for ORF71, based on the appearance of an apparent smearing pattern around ~2 kb. These findings are also consistent with earlier published observations on RRV ORF71 transcription (10). Given that ORF71 is a putative latent gene, we speculated that messages detected with an ORF71 probe were specific to transcripts anti-sense to this ORF, and thus might be linked to downstream R15 and ORF74.

Identification of the 5′ and 3′ ends of RRV R15-ORF74 transcripts. The 5.5 kb and 3.0 kb messages detected by Northern analysis are both much longer than the expected ~2.0 kb for an R15-ORF74 bi-cistronic message. We speculated that the 5.5 kb transcript

could represent a message that initiates further upstream of R15, or which reads through the stop codon of ORF74 and terminates farther downstream, whereas the identity of the 3.0 kb message was initially uncertain. To address these issues, we examined the identity of the 5′ and 3′ ends of these transcripts by rapid amplification of cDNA ends (RACE) analysis. 3′ RACE was performed with 72 hr/untreated RNA from RRV infected primary rhesus fibroblasts, utilizing an ORF74 specific primer that binds at nucleotide position 124102 of the RRV genome (within ORF74 sequence), along with a polyA specific primer (Fig. 4.2A). A strong signal for a single product of approximately 800 bp was obtained (Fig. 4.2B), which was then isolated and cloned for sequencing. Examination of five 3′ RACE cDNA clones revealed that all of the amplified products terminated at the same location, a stretch of A residues located 95 bases after the stop codon for ORF74. Therefore, it appears that all transcripts terminating after ORF74 utilize a non-conventional polyA site (AUUAAA) starting at nucleotide 125021 of the viral genome (Fig. 4.2D). Using a forward primer specific for the 5′ end of R15 in 3′ RACE (Fig. 4.2A), no products were obtained, suggesting a lack of any polyA signals upstream of nt 125021 (data not shown). No product corresponding to the entire R15-ORF74 region (~2 kb) was obtained from a 3′ RACE reaction using this same 5′ R15 primer, likely due to the large size of the region to be amplified. These findings demonstrate that transcripts encoding RRV R15 and ORF74 appear to terminate directly after ORF74 sequence, and that no transcripts extend pass this region into ORF75 sequence. To confirm that messages extending through ORF75 do not extend into ORF74 sequence, 3′ RACE was performed with an ORF75 specific primer (Fig. 4.2A). A single product was obtained in

this reaction and DNA sequence analysis of the product indicated that ORF75 messages do not extend beyond ORF75 into ORF74 sequence (data not shown).

Since no transcripts extend downstream of ORF74, the transcripts detected by Northern analysis are likely due to initiation of transcription upstream of R15 sequence. In the case of the 5.5 kb message, the sequence upstream of R15 would be estimated to be approximately 3.4 kb in length, suggesting that transcription would be initiating in the region of the genome containing ORF71, which is consistent with our Northern blot analysis with an ORF71 probe (Fig. 4.1E). To determine whether the 5′ initiation site of the 5.5 kb transcript originated within ORF71, we performed 5′ RACE using a primer specific for the 5′ end of ORF71 sequence, near where the predicted start site of the 5.5 kb transcript lies (Fig. 4.2A). From this RACE reaction we obtained a predominant product of 0.3 kb (Fig. 4.2C). The 5′ RACE product was purified and five individual cDNA clones were sequenced. The sequences of these five clones were all identical, and revealed that a transcript indeed initiates in the region of the viral genome containing ORF71 (at nt 119441) and extends toward R15 (Fig. 4.2E). The procedure used for 5′ RACE (RNA-Ligase-Mediated RACE) is such that only RNA species with a 5′ cap will be amplified (96), ruling out the possibility of amplifying fragments of incomplete mRNAs or those lacking a cap structure.

To further confirm the 5′ RACE data, we performed RNase protection analysis on 72 hr/untreated RRV-infected primary rhesus fibroblast RNA. Utilizing a probe overlapping the predicted start site, we obtained some evidence for a protected fragment corresponding to the predicted start site identified by 5′ RACE (data not shown). However, in this same experiment we also obtained a major product corresponding to full

protection with this probe, which suggests that other transcripts initiating upstream of our predicted start site may overlap this region.

Overall, this implies that the 5.5 kb transcript represents one large transcript initiating in ORF71 sequence, and extending through ORF74. Examination of the sequence directly upstream of the predicted start site revealed the absence of a recognizable TATA motif, suggesting that transcriptional initiation of the transcript is through a TATA-independent mechanism. However, the presence of binding sites for several cellular transcription factors was noted (i.e. c-Jun and AP-1), indicating that this region may support efficient transcription of downstream ORFs (Fig. 4.2E).

Defining the relative transcription start site of the smaller 3.0 kb transcript was less straightforward, as our data accumulated thus far suggested two possibilities. First, that the 3.0 kb transcript could be a separate transcript initiating approximately 1.0 kb upstream of R15, or second, that the transcript could be a spliced version of the larger 5.5 kb transcript. Given our previous findings, we had no evidence to suggest the potential presence of any transcripts that initiate directly upstream of R15. However, to examine this possibility, we used a primer antisense to the exact 5′ end of R15 sequence in 5′ RACE (Fig. 4.2A), but were unsuccessful at amplifying any product, even using varying reaction conditions. We also utilized primers that were specific for regions further upstream of R15, specifically the 5′ ends of ORF72 and ORF73 sequence (Fig. 4.2A), but again no RACE products were obtained. When examining this region upstream of R15 we found a high degree of predicted secondary structure, which could account for a lack of products in RACE reactions, although we speculate that lack of products is actually due to the absence of R15 and ORF74 containing transcripts initiating in these regions.

To examine the possibility that the 3.0 kb transcript could be derived from a larger spliced transcript initiating within ORF71 sequence, we performed RT-PCR on 72 hr/untreated RNA using primers that are specific for R15 and ORF71. Specifically, the 5′ primer used (primer B, Fig. 4.3A) was specific for ORF71 sequence located 100 bp downstream from 5′ end of the sequence obtained in 5′ RACE, and the 3′ primer was specific for the 5′ end of R15 sequence (primer A, Fig. 4.3A). From this experiment, we obtained a single 0.7 kb product in reactions containing RT enzyme (Fig. 4.3B), which suggests that the region upstream of R15 does in fact contain a splice site, potentially accounting for the smaller 3.0 kb transcript observed by Northern blot analysis. Importantly, using a primer specific for the exact 3′ end of ORF71 (230 bp upstream of the predicted start site of R15-ORF74 transcripts; primer C, Fig. 4.3A) in RT-PCR with the same R15 primer as above (primer A, Fig 4.3A), we did not obtain any products (Fig. 4.3B), indicating that any potential transcripts initiating upstream of nt 119441 are not connected to R15 sequence.

Cloning and sequencing of the 0.7 kb RT-PCR product indicated that a splice occurs between nt 119809 and nt 122533, removing approximately 2.7 kb of sequence, including the sequence for ORF73 and the majority of ORF72 (Fig. 4.3C). To confirm that this predicted splice event is occurring, we generated an oligo probe for Northern analysis specific for ORF73 sequence (antisense to R15-ORF74 message). If the smaller 3.0 kb band does represent a spliced message, it should not be detected by Northern blot when using this ORF73 oligo probe, while the larger 5.5 kb band would still remain detectable. Indeed, we detected only the 5.5 kb transcript with the ORF73 oligo probe using 72 hr/untreated RNA (Fig. 4.3D). This result agrees with our RT-PCR data, and

suggests that the 3.0 kb band seen in Northern blots for R15 and ORF74 represents a spliced version of a larger transcript, and may be derived from the 5.5 kb message also detected in these Northerns. We were unsuccessful in amplifying both the region upstream of R15 in its unspliced form, and the entire 5.5 kb transcript (from ORF71 through ORF74) by RT-PCR, which we speculate could be due to the presence of extensive secondary structure in the transcript that inhibit the RT reaction, or general limits of the RT reaction.

RT-PCR analysis of R15-ORF74 bi-cistronic message. Northern blot analyses suggest that R15 and ORF74 are co-transcribed on the same message. Therefore, we sought to confirm this by RT-PCR analysis. This approach would also allow us to determine if this transcript was spliced in the region encoding both ORFs, as is the case of HHV-8 K14 and ORF74, in which 149 bp between the two ORFs is spliced from the K14-ORF74 containing transcript (35, 85, 120, 161). We designed primers to bind at the exact 5′ end of R15 sequence and the exact 3′ end of ORF74 sequence to amplify the corresponding message from RNA obtained from RRV-infected primary rhesus fibroblasts. The expected size for this product would be 2.1 kb for an unspliced message containing both ORFs, while anything smaller than this size would represent potential spliced message(s). Using 72 hr/untreated RNA in this analysis, we amplified two predominant products. Specifically, we detected a 2.1 kb product likely representing the entire unspliced region, and a more abundant 1.7 kb product, indicating that splicing of the 2.1 kb message is taking place (Fig. 4.4A). No products were detected in control reactions containing no RT enzyme. The finding that the 1.7 kb product is in greater abundance compared to the 2.1

kb product suggests that this spliced message may be the predominant form of the transcript found in RRV-infected cells undergoing lytic replication.

To identify the sequence of the spliced message, and confirm the identity of the unspliced message, we isolated both products obtained by RT-PCR and sequenced five cDNA clones of each. The sequences of all 2.1 kb cDNA clones were identical, and confirmed the identity of the full-length, and therefore unspliced, R15 and ORF74 region of the bi-cistronic transcripts. Sequences from the cDNA clones corresponding to the more abundant 1.7 kb species were all identical, and demonstrated the presence of a splice donor at nt 123555 (within R15 sequence) and a splice acceptor at nt 123916 (8 nt upstream of the ORF74 ATG) (Fig. 4.4C). The donor sequence motif (G′*GTGGGT*) is identical to the donor sequence identified in the splice of K14 and ORF74 in HHV-8, while the acceptor motif (*TGTCAG*′A) is more divergent from the motif found in HHV-8 (*TTGTAG*′G) (35, 85, 120, 161). Unlike what has been reported for HHV-8, in which neither K14 or ORF74 coding sequence is altered, the splice event in the RRV transcript removes 72 bp from the 3′ end of R15 coding sequence, making the stop codon for this shortened form of R15 a TGA located 8 bp downstream of the ATG for ORF74 (Fig. 4.4C). This splice would therefore affect the predicted vCD200 expression pattern of the transcript, creating an altered form of vCD200 with 24 aa deleted from the C terminus (amino acids 230-254), and a series of 6 new amino acids in its place (TTTWTP). Importantly, the 24 aa region deleted from vCD200 contains the predicted transmembrane domain of this protein (amino acids 229-250), suggesting there may be a soluble form of vCD200 expressed during lytic replication (Fig. 4.4D).

To confirm that the spliced R15-ORF74 region is directly linked to upstream ORF71sequence, as suggested by Northern analysis, we performed RT-PCR using a 5′ primer specific for a region of ORF71 predicted to be contained in R15-ORF74 transcripts with a 3′ primer specific for the exact 5′ end of ORF74 (Fig. 4.4E). In this reaction, we obtained an approximately 1.4 kb product, corresponding in size to that predicted for a dually-spliced transcript initiating in ORF71 and extending to ORF74 (data not shown). Sequencing of this cDNA product revealed that it contained both splices identified in our previous RT-PCR experiments, and demonstrates that both splicing events are present in the same transcript in infected cells (the sequence of this cDNA has been submitted to GenBank). This also indicates that the spliced bi-cistronic R15-ORF74 sequence is directly linked to ORF71 sequence, further supporting our earlier results that suggested R15-ORF74 containing transcripts initiate in ORF71 sequence.

Examination of expression patterns of R15 and ORF74 from spliced and unspliced bi-cistronic messages. First, we wanted to test the ability of cellular machinery to splice transcripts generated from the 2.1 kb R15-ORF74 cDNA. CHO cells were transfected with vector containing the 2.1 kb R15-ORF74 cDNA or empty vector, and RNA was isolated at 48 hrs post-transfection. RT-PCR was then performed with a 5′ R15-specific primer and a 3′ ORF74-specific primer. Interestingly, both species of R15-ORF74 bi-cistronic transcripts (2.1 kb and 1.7 kb) were present within these cells (data not shown). CHO cells transfected with empty vector did not test positive for either transcript. Therefore, in cells transfected with the full-length/unspliced 2.1 kb R15-ORF74 cDNA

expressing vector, both spliced and unspliced versions of the R15-ORF74 message are present.

After discovering that R15 and ORF74 are encoded on the same bi-cistronic late-lytic messages, and that these transcripts contain a splice site between the two ORFs, we next wanted to examine the protein expression patterns from transcripts that have been spliced or remain unspliced in this region. To facilitate expression analyses without antibodies to these viral proteins, we performed PCR using a sequenced R15-ORF74 cDNA clone of each transcript variant as a template (spliced/1.7 kb or unspliced/2.1 kb), to introduce an internal FLAG-epitope tag in frame with vCD200, and to introduce an HA-epitope tag to the C-terminus of vGPCR. To avoid disruption of the predicted N-terminal signal sequence of RRV vCD200 (124), a FLAG tag was introduced upstream of the identified splice site at nt 632 of R15. The internal FLAG-tagged R15 constructs were named 1.7 kb R15-FLAG and 2.1 kb R15-FLAG, while the C-terminal HA tagged ORF74 constructs were named 1.7 kb ORF74-HA and 2.1 kb ORF74-HA.

To initially assess the expression from these constructs, CHO cells were transiently transfected with empty vector, 1.7 kb R15-FLAG, 1.7 kb ORF74-HA, 2.1kb R15-FLAG, or 2.1 kb ORF74-HA. Approximately 48 hr post-transfection, these cells were stained with antibodies specific for the FLAG or HA epitopes and examined by immunofluorescent confocal microscopy. Cells transfected with the full-length 2.1 kb R15-FLAG showed specific staining, with the cellular distribution of vCD200-FLAG appearing mostly cytosolic, with some areas of apparent membrane staining (Fig. 4.5A). A similar staining pattern was observed with cells transfected with 2.1 kb ORF74-HA (Fig. 4.5B), demonstrating that vCD200 and vGPCR proteins are both made from this

full-length species of transcript. To our knowledge, this demonstrates for the first time that a viral GPCR can be expressed as the second ORF on a bi-cistronic transcript.

When examining staining of cells expressing the spliced 1.7 kb R15-FLAG transcript, we found that the vCD200 staining was generally cytosolic, and importantly, absent from the plasma membrane (Fig. 4.5C). The pattern of vCD200 expression from the 1.7 kb R15-FLAG vector suggests that the truncated version of vCD200 expressed from the spliced transcript is no longer localized to the plasma membrane, the predicted outcome of deleting the RNA sequence encoding the putative transmembrane region of the protein. vGPCR staining is also detected in the cytoplasm and on the surface of cells transfected with the 1.7 kb R15-ORF74 cDNA (Fig. 4.5D). Therefore, splicing of the 2.1 kb R15-ORF74 transcript does not abrogate vGPCR expression.

Next, we wanted to determine if vCD200 was indeed capable of being secreted from cells expressing the spliced 1.7 kb or 2.1 kb cDNAs. Western blot analysis of lysates from transiently transfected CHO cells demonstrated that a band of approximately 40 kDa for vCD200-FLAG is detected in cells expressing either 1.7 kb or 2.1 kb R15-FLAG, but not in cells transfected with vector alone (Fig. 4.6A). The predicted size of full-length vCD200-FLAG is 28 kDa, however, the protein has several potential glycosylation sites, which likely accounts for the discrepancy in the size and the diffuse property of the protein detected by Western blot. Also, since the splicing event that removes the transmembrane region of vCD200 deletes a total of 18 aa residues of protein sequence, both the full-length and spliced species of vCD200 are likely represented by the same approximately 40 kDa band in cells transfected with 2.1 kb R15-FLAG construct. To determine whether a soluble version of vCD200 was being secreted from

cells expressing spliced 1.7 kb R15-ORF74 cDNA, supernatants from transiently transfected CHO cells were collected and concentrated for Western blot analysis. As predicted, supernatants from cells transfected with vectors expressing either 1.7 kb or 2.1 kb R15-FLAG contained significant amounts of vCD200 protein, indicating that the 1.7 kb cDNA is indeed capable of producing soluble/secreted vCD200 protein (Fig. 4.6B).

We also sought to confirm the expression of full-length vGPCR from both the 1.7 kb and 2.1 kb cDNAs. Thus, vGPCR expression from either the 1.7 kb or 2.1 kb ORF74-HA constructs was examined by immunoprecipitation of HA tagged protein from transiently transfected CHO cells, followed by Western blot analysis. Detection of a band for the predicted size of the RRV vGPCR in cells transfected with either 1.7 kb or 2.1 kb ORF74-HA constructs demonstrates that full-length protein is capable of being produced from either spliced or unspliced cDNAs (Fig. 4.6C), and suggests that translation of ORF74 still occurs even after splicing has taken place in the region upstream of ORF74 sequence.

DISCUSSION

HHV-8 is the accepted etiological agent of human malignancies including KS, MCD, PEL, and some NHLs. Prior to highly active antiretroviral therapy, KS lesions were the most common disease manifestation observed in AIDS patients, while MCD and PEL are more rare forms of lymphoproliferative disease caused by HHV-8. To understand the pathogenesis of this virus, we utilize rhesus macaque rhadinovirus (RRV), the rhesus macaque homologue of HHV-8, to infect SIV-infected monkeys as a model for HIV/HHV-8 infection. Understanding differences and similarities between these two viruses is critical in continued development of the RRV/rhesus macaque animal model, and for development of potential treatments for HHV-8 associated diseases.

In this study, we have examined the transcription from two viral ORFs encoded by RRV, R15 and ORF74, whose homologues in HHV-8 have been postulated to be involved in the development of viral-mediated disease. In studies of the transcription of these ORFs in HHV-8, it was determined that both ORFs are encoded on bi-cistronic messages, and that these transcripts are expressed as early-lytic genes. Although both proteins encoded by these HHV-8 ORFs are believed to be expressed from this bi-cistronic message, the actual protein expression pattern from the HHV-8 transcripts has never been examined. Comparing transcriptional patterns of ORFs shared between RRV and HHV-8 can lend insight into whether or not the products of these ORFs indeed play a similar role during viral infection and disease development.

Northern blot and RT-PCR analyses revealed that RRV R15 and ORF74 are transcribed as bi-cistronic messages, similar to HHV-8 K14/ORF74. However, unlike the early-lytic expression pattern of HHV-8 K14 and ORF74, RRV R15 and ORF74 are

transcribed as late-lytic genes. Although true differences could exist in the patterns of transcription of these genes between HHV-8 and RRV, we believe the discrepancies seen in relation to the assignment of classes of lytic transcripts between these viruses are more likely due to differences in the systems used to analyze lytic transcription by these viruses. Specifically, all of the studies done to date analyzing K14 and ORF74 transcription in HHV-8 have utilized latently-infected B cells induced to undergo lytic replication using phorbol esters, such as 12-*O*-tetradecanoylphorbol-13-actetate (TPA) or *n*-butyrate (35, 85, 120, 161). In these cultures, a small percentage of latently HHV-8-infected cells spontaneously undergo lytic reactivation (~1-2%), even in the absence of drug induction. Therefore, lytic transcripts may already be present to some extent in these cultures even before induction, which could complicate the definitive assignment of a transcript to a particular class of lytic transcript. On the other hand, RRV infection in our *in vitro* system is strictly lytic, allowing for tight regulation of viral gene expression after infection, and eliminating the background of latent gene transcription. Taken together, the RRV system is more accurate when making the assignment of viral genes to a particular lytic class.

From Northern analysis for RRV R15 and ORF74, we observed two potential sizes of transcripts, both larger than the predicted sizes we expected for a bi-cistronic message encoding these two ORFs. From the identification of the 5′ and 3′ ends of these transcripts by RACE analysis, we learned that transcripts extending through ORF74 do not extend into downstream ORFs, and that the 5′ end appears to initiate within ORF71 sequence. Analysis of the sequence upstream of the transcriptional start site predicted by 5′ RACE did not reveal any traditional TATA-like motifs that might be involved in

transcriptional initiation of the R15-ORF74 message, although this region does contain binding sequences for several known transcription factors. This suggests that transcription of the R15-ORF74 messages are likely TATA-independent, a finding that is commonly seen with viral late promoters, including HHV-8 (33, 178). An attempt to confirm the 5′ RACE data by RNAse protection analysis was not definitive, and suggests that in addition to the predicted start site identified by RACE, other transcripts may indeed overlap this region and extend through ORF71 sequence. This is especially likely since the RRV lytic origin of DNA replication is located directly upstream of ORF71 (128), and is thought to be a transcriptionally active region, which contains multiple predicted ORFs based on computer analysis. Therefore, attempting to identify transcriptional start sites initiating in ORF71 using this technique may be complicated by overlapping transcripts that emanate upstream of this region of the genome. In the case of the 3′ end of the R15-ORF74 transcript, it was found that the poly(A) site utilized is identical to that identified in analysis of HHV-8 ORF74 transcription, terminating directly after ORF74.

Examination of the region upstream of R15 revealed that 2.7 kb of sequence is spliced from a larger transcript containing this ORF, likely represented by the 5.5 kb transcript detected by Northern analysis. This splicing results in the production of a form of the R15-ORF74 message that correlates well with the 3.0 kb band observed by Northern analysis. Specifically, the entire ORF73 coding sequence, as well as a majority of ORF72 coding sequence, is removed by splicing. The size of such a large un-translated region (UTR) in the larger R15-ORF74 containing transcript was unexpected, as was the presence of a splice in this region to produce a smaller version of this transcript. This

pattern of transcription is different than what has been seen with HHV-8 K14-ORF74, which has been suggested to only be produced as a 2.8-3.2 kb transcript that initiates directly upstream of K14 sequence. However, it is of interest that in several studies examining K14-ORF74 transcription, larger size transcripts have also been detected, but have essentially been unexamined. Kirshner, *et al.* detected a ~9 kb band by Northern blot of RNA from induced cultures of BCBL-1 cells using an ORF74 specific probe, and speculate that it may be due to read-through of transcripts through the ORF74 poly(A) site (85). In addition, Talbot, *et al.* detected a ~9.5 kb band by Northern blot using RNA from induced cultures of BCP-1 cells with a vCD200 specific probe, which they did not further identify (161). Interestingly, they also found that this 9.5 kb band was detected using a probe for ORF71, suggesting that these two ORFs could be expressed together on a single transcript spanning the entire ORF71-ORF74 region. If true, this would be very similar to the pattern of transcription we have found for RRV R15 and ORF74, in which transcripts encoding these ORFs initiate in ORF71 sequence. Further studies would be required to determine the exact identity of the larger K14/ORF74 messages, and to determine whether HHV-8 transcription in this region may actually mimic that found in RRV.

The purpose of such a large UTR in the transcripts containing R15 and ORF74 during lytic RRV infection is unclear. Although both the 5.5 kb and spliced 3.0 kb transcripts are present in infected cells in relatively equal abundance, it is possible that the spliced message is preferentially used for translation of vCD200 and vGPCR compared to the 5.5 kb message, although this is currently unknown. The region upstream of R15 was examined for the presence of unidentified ORFs utilizing computer

software, however, none were predicted to exist in this region (data not shown). Therefore, it appears that the 5.5.kb transcript may be produced to yield splice variants that encode vCD200 and vGPCR, and may simply represent unprocessed template awaiting splicing.

Further examination of the transcriptional splicing pattern within the R15 and ORF74 coding sequence by RT-PCR revealed that a second splicing event removes 360 bp of sequence in the R15-ORF74 region. Therefore, from the initial 5.5 kb transcript that is produced, there appears to be two major splicing events that take place, such that four different forms of R15-ORF74 containing message could exist at one time. Due to the relatively small size of the splice event in the R15-ORF74 region, distinguishing between the different forms of spliced message is not possible by Northern blot analysis, but may account for the diffuse nature of the bands we detected in our studies. However, RT-PCR analysis using primers for ORF71 sequence predicted to be contained in R15-ORF74 transcripts, along with a primer corresponding to ORF74 sequence, resulted in the detection of a dually-spliced product containing both splice events, while no single spliced products were identified. This may suggest that the predominant form of R15-ORF74 transcripts within infected cells contains both splices.

Upon examination of the sequence removed by the splicing event in the R15-ORF74 region, we found that the splice alters the coding capabilities of R15, deleting the coding sequence for the putative transmembrane domain of vCD200. Thus, R15-ORF74 transcripts containing this splice have the potential to encode for a soluble form of vCD200, and our immunofluorescence and Western blot data support this hypothesis. This is a novel finding for any CD200 or viral CD200 homologue. Western blot analysis

and immunofluorescence data also demonstrated that full-length vGPCR is translated from spliced and unspliced R15-ORF74 transcript species. This suggests that the splice removed from the region directly upstream of ORF74 does not alter the expression pattern of the vGPCR. Translation of RRV ORF74 from these bi-cistronic transcripts could be occurring through an internal ribosomal entry site (IRES)-mediated mechanism, or by other mechanisms such as ribosomal scanning, or translational re-initiation, ideas which have also been suggested to be involved in initiation of HHV-8 ORF74 translation (85, 161). Importantly, the finding that RRV vGPCR is in fact expressed from different spliced forms of bi-cistronic transcripts is intriguing, and to our knowledge demonstrates for the first time that a viral GPCR protein is capable of being expressed as the 3′ ORF on a bi-cistronic message. The exact importance of the bi-cistronic expression pattern of the vCD200 and vGPCR proteins in RRV and HHV-8 is yet to be determined. However, the tightly linked expression of these proteins in both viruses would suggest an essential function, either directly or indirectly, or perhaps some interplay between the activities that each protein regulates that may be critical to some aspect of the viral life cycle.

The presence of soluble RRV vCD200 during RRV infection could have major implications in altering the function of the immune system of an infected host. The RRV vCD200 protein is similar in sequence to human CD200 (huCD200), and to HHV-8 vCD200, but its function has yet to be understood. huCD200 has been demonstrated to play important roles in controlling the inflammatory response induced by cells of myeloid lineage. Specifically, engagement of the CD200 receptor on cells of myeloid-lineage induces these cells to produce an anti-inflammatory (TH2) response (66, 77, 174), while vCD200 encoded by HHV-8 K14 elicits a pro-inflammatory (TH1) response from these

cells, a function exactly opposite of huCD200 (36). Whether the RRV vCD200 protein behaves as an anti-inflammatory or pro-inflammatory protein, the implications that the presence of a soluble CD200 homologue may have during viral infection are substantial, especially in its potential contributions to virus-induced disease. Studies investigating the function of RRV vCD200 are currently underway.

Figure 4.1 Northern blot analysis of RRV R15 and ORF74 transcripts. (A) The region in the RRV genome containing ORFs R15 (vCD200) and ORF74 (vGPCR) is shown. The region is located at the extreme right end of the RRV genome. Viral nucleotide numbers are noted and ORFs are drawn to scale. (B-D) RNA from RRV-infected rhesus fibroblasts treated with cycloheximide (CHX), phosphonoacetic acid (PAA), or untreated cultures were collected at 24 hrs, 48 hrs, and 72 hrs post-infection, respectively. Approximately 10 μg of total RNA was run on denaturing agarose gels, and transferred to nitrocellulose for hybridization to dsDNA probe for ORF74 (B), dsDNA probe for R15 (C), an oligonucleotide probe for R15 (D), and dsDNA probe for ORF71 (E). A rhesus GAPDH probe was utilized to demonstrate equal amounts of RNA for each lane in B and C.

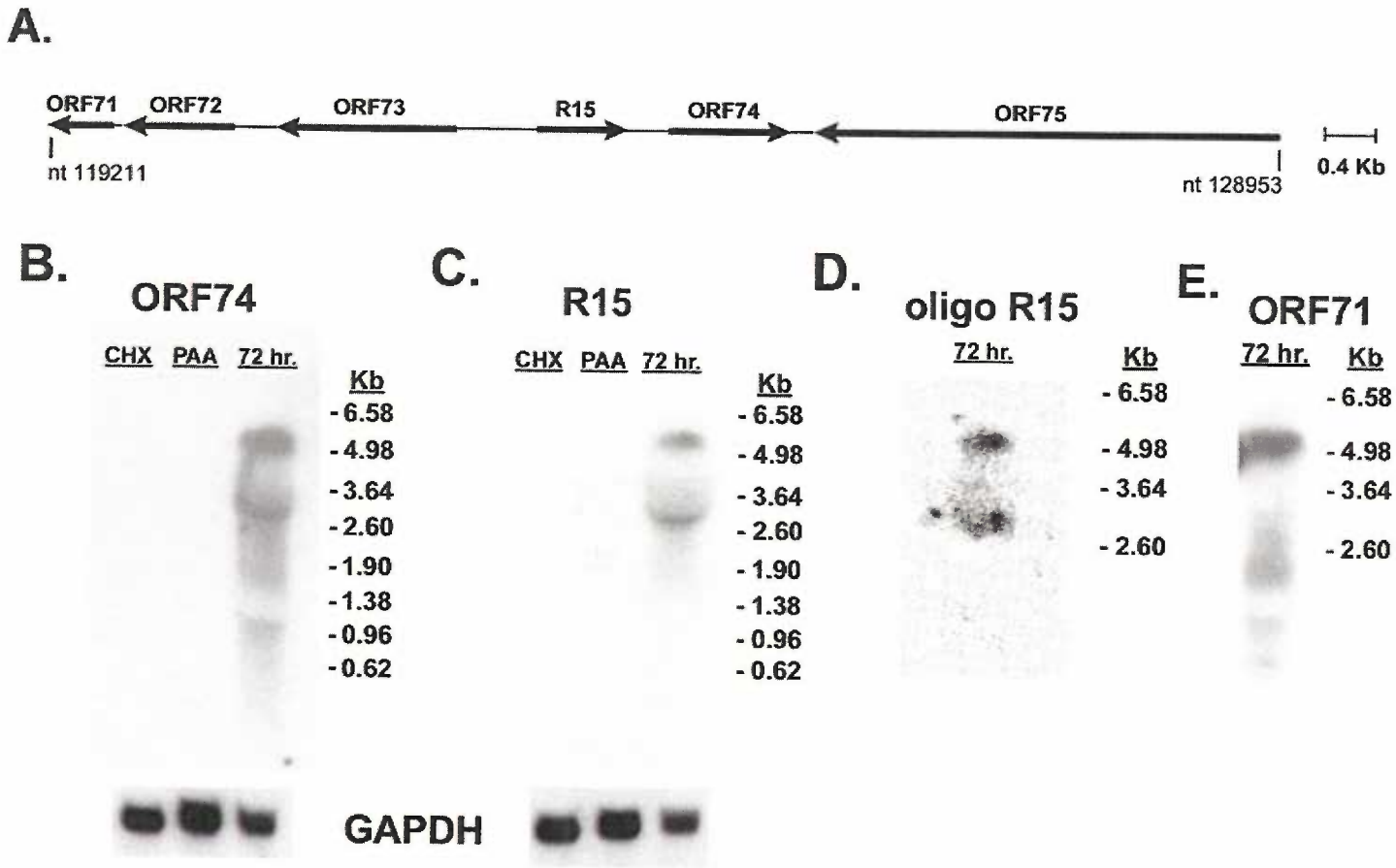
A.
ORF71
ORF72
ORF73
R15
ORF74
ORF75
nt 119211
nt 128953
0.4 Kb
B.
ORF74
CHX PAA 72 hr.
Kb
- 6.58
- 4.98
- 3.64
- 2.60
- 1.90
- 1.38
- 0.96
- 0.62
GAPDH
C.
R15
CHX PAA 72 hr.
Kb
- 6.58
- 4.98
- 3.64
- 2.60
- 1.90
- 1.38
- 0.96
- 0.62
D.
oligo R15
72 hr.
Kb
- 6.58
- 4.98
- 3.64
- 2.60
E.
ORF71
72 hr.
Kb
- 6.58
- 4.98
- 3.64
- 2.60

Figure 4.2 5′ and 3′ RACE analysis of RRV R15 and ORF74 transcripts. (A) Diagram of region analyzed; the arrows indicate oligonucleotide primers used for RACE analysis, and those denoted with an asterisk (*) gave specific products. Agarose gel of products obtained from a 3′ RACE reaction with ORF74 primer (B), and a 5′ RACE reaction with ORF71 primer (C). (D) A portion of the consensus 3′ RACE product DNA sequence; the 3′ end of ORF74 sequence along with the putative poly(A) site (ATTAAA) and poly(A) tail are noted. (E) ORF71 DNA sequence with 5′ RACE sequence in bold and italicized (the transcription start site is noted by +1). Predicted binding sites for transcription factors, c-Jun and AP-1 are also noted along with a CAAT box. No TATA box was identified.

A.

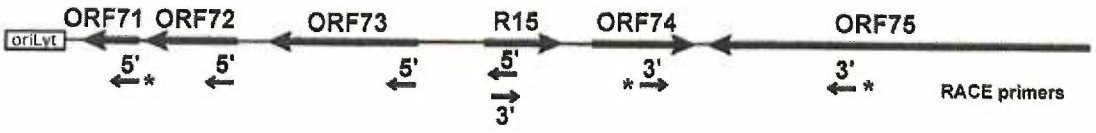

B.

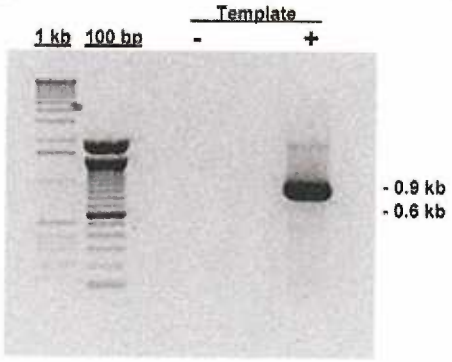

C.

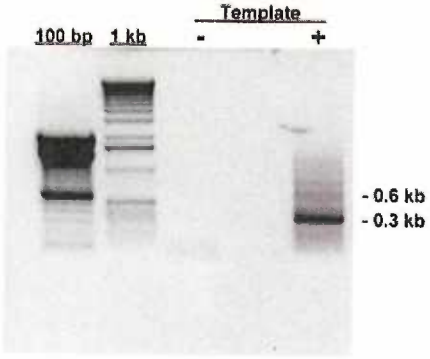

D.

nt 124927 GTTTTTCCACTTCAGGTAGTTTATGAGACACTCA
ORF74
nt 124961 CGCGACACTTGGTTGGATTGTTTGTGTACATTT

nt 124994 ATTTTCATTTTGTGTACATTTATTTTC**ATTAAA**G

nt 125028 CGATCTGACCTGCAGACCTTAAAAAAAAAAAA
polyA

E.

nt 119295 TGAGGGGCTGACCAGGGCCGCCTTTTCCATTT
c-Jun
nt 119327 GCGAGAGCCACCGAAAAAAGGTGGGTGACTG
c-Jun
nt 119358 GTTGCGCCTGCGACCAAGCTGGTCGCCCGTTA

nt 119390 GAAAAACTAAATTTTTCACGTCCCTTTCTGAG
AP-1
+1
nt 119422 AGCTGGCGGTCAATGGAGA***GCATCAGGTGTTT***
CAAT Box
nt 119454 ***GTATGGACTAAAGTAACTGGGGCTGGACCGGA***

Figure 4.3 Analysis of 5.5 kb R15-ORF74 transcript for splicing upstream of R15. (A) Depiction of RT-PCR primers, ORF73 oligonucleotide probe used and the predicted splicing of the 5.5 kb message. (B) Agarose gels of RT-PCR reaction products obtained using 72 hr/untreated RNA with noted primers. A single product was obtained in reactions using primers A and B (A/B rxn), while no product was obtained when using a primer that binds outside of the predicted transcriptional start site in place of primer B (A/C rxn). Reaction A/B without RT (A/B Rxn –RT) produced no products, and the integrity of the RNA in the A/C reactions was confirmed using primers for GAPDH. (C) Sequence of the cDNA product from reaction A/B, noting the region spliced from the 5.5 kb message. (D) Northern blot analysis of 72 hr/untreated RNA using ORF73 oligonucleotide probe.

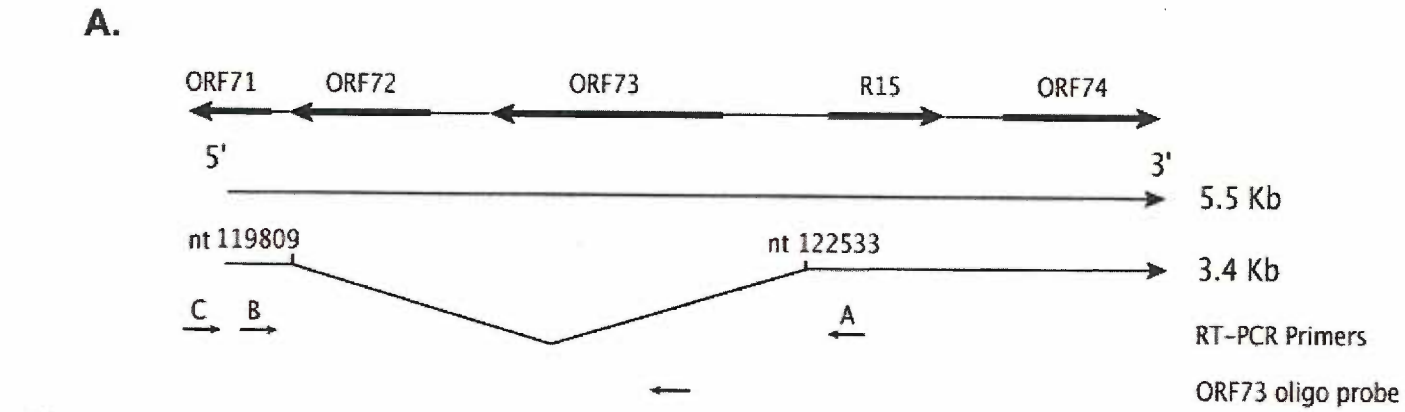

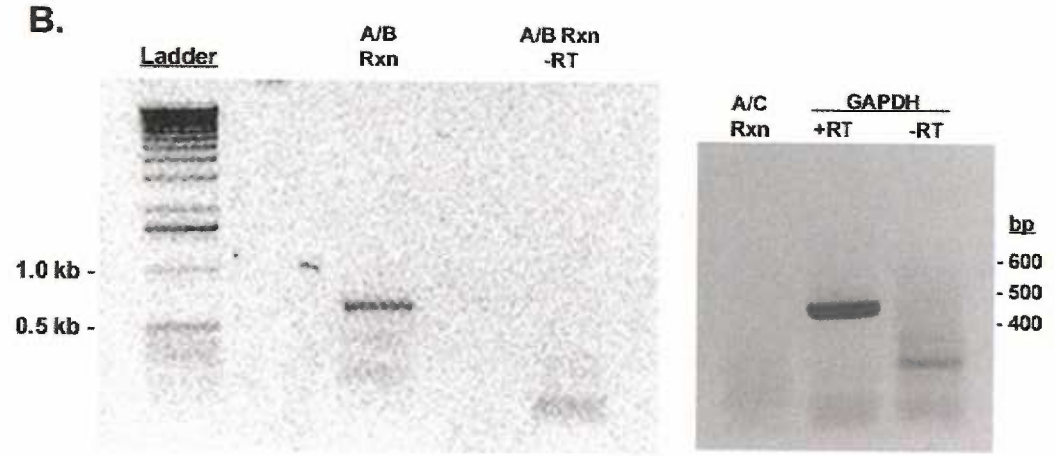

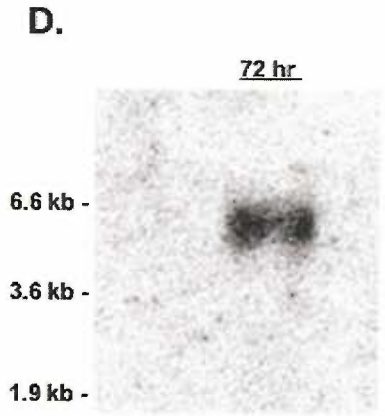

C.

AGCGTTTGATAAATCACGACGAACCGCGG - - - - - - - - - - - - - - - - - AAAGTCTGTTCCGCCGCGCAGCGCGCGGCC

nt 119809 nt 122533

Figure 4.4 Analysis of splicing pattern within the bi-cistronic R15-ORF74 transcript. (A) Agarose gel of RT-PCR reaction products obtained using 72 hr/untreated RNA with 5′ R15 and 3′ ORF74 primers. Two bands are detected, one unspliced (2.1 kb), and the other representing a spliced transcript (1.7 kb). (B) Depiction of the R15-ORF74 region, and the predicted splicing pattern based on RT-PCR. (C) DNA sequence alignment of portions of unspliced (2.1 kb) and spliced (1.7 kb) RT-PCR products. Dashes represent region spliced from 1.7 kb message, stop codons for R15 are in gray and the start codons for ORF74 are in black. Note that the stop codon for the spliced R15 sequence is within ORF74 sequence, but in a different reading frame. (D) Diagram of splicing of the bi-cistronic R15-ORF74 transcript. The unspliced transcript loses 360 bp of sequence during splicing, resulting in removal of the coding sequence for the predicted vCD200 transmembrane domain, and generating a transcript potentially encoding a soluble form of vCD200. (E) Diagram of the dually-spliced 3.1 kb R15-ORF74 transcript produced from a larger precursor, and the location of RT-PCR primers used to amplify cDNA containing both splice events. RT-PCR using the indicated primers demonstrates that both splicing events are found in the same message, and that ORF74 sequence is linked to ORF71 sequence in these transcripts.

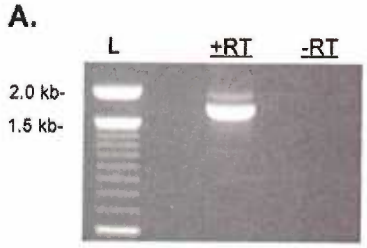

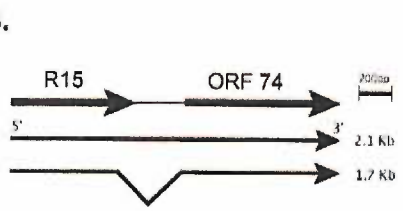

C.

```
2.1Kb RT-PCR  601 TGCCTGGTCACTCATATAGGCGGTTTGGCCGCGGCGGCGGCCCCTGGACCCCGTGTTTTCGGATCCCCTGGAAGGGACGAGCCACTACGTGGTGGGTGTGG 700
1.7Kb RT-PCR  601 TGCCTGGTCACTCATATAGGCGGTTTGGCCGCGGCGGCGGCCCCTGGACCCCGTGTTTTCGGATCCCCTGGAAGGGACGAGCCACTACGTG---------- 680

2.1Kb RT-PCR  701 TGGCAGCGGCCGCCGTTTTAGGCATTTTTTTAACGGGTGTTTTTTTGTATAGGTCTATGTGAGCGCGCGTGTCCCCCGTGTCTAGTGTTTTGTTCCCCAG 800
1.7Kb RT-PCR  681 ---------- 680

2.1Kb RT-PCR  801 TGAGTGTCTCCATGACAAATACAAATTTGAGGCTGGCTTTTTAGGGTGGTTCTTGTGCGACGCTTCCTGTGTAACTGCATACACCGGGGTGTCGCCAGGG 900
1.7Kb RT-PCR  681 ---------- 680

2.1Kb RT-PCR  901 AAACCGCGTCTCCCCTTTATGTCGCTCGCCCTCCAGAGCGAAAGTGAGAATGGTTCCTGGGGCGTTTTGGCGTTGAGAGAGTCGGGCGATGTTGCCGT 1000
1.7Kb RT-PCR  681 ---------- 680

2.1Kb RT-PCR  1001 AGCGGCGTCTGCAAAGGCTCACCCGCTTCTGTTTTTTTCTTTTGTCAGACAACAACATGGACGCCTTGAACAATAACCTTAACCTGCTGATGGATTTT 1100
1.7Kb RT-PCR  681 ----------ACAACAACATGGACGCCTTGAACAATAACCTTAACCTGCTGATGGATTTT 740

2.1Kb RT-PCR  1101 CTGTCTAACTATTCGAATAGCTACAGTAGTTATGACGACAATATGTCTTACACCTTAGACACGGAATCCACGCTGTGTCGGCTGACGGTGGTTTTCCCAC 1200
1.7Kb RT-PCR  741 CTGTCTAACTATTCGAATAGCTACAGTAGTTATGACGACAATATGTCTTACACCTTAGACACGGAATCCACGCTGTGTCGGCTGACGGTGGTTTTCCCAC 840
```

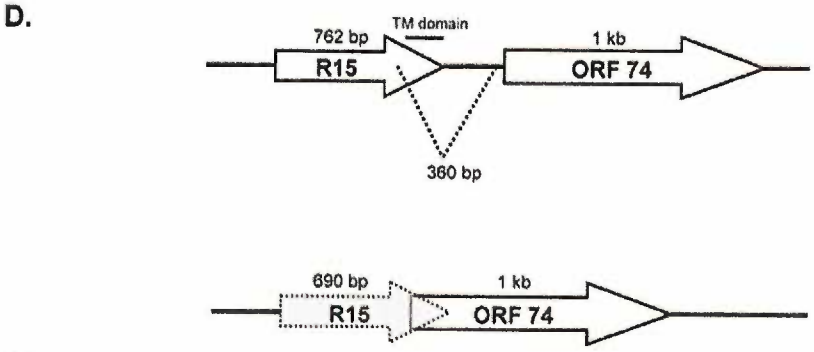

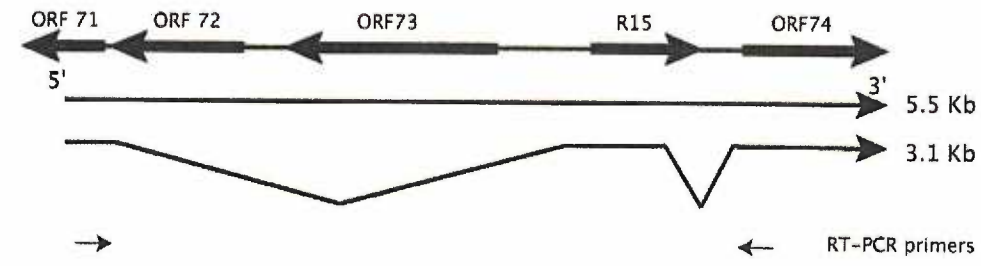

Figure 4.5 Immunofluorescent confocal microscopy of CHO cells transiently expressing epitope-tagged 1.7 kb or 2.1 kb bi-cistronic R15-ORF74 cDNAs. vCD200 contains an internal FLAG epitope tag , while vGPCR contains a C-terminal HA epitope tag. vCD200 expressed from the 2.1 kb cDNA (A) is detected throughout the cytoplasm and at the cell surface, while vCD200 expressed from the 1.7 kb cDNA (C) only displays a cytoplasmic staining pattern. The staining pattern for vGPCR is similar for the 2.1 kb (B) and 1.7 kb (D) versions of cDNA, with protein detected throughout the cytoplasm, as well as at the cell surface. The field shown in panels A, C and D is 512 x 512 microns, panel B is 1024 x 1024 microns.

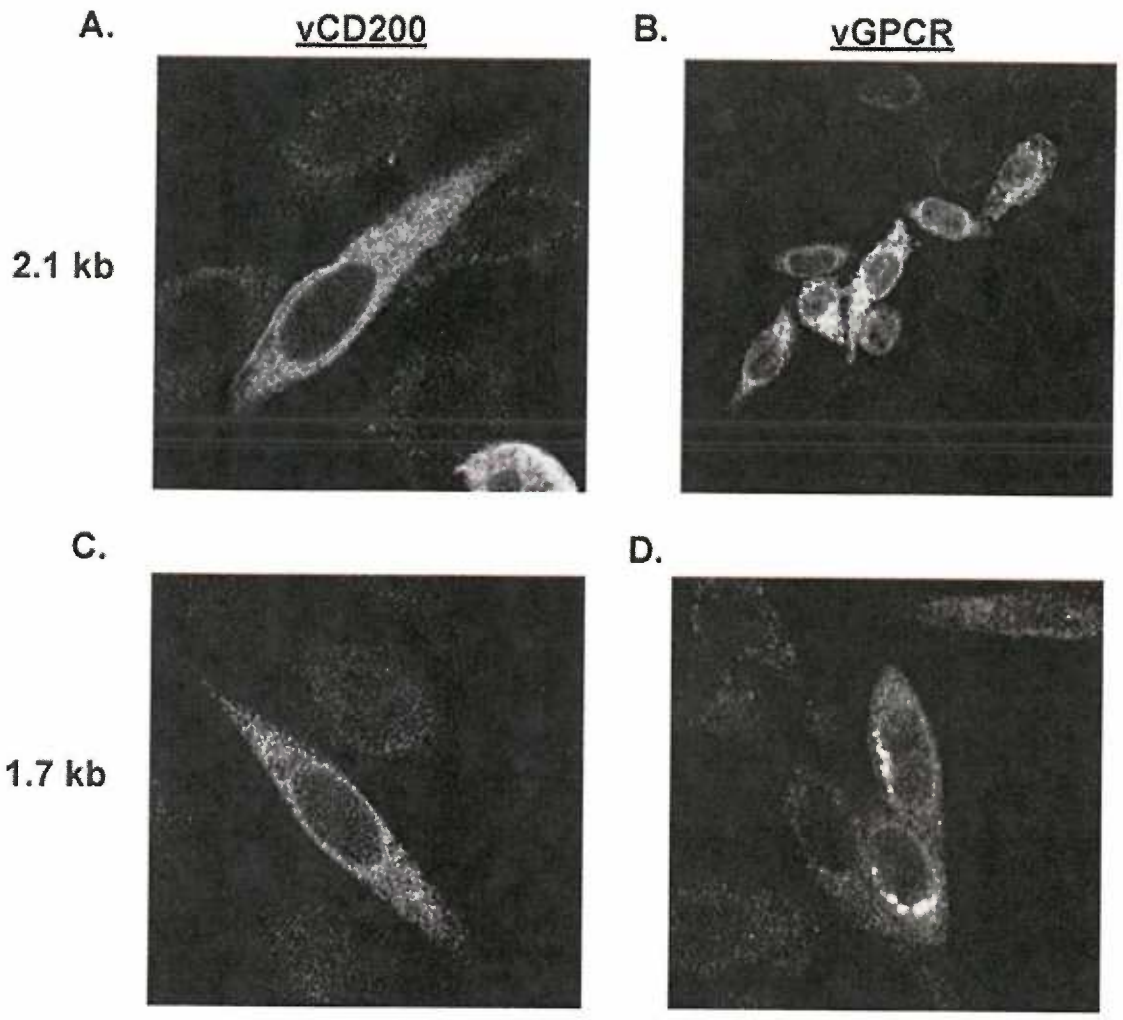
A.
vCD200
B.
vGPCR
2.1 kb
C.
D.
1.7 kb

Figure 4.6 Western blot analysis of vCD200 and vGPCR expression. Total cell lysates (A) or supernatants (B) from CHO cells transfected with empty vector, 1.7 kb R15-FLAG, or 2.1 kb R15-FLAG were analyzed for recombinant vCD200-FLAG expression. (C) anti-HA Western of immunoprecipitated lysates from CHO cells transfected with empty vector, 1.7 kb ORF74-HA, 2.1 kb ORF74-HA, or HA-ORF74 expressing control vector.

A.

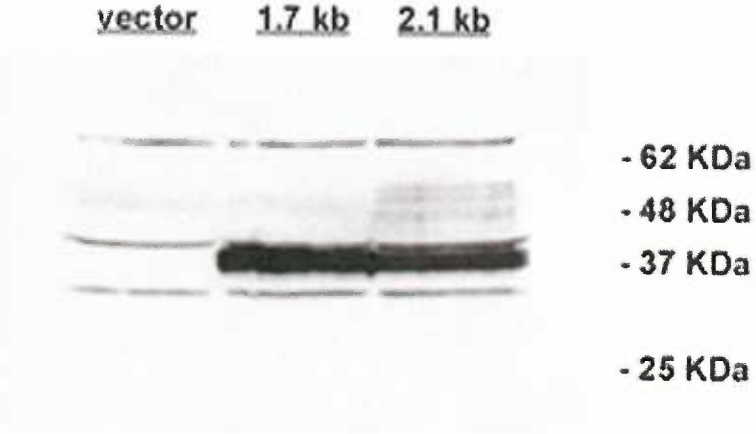
vector
1.7 kb
2.1 kb
- 62 KDa
- 48 KDa
- 37 KDa
- 25 KDa

B.

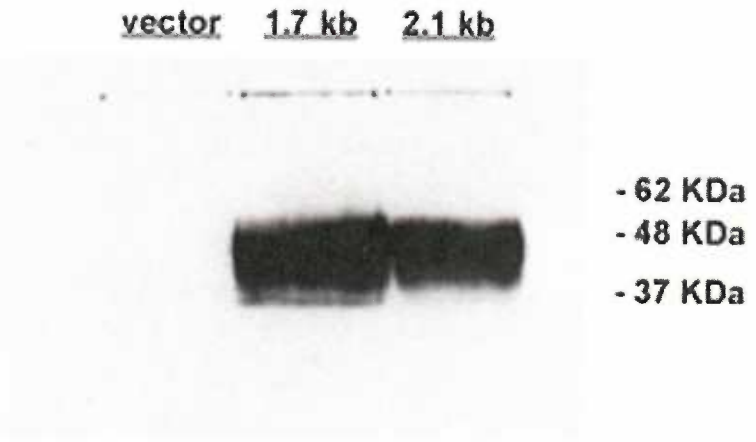
vector
1.7 kb
2.1 kb
- 62 KDa
- 48 KDa
- 37 KDa

C.

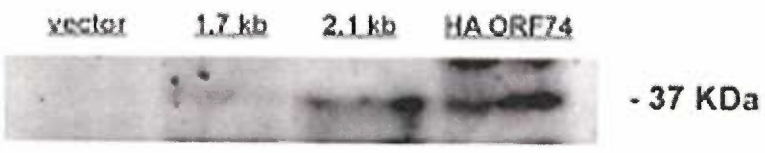
vector
1.7 kb
2.1 kb
HA ORF74
- 37 KDa

Chapter 5

SUMMARY AND CONCLUSIONS

1. RRV ORF74 Encodes a vGPCR Similar to the HHV-8 vGPCR

a. *Preliminary Characterization of the RRV vGPCR*

In chapter 2 of this thesis, the preliminary analysis of the RRV vGPCR is described. This work established that RRV ORF74 encodes a protein with general properties of a GPCR, and that this protein is similar in sequence to the vGPCR of HHV-8. Analysis of the activities of the RRV vGPCR revealed that NIH3T3 cells expressing this viral protein display a transformed phenotype *in vitro* and *in vivo*, indicating that like the HHV-8 vGPCR, the RRV vGPCR is oncogenic, and thus has the potential to contribute to viral-mediated transformation. Expression of the RRV vGPCR in NIH3T3 cells was also found to induce the secretion of vascular endothelial growth factor (VEGF), an angiogenic cytokine known to play a major role in the development of KS (38, 103). Therefore, as has been suggested for the HHV-8 vGPCR, increased VEGF secretion may play a significant role in tumorigenesis induced by expression of the RRV vGPCR. Examination of the signaling properties of the RRV vGPCR revealed that the receptor possesses constitutive signaling abilities similar to its HHV-8 counterpart, and can activate the ERK1/2 pathway in a ligand-independent manner. Also, as is the case for the HHV-8 vGPCR, we found that RRV vGPCR signaling is responsive to the cellular

chemokine GROα, suggesting that chemokine modulation may significantly affect the constitutive signaling abilities of this receptor. Although the signaling properties of the RRV and HHV-8 vGPCRs did appear similar in these studies, an observation was made that the HHV-8 vGPCR might have a slightly higher ability to activate ERK signaling in NIH3T3 cells compared to the RRV vGPCR. These findings could be due to variances in protein expression in these experiments, or actual differences in signaling abilities of the receptors in this cell type. Nevertheless, these studies indicate overall that the RRV encoded vGPCR behaves in a similar manner to the vGPCR of HHV-8.

b. ***Analysis of the RRV and HHV-8 vGPCRs in B cells***

Chapter 3 of this thesis describes the analysis of the properties of both the RRV and HHV-8 vGPCRs in human B cells, and presents novel findings for both receptors in a cell type relevant to RRV and HHV-8 infection and disease development *in vivo*. In this work we demonstrated that the RRV and HHV-8 vGPCRs regulate similar signaling pathways in B cells, and specifically that both can activate ERK1/2 and Akt/GSK-3 in a constitutive manner in this cell type. In addition, both vGPCRs also display responsiveness to the chemokine IP-10 in B cells, which inhibits the constitutive signaling of these receptors. This finding not only expands the repertoire of chemokines known to bind the RRV vGPCR, but also indicates that the RRV and HHV-8 receptors may share a similar chemokine binding pattern overall. We also determined that the G protein coupling patterns of both vGPCRs are similar in B cells, with both utilizing $G\alpha_i$-independent pathways to activate ERK1/2 and Akt/GSK-3 signaling. Further, signaling by the RRV and HHV-8 vGPCRs to these pathways in B cells is partially dependent on

PI3K. Some of these findings differ from those of previously published studies examining the HHV-8 vGPCR in other cell types, and indicate that the cell types in which they are expressed are extremely important in determining the signaling patterns of these vGPCRs. Therefore, in order to accurately delineate all of the pathways affected by both vGPCRs, and the potential involvement of these pathways in disease development, examination of the signaling patterns of these receptors in cell types relevant to natural RRV and HHV-8 infections *in vivo* will be necessary. This idea will be especially important when attempting to identify signaling pathways as possible targets for therapeutics to treat viral-associated diseases induced by vGPCR expression.

Finally, in these studies we also found that both the RRV and HHV-8 vGPCRs have anti-apoptotic effects in B cells, since expression of either vGPCR was able to inhibit the caspase-mediated cleavage of PARP induced by an apoptotic stimulus. Although the exact signaling pathways utilized by the vGPCRs to induce this effect were not specifically identified, this activity is likely at least partially mediated by activation of Akt, since we found that this pathway was constitutively upregulated in cells expressing the receptors, and since caspase-9 is a known target of Akt (27). Overall, these data suggest that the RRV and HHV-8 vGPCRs may promote B cell survival when expressed in infected cells. This finding could have major implications for the roles these receptors play in the viral life cycle, and in the development of B cell malignancies associated with viral infection *in vivo*, as will be discussed later.

2. Unique Properties of RRV ORF74 Transcription

a. *RRV ORF74 is Transcribed as Part of a Spliced Late-Lytic Bi-cistronic Message*

Chapter 4 describes the transcriptional analysis of RRV ORF74 in the context of *de novo* lytic viral infection *in vitro*. In these studies we demonstrated that RRV ORF74 is expressed as a complex dually spliced bi-cistronic transcript with the upstream ORF R15, which encodes the viral homologue of the cellular immuno-regulatory protein CD200 (vCD200). This bi-cistronic pattern of RRV ORF74 expression is similar to what is seen in HHV-8, in which ORF74 is also transcribed with an upstream vCD200-encoding ORF (ORF K14). However, the exact identities of the upstream regions of these transcripts appear to differ significantly between these viruses. Specifically, the RRV R15-ORF74 transcript initiates ~3 kb upstream of R15 in the region of the viral genome containing ORF71, with a post-transcriptional splicing event removing most of the transcript prior to R15 sequence, while the HHV-8 K14-ORF74 transcript has been reported to initiate in a region of the viral genome directly upstream of K14, and does not display splicing events in this region. Importantly, the RRV R15-ORF74 transcript also appears to possess a late-lytic pattern of expression, versus the early-lytic pattern suggested for HHV-8 K14-ORF74 transcript. These differences in expression patterns between these ORFs could represent actual variances in transcription between these viruses, but may also be due to differences in the systems used to analyze transcription. Overall, these data suggest that although similar, significant differences may exist between RRV and HHV-8 in terms of viral gene transcription, and in particular, transcription of ORF74.

b. ***Splicing of RRV R15-ORF74 Transcripts Produces Soluble vCD200***

A major finding from our transcriptional studies of RRV ORF74 was the identification of a splice site in the intergenic region between R15 and ORF74, which removes the portion of the transcript encoding the transmembrane domain of vCD200. Importantly, this splicing event does not alter the sequence encoding ORF74. A similar splicing event occurs in the HHV-8 K14-ORF74 transcript, however, this splice does not remove any sequence for K14, suggesting that splicing has no effects on translation of HHV-8 vCD200 (85, 120). Examination of the protein production pattern from the spliced version of the RRV R15-ORF74 transcript reveals that as anticipated, deletion of the portion of the transcript encoding the vCD200 transmembrane domain results in the production of a soluble form of vCD200. The production of a soluble form of RRV vCD200 is a novel finding for any CD200-like protein, and could have major implications for a role for this protein in RRV pathogenesis. Specifically, the presence of a soluble vCD200 during infection may allow for the regulation of the host immune response, likely producing anti-inflammatory effects similar to cellular CD200. Further work determining the exact functions of RRV vCD200 is currently underway, and should shed light on the properties of this protein and its potential role in disease development.

In addition to the novel findings described, the information obtained on the transcription of RRV ORF74 will be extremely critical to the development of any modified viruses containing altered ORF74 sequence. This idea is based on the fact that some alterations of ORF74 sequence could have significant effects on the expression of vCD200 from R15, given the unique splicing patterns of the bi-cistronic R15-ORF74

transcript. Therefore, this information must be taken into consideration before any attempts are made to disrupt the coding sequence for RRV ORF74 in any manner.

c. *Efficient Translation of the RRV vGPCR from Bi-cistronic Messages*

Although the HHV-8 vGPCR is believed to be expressed from bi-cistronic K14-ORF74 transcripts, the protein expression pattern from these bi-cistronic messages has never been examined. Work presented in chapter 4 demonstrates that in the case of RRV, the vGPCR can be efficiently expressed in full-length as the second ORF on a bi-cistronic message, suggesting that this is also likely true for HHV-8. The mechanisms involved in translation of these ORFs from bi-cistronic transcripts are unknown, but may include the use of an internal ribosomal entry site (IRES), leaky ribosomal scanning, or translational reinitiation. Future work should determine the exact mechanisms involved in translation of the RRV vGPCR.

The potential importance of the co-expression of the RRV vGPCR with the viral CD200 homologue is unknown. Currently, we can only speculate that RRV vCD200 may have anti-inflammatory effects similar to cellular CD200, and that interactions of this protein with the target CD200 receptor on myeloid lineage cells regulates the production of various cytokines involved in an anti-inflammatory response. If true, one possibility may be that some of these cytokines are capable of interacting with and regulating the vGPCR, and therefore that co-expression of these viral proteins is somehow beneficial to the virus. Alternatively, the co-expression of these ORFs may not have a significant correlation, and could just be an example of optimized utilization of viral coding

sequence. Whatever the case may be, this will be an important area for future investigation.

3. Putative Functions of the vGPCR in the Life Cycle and Pathogenesis of RRV

Based on the analyses we have performed, the RRV vGPCR appears to behave in a similar fashion to the vGPCR of HHV-8, and the ORFs encoding both proteins are expressed at a similar time during the viral life cycle, namely during lytic replication. Although some differences in the transcriptional patterns appear to exist, both vGPCRs are likely produced at a time point critical to some aspect of the viral life cycle, and may play similar roles in disease development. Therefore, many of the same ideas put forth concerning the role of the HHV-8 vGPCRs in the viral life cycle and viral pathogenesis (see chapter 1, section 4e for a detailed discussion) also apply to the RRV vGPCR.

Essentially, the RRV vGPCR could be envisioned to be expressed in two potential scenarios in an infected cell, with the first being expression of the vGPCR during the normal lytic replication cycle (Fig. 5.1A). In this case, the vGPCR may be expressed for a sufficient period of time before the ultimate lysis and destruction of an infected cell, and thus could be involved in enhancing viral replication by activating proliferative signaling pathways such as ERK, or by promoting prolonged cell survival by activating anti-apoptotic pathways such as PI3K/Akt. In addition, cytokines and growth factors induced by transient vGPCR expression in these cells could act in a paracrine fashion, having angiogenic and growth promoting effects on neighboring cells, or potentially recruiting more target cells into a region of active viral replication. The possibility also

exists that the vGPCR is involved in the chemotaxis or homing of infected cells in response to chemokines, which could be a mechanism of viral spread mediated by the vGPCR.

The second scenario involves expression of the vGPCR in an infected cell without concurrent viral replication (Fig. 5.1B). This could be due to the aberrant induction of vGPCR expression (e.g. deregulated ORF74 transcription in a latently infected cell), or due to its expression during an abortive lytic replication cycle. In either case, viral replication would not destroy the cell, and the vGPCR could be expressed to sufficient levels to activate various signaling pathways that have effects on growth and survival (ERK, Akt, etc.), ultimately leading to direct transformation of the cell expressing the receptor. This expression pattern of the vGPCR could also induce the secretion of cytokines and growth factors, which then may have paracrine or autocrine effects, promoting angiogenesis, increased cell growth, and cell recruitment. vGPCR expression in these cells could also possibly allow for their chemotaxis and homing in response to chemokines.

Importantly, the development of HHV-8-like diseases in RRV infected macaques, most notably retroperitoneal fibromatosis (RF) and B cell hyperplasia, might be partially explained by expression of the vGPCR in RRV infected cells. Based on our findings that the RRV vGPCR has transforming potential, induces the secretion of the angiogenic cytokine VEGF, and has anti-apoptotic effects in cells that express the receptor, expression of this protein in RRV-infected rhesus macaques likely plays some role in the development of disease. Indeed, previous data from our lab has shown that RRV ORF74 transcripts can be detected in samples of RF tissue from RRV-infected macaques,

suggesting that the RRV vGPCR could potentially be associated with the development of RF, although this remains to be fully investigated. In the case of RRV-associated B cell hyperplasia, data suggests that the virus can establish an infection in B cells *in vivo* (17), and in this thesis, some direct evidence is presented that expression of the RRV vGPCR can have effects on the growth of B cells in which the receptor is expressed. Specifically, B cells expressing the RRV vGPCR display an increased resistance to apoptosis, suggesting that expression of this protein in infected B cells could promote the survival of these cells. Indeed, activation of anti-apoptotic mechanisms is often associated with the development of cancers (133), and in the case of vGPCR enhanced survival of infected B cells, this could be a potential mechanism of promoting abnormal B cell growth. In addition, activation of pathways such as ERK1/2 by the RRV vGPCR may also promote increased cellular proliferation, which could also contribute to the development of lymphoproliferative disorders. However, an important note to make is that we have obtained no evidence that B cells expressing either the RRV or HHV-8 vGPCRs display increased rates of proliferation, although further experiments will need to be performed to completely rule out this possibility. Nevertheless, all of the information we have obtained thus far suggests that the expression of the RRV vGPCR in B cells of RRV-infected macaques could play a role in the development of B cell abnormalities.

Figure 5.1 Potential scenarios of RRV vGPCR expression in infected cells. RRV infection of a target cell (e.g. B cells) could lead to two possible scenarios of RRV vGPCR expression. (A) Expression during a normal lytic replication cycle would result in transient vGPCR expression, which could cause activation of cellular signaling pathways such as ERK and Akt, promoting increased viral replication before the ultimate destruction of the cell and release of viral progeny. This pattern of expression may also induce cytokine secretion, which could have various effects on neighboring cells, and possibly promote disease development. (B) vGPCR expression without concurrent viral replication (e.g. aberrant expression or expression during an abortive lytic replication cycle) could result in direct transformation of an infected cell, due to constitutive activation of signaling pathways such as ERK and Akt by the vGPCR, while increased cytokine production by these cells might have paracrine or autocrine effects that promote disease development. In addition, in both scenarios, the RRV vGPCR could potentially play a role in chemotaxis and homing of infected cells.

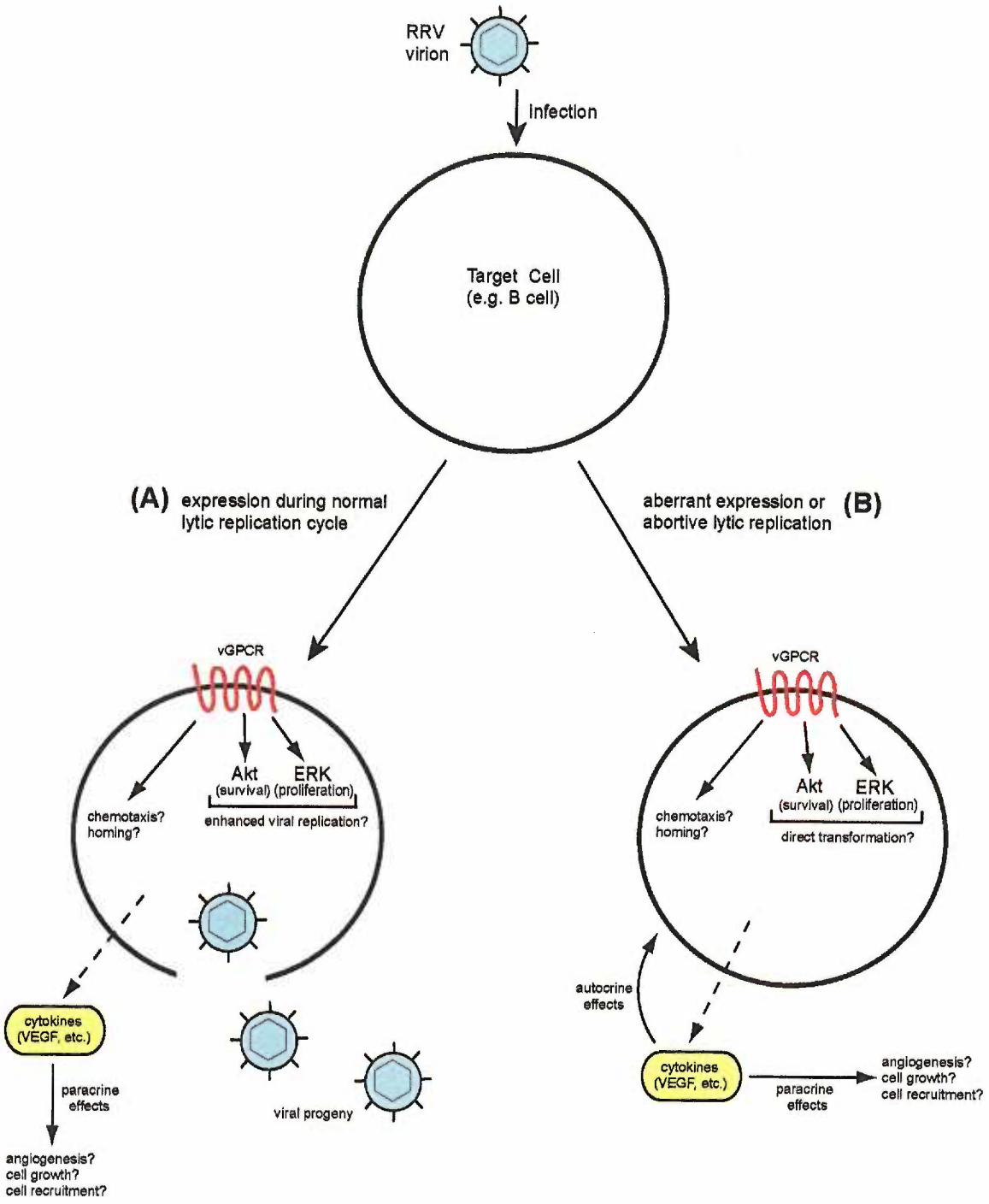
RRV
virion
Infection
Target Cell
(e.g. B cell)
(A) expression during normal
lytic replication cycle
aberrant expression or
abortive lytic replication (B)
vGPCR
Akt
ERK
(survival) (proliferation)
chemotaxis?
homing?
enhanced viral replication?
cytokines
(VEGF, etc.)
paracrine
effects
angiogenesis?
cell growth?
cell recruitment?
viral progeny
vGPCR
Akt
ERK
(survival) (proliferation)
chemotaxis?
homing?
direct transformation?
autocrine
effects
cytokines
(VEGF, etc.)
paracrine
effects
angiogenesis?
cell growth?
cell recruitment?

4. Utility of RRV as a Model System for Studies of the HHV-8 vGPCR

The major goal of this work was to compare the properties of the RRV-encoded vGPCR to those of the vGPCR of HHV-8, and to ultimately determine the utility of RRV as a model system to study the contributions of these receptors to the viral life cycle and virus-associated diseases. As discussed in chapter 1, the HHV-8 vGPCR has been implicated by numerous studies to be a major determinant of viral pathogenesis, and in particular, is thought to play a major role in promoting the transforming potential of the virus. Our studies have shown that the RRV and HHV-8 vGPCRs are highly similar proteins that behave in nearly identical fashions, at least in the experiments performed thus far. Specifically, both are constitutively signaling receptors that are responsive to exogenous chemokines, and their expression induces cytokine secretion, causes cellular transformation, and promotes cell survival. In addition, the signaling mechanisms utilized by both receptors appear to be similar, further suggesting that these receptors are homologous proteins.

The only major difference between the RRV and HHV-8 vGPCRs that we have identified from our work concerns the transcriptional expression patterns of the ORFs encoding these proteins. In particular, although these ORFs have a similar bi-cistronic pattern of expression, we found that they may possess different kinetics of lytic expression, and that major differences in transcriptional initiation sites and splicing patterns exist in the transcripts encoding these ORFs. Nevertheless, the fact that ORF74 sequence is completely maintained in the spliced versions of both the HHV-8 K14-ORF74 and RRV R15-ORF74 transcripts, and that both transcripts are expressed during

the lytic cycle, implies that these viral ORFs provide similar functions to the virus, and may also have similar effects in disease development.

In conclusion, RRV is the rhesus macaque homologue of HHV-8, and encodes a vGPCR that appears homologous to the vGPCR of HHV-8. Therefore, RRV provides an excellent model system for the analysis of the roles of the HHV-8 vGPCR in the viral life cycle and viral pathogenesis. Ultimately, RRV should prove invaluable to studies examining potential methods to treat viral malignancies associated with vGPCR expression *in vivo*.

Appendices

Appendix 1

Analysis of RRV vGPCR Mutants

Introduction: The IRC motif of the RRV vGPCR, located from amino acid residues 143 to 145, is similar to the VRY motif found in this location in the HHV-8 vGPCR. These motifs are variants of a highly conserved DRY motif found in most GPCRs, which is located in the second intracellular loop at the junction of the third transmembrane domain. Initial studies with the chemokine receptor CXCR2, the cellular homologue of the HHV-8 vGPCR, suggested that replacement of the charged aspartic acid (D) residue in the DRY motif with a hydrophobic valine (V) residue conferred constitutive signaling abilities to this receptor (24). Therefore, the speculation was made that the VRY motif found in the HHV-8 vGPCR played a role in the constitutive activity and transforming potential of this receptor. Thus, we performed mutagenesis analysis on the IRC motif in the RRV vGPCR, to determine the potential contributions of isoleucine 143 (I143) and cysteine 145 (C145) to the activities of the receptor. We anticipated that changing I143 to a D residue might reduce the receptors constitutive activity, since this alteration would change the IRC motif to DRC, which is more similar to the DRY sequence found in CXCR2. Alternatively, changing the C145 residue of the RRV vGPCR to a tyrosine (Y) would change the IRC motif to IRY, which closely mimics the VRY motif of HHV-8 vGPCR, suggesting that this mutated version of the receptor could possibly display higher levels of constitutive activity than the wild type receptor.

Materials and Methods: The sequence for wild type RRV ORF74 was altered by PCR-based mutagenesis, and the presence of the desired mutations was confirmed by sequence analysis. These products were then cloned into the retroviral vector pLNCX to generate two constructs; RRV ORF74 I143D, and RRV ORF74 C145Y. Next, stable NIH3T3 clones were generated and tested for expression by RT-PCR (data not shown), and phospho-ERK Westerns and soft-agarose assays were performed using these clones. The methods utilized to perform these experiments are described in detail in the material and methods section of chapter 2.

Results: Two clones each of the I143D (clones 1 and 2) and C145Y (clones 18 and 19) mutants were initially tested for their abilities to activate ERK signaling, compared to two wild type RRV ORF74 clones (clones 3 and 7), a vector control clone (pLNCX-6), and wild type NIH3T3 cells. This experiment demonstrated that either alteration of the IRC motif in the RRV vGPCR had no apparent effect on the receptor's ability to constitutively activate ERK1/2 (Fig. A.1A), suggesting that differences in this motif compared to wild type CXCR2 or the HHV-8 vGPCR do not account for the receptors constitutive signaling abilities. Next, we tested these same clones for their ability to grow in soft-agarose media, to determine the effects of the mutations on the transforming abilities of the RRV vGPCR. Figure A.1B shows representative images of one of these assays, in which we found that neither mutation affected the ability of the RRV vGPCR to induce cellular transformation, with both mutant forms of the vGPCR displaying similar abilities to grow in soft-agarose as is seen with the wild type vGPCR. No growth was detected with a vector control clone in these assays.

Conclusions: Alterations of the I or C residues of the RRV vGPCR IRC motif do not appear to affect the constitutive signaling or transforming abilities of the receptor. Interestingly, shortly after we performed these analyses, several studies examining the HHV-8 vGPCR indicated that mutation of the V residue of the VRY motif to aspartic acid (D) does not affect the constitutive signaling properties of this receptor (76, 129, 140, 148). This supports our findings, and indicates that the IRC motif of RRV vGPCR and the VRY motif of the HHV-8 vGPCR do not appear to be the major determinants of receptor activity, and suggests that multiple residues or regions of these vGPCRs are likely involved in determining their overall activities.

Figure A.1 Analysis of RRV vGPCR mutants. (A) phospho-ERK Western of lysates from wild type NIH3T3 cells, a vector control NIH3T3 clone (pLNCX-6), or NIH3T3 clones expressing wild type RRV vGPCR (ORF74-3 and ORF74-7), I143D RRV vGPCR (I143D-1 and I143D-2), or C145Y RRV vGPCR (C145Y-18 and C145Y-19). Blots were probed with anti-phospho-ERK1/2 antibody (pERK), then stripped and reprobed with total ERK antibody (ERK). (B) Soft-agarose assay of mutant RRV vGPCR expressing NIH3T3 clones (I143D and C145Y) , and a vector control clone (pLNCX).

A.

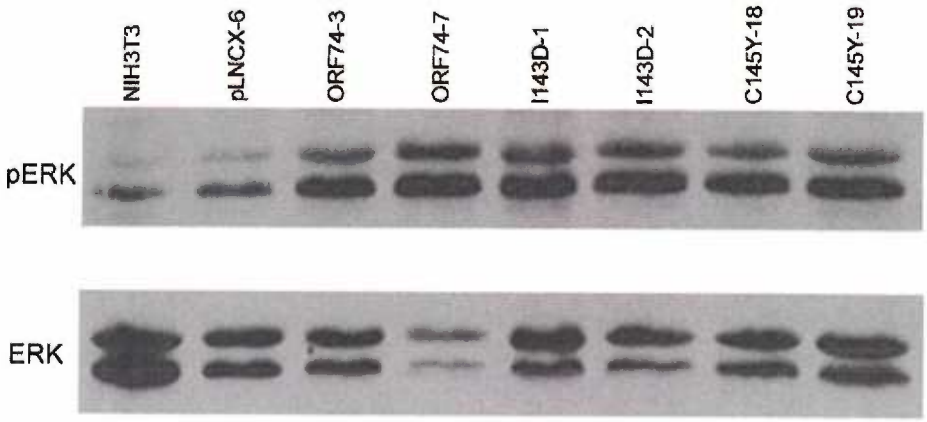
NIH3T3
pLNCX-6
ORF74-3
ORF74-7
I143D-1
I143D-2
C145Y-18
C145Y-19
pERK
ERK

B.


pLNCX
I143D ORF74
C145Y ORF74

Appendix 2

Construction of an RRV Bacterial Artificial Chromosome (BAC)

Introduction: Accurate determination of the roles of individual herpesvirus genes in the viral life cycle and pathogenesis requires mutagenesis of these genes in the context of the virus. In the past, the most common approach to constructing these mutant viruses was by performing site-directed mutagenesis via homologous recombination in eukaryotic cells, using viral genomic DNA and plasmid DNA containing the mutation of interest. Some major drawbacks to this approach are the inefficiency of the recombination event, and the large amount of time required to successfully generate and identify a mutant virus. However, recently a new approach has been developed that alleviates many of the issues associated with this method of producing a recombinant mutant virus (see reference (2) for a detailed review). This method involves cloning the entire viral genome as a bacterial artificial chromosome (BAC), which can be propagated in *E.coli*. This allows for mutagenesis of the viral genome in bacteria utilizing prokaryotic recombination machinery, and recovery of infectious mutant virus by transfection of purified BAC DNA into eukaryotic cells. In general, having the viral genome in bacteria significantly reduces the amount of time and labor involved in constructing a mutant virus. After the initial cloning of mouse cytomegalovirus (MCMV) as a BAC (105), the genomes of numerous other herpesvirsues have also been cloned as BACs, including human CMV, HSV, pseudorabiesvirus (PRV), EBV, HHV-8, and MHV-68 (2). An RRV BAC has not been

generated, but would be extremely beneficial for the generation of gene mutants, and in particular, mutants of RRV ORF74. Therefore, we began work to construct a BAC of RRV_{17577} for use in production of recombinant mutants of RRV. Some of the preliminary work on this project is described here.

Materials and Methods: The procedure for generating a recombinant RRV BAC is outlined in figure A.2. For generation of the RRV BAC, we are utilizing the BAC cassette pKSO-*gpt* derived from the vector pHA1. The cassette contains a bacterial origin of replication, a chloramphenicol resistance gene, and the *E.coli* gene guanosine phosphoribosyl transferase (*gpt*). The presence of *gpt* allows for the selection of recombinant virus containing the BAC plasmid in eukaryotic cells, using xanthine and mycophenolic acid. To introduce the BAC cassette into the RRV genome, a linearized version of the cassette was cloned into a plasmid containing ~2 kb of RRV sequence, and specifically, was inserted between the sequences for ORFs 57 and R6 of RRV, with ~1 kb of flanking RRV DNA sequence on each side of the cassette (see figure A.2). Importantly, this region was recently utilized in the construction of a recombinant version of RRV expressing green fluorescent protein (GFP), and analysis of this region in the GFP virus suggests that insertion does not disrupt expression of any surrounding ORFs.

Results and Future Directions: Thus far, we have begun selecting for a recombinant RRV BAC virus after transfecting primary rhesus fibroblasts with viral genomic DNA and the BAC recombination plasmid. After this virus is obtained, we will be able to isolate circular RRV BAC DNA and introduce this into *E.coli* for propagation.

Ultimately, the RRV BAC will be used for mutagenesis studies of particular RRV ORFs of interest, and should contribute greatly to studies of RRV.

Figure A.2 General outline of procedures used for generation of a recombinant RRV BAC. A recombination plasmid has been generated to introduce the BAC cassette into the RRV genome. The BAC cassette contains a bacterial origin of replication, and the *E.coli* gene *gpt*, which allows for selection of recombinant RRV BAC virus with mycophenolic acid and xanthine. The BAC cassette was inserted into a plasmid containing ~2 kb of RRV genomic DNA, and specifically, was placed between ORFs 57 and R6. ~1 kb of flanking viral sequence is located on either side of the cassette. Co-transfection of a linearized version of this plasmid with RRV genomic DNA is performed in primary rhesus fibroblasts, and recombinant virus is then selected. After recombinant virus is isolated, this virus will be used to infect primary rhesus fibroblasts, and circularized RRV BAC DNA will be purified from these cells. Next, *E.coli* will be transformed with this circular DNA, resulting in the production of bacteria harboring the entire RRV genome as a BAC. Once in *E.coli*, mutations can be easily introduced to the RRV genome. After mutagenesis, BAC DNA will be isolated and transfected into eukaryotic cells, resulting in the production of infectious mutant virus. The figure is not drawn to scale.

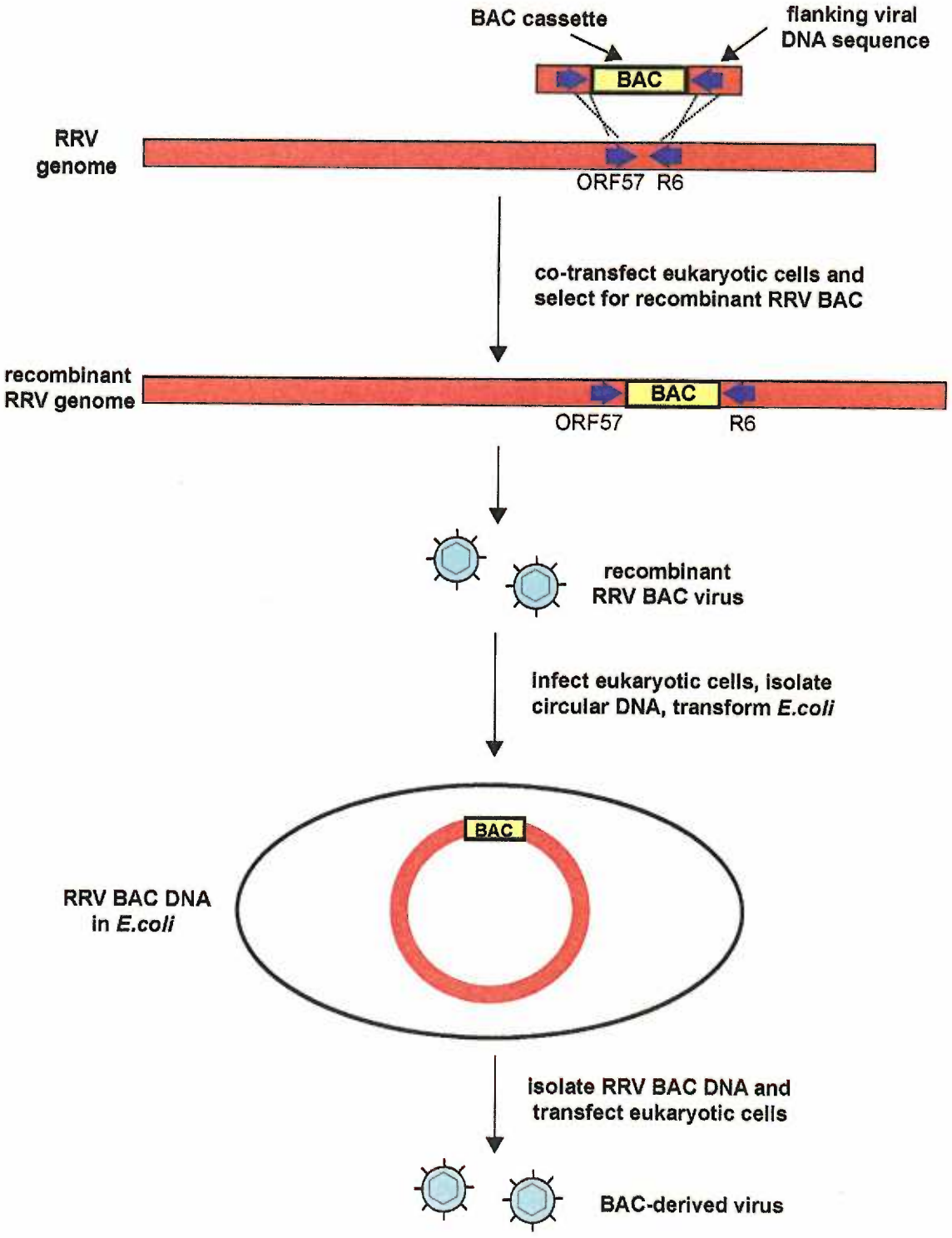
BAC cassette
flanking viral DNA sequence
BAC
RRV genome
ORF57 R6
co-transfect eukaryotic cells and select for recombinant RRV BAC
recombinant RRV genome
BAC
ORF57
R6
recombinant RRV BAC virus
infect eukaryotic cells, isolate circular DNA, transform E.coli
BAC
RRV BAC DNA in E.coli
isolate RRV BAC DNA and transfect eukaryotic cells
BAC-derived virus

REFERENCES

1. **Ablashi, D. V., L. G. Chatlynne, J. E. Whitman, Jr., and E. Cesarman.** 2002. Spectrum of Kaposi's sarcoma-associated herpesvirus, or human herpesvirus 8, diseases. Clin Microbiol Rev **15:**439-64.

2. **Adler, H., M. Messerle, and U. H. Koszinowski.** 2003. Cloning of herpesviral genomes as bacterial artificial chromosomes. Rev Med Virol **13:**111-21.

3. **Ahuja, S. K., and P. M. Murphy.** 1993. Molecular piracy of mammalian interleukin-8 receptor type B by herpesvirus saimiri. J Biol Chem **268:**20691-4.

4. **Alexander, L., L. Denekamp, A. Knapp, M. R. Auerbach, B. Damania, and R. C. Desrosiers.** 2000. The primary sequence of rhesus monkey rhadinovirus isolate 26-95: sequence similarities to Kaposi's sarcoma-associated herpesvirus and rhesus monkey rhadinovirus isolate 17577. J Virol **74:**3388-98.

5. **Aluigi, M. G., A. Albini, S. Carlone, L. Repetto, R. De Marchi, A. Icardi, M. Moro, D. Noonan, and R. Benelli.** 1996. KSHV sequences in biopsies and cultured spindle cells of epidemic, iatrogenic and Mediterranean forms of Kaposi's sarcoma. Res Virol **147:**267-75.

6. **Amaral, M. C., S. Miles, G. Kumar, and A. E. Nel.** 1993. Oncostatin-M stimulates tyrosine protein phosphorylation in parallel with the activation of p42MAPK/ERK-2 in Kaposi's cells. Evidence that this pathway is important in Kaposi cell growth. J Clin Invest **92:**848-57.

7. **Ambinder, R. F.** 2000. Gammaherpesviruses and "Hit-and-Run" oncogenesis. Am J Pathol **156:**1-3.

8. **Aoki, Y., E. S. Jaffe, Y. Chang, K. Jones, J. Teruya-Feldstein, P. S. Moore, and G. Tosato.** 1999. Angiogenesis and hematopoiesis induced by Kaposi's sarcoma-associated herpesvirus-encoded interleukin-6. Blood **93:**4034-43.

9. **Arai, H., and I. F. Charo.** 1996. Differential regulation of G-protein-mediated signaling by chemokine receptors. J Biol Chem **271:**21814-9.

10. **Arvanitakis, L., E. Geras-Raaka, A. Varma, M. C. Gershengorn, and E. Cesarman.** 1997. Human herpesvirus KSHV encodes a constitutively active G-protein-coupled receptor linked to cell proliferation. Nature **385:**347-50.

11. **Arvanitakis, L., E. A. Mesri, R. G. Nador, J. W. Said, A. S. Asch, D. M. Knowles, and E. Cesarman.** 1996. Establishment and characterization of a primary effusion (body cavity-based) lymphoma cell line (BC-3) harboring kaposi's sarcoma-associated herpesvirus (KSHV/HHV-8) in the absence of Epstein-Barr virus. Blood **88:**2648-54.

12. **Arvin, A. M.** 1996. Varicella-zoster virus. Clin Microbiol Rev **9:**361-81.

13. **Arya, M., H. R. Patel, and M. Williamson.** 2003. Chemokines: key players in cancer. Curr Med Res Opin **19:**557-64.

14. **Bais, C., B. Santomasso, O. Coso, L. Arvanitakis, E. G. Raaka, J. S. Gutkind, A. S. Asch, E. Cesarman, M. C. Gershengorn, E. A. Mesri, and M. C. Gerhengorn.** 1998. G-protein-coupled receptor of Kaposi's sarcoma-associated herpesvirus is a viral oncogene and angiogenesis activator. Nature **391:**86-9.

15. **Bais, C., A. Van Geelen, P. Eroles, A. Mutlu, C. Chiozzini, S. Dias, R. L. Silverstein, S. Rafii, and E. A. Mesri.** 2003. Kaposi's sarcoma associated

herpesvirus G protein-coupled receptor immortalizes human endothelial cells by activation of the VEGF receptor-2/ KDR. Cancer Cell **3:**131-43.

16. **Bechtel, J. T., Y. Liang, J. Hvidding, and D. Ganem.** 2003. Host range of Kaposi's sarcoma-associated herpesvirus in cultured cells. J Virol **77:**6474-81.

17. **Bergquam, E. P., N. Avery, S. M. Shiigi, M. K. Axthelm, and S. W. Wong.** 1999. Rhesus rhadinovirus establishes a latent infection in B lymphocytes in vivo. J Virol **73:**7874-6.

18. **Birkenbach, M., K. Josefsen, R. Yalamanchili, G. Lenoir, and E. Kieff.** 1993. Epstein-Barr virus-induced genes: first lymphocyte-specific G protein-coupled peptide receptors. J Virol **67:**2209-20.

19. **Blackbourn, D. J., D. Osmond, J. A. Levy, and E. T. Lennette.** 1999. Increased human herpesvirus 8 seroprevalence in young homosexual men who have multiple sex contacts with different partners. J Infect Dis **179:**237-9.

20. **Boshoff, C., D. Whitby, T. Hatziioannou, C. Fisher, J. van der Walt, A. Hatzakis, R. Weiss, and T. Schulz.** 1995. Kaposi's-sarcoma-associated herpesvirus in HIV-negative Kaposi's sarcoma. Lancet **345:**1043-4.

21. **Bouchard, V. J., M. Rouleau, and G. G. Poirier.** 2003. PARP-1, a determinant of cell survival in response to DNA damage. Exp Hematol **31:**446-54.

22. **Boulanger, E., J. Briere, P. Gaulard, D. Droz, and E. Oksenhendler.** 2003. HHV8-related non-Hodgkin's lymphoma of the spermatic cord in a patient with HIV-associated multicentric Castleman disease. Am J Hematol **72:**70-1.

23. **Breitwieser, G. E.** 2004. G protein-coupled receptor oligomerization: implications for G protein activation and cell signaling. Circ Res **94:**17-27.

24. **Burger, M., J. A. Burger, R. C. Hoch, Z. Oades, H. Takamori, and I. U. Schraufstatter.** 1999. Point mutation causing constitutive signaling of CXCR2 leads to transforming activity similar to Kaposi's sarcoma herpesvirus-G protein-coupled receptor. J Immunol **163:**2017-22.

25. **Cannon, M., N. J. Philpott, and E. Cesarman.** 2003. The Kaposi's sarcoma-associated herpesvirus G protein-coupled receptor has broad signaling effects in primary effusion lymphoma cells. J Virol **77:**57-67.

26. **Cannon, M. L., and E. Cesarman.** 2004. The KSHV G protein-coupled receptor signals via multiple pathways to induce transcription factor activation in primary effusion lymphoma cells. Oncogene **23:**514-23.

27. **Cardone, M. H., N. Roy, H. R. Stennicke, G. S. Salvesen, T. F. Franke, E. Stanbridge, S. Frisch, and J. C. Reed.** 1998. Regulation of cell death protease caspase-9 by phosphorylation. Science **282:**1318-21.

28. **Casarosa, P., R. A. Bakker, D. Verzijl, M. Navis, H. Timmerman, R. Leurs, and M. J. Smit.** 2001. Constitutive signaling of the human cytomegalovirus-encoded chemokine receptor US28. J Biol Chem **276:**1133-7.

29. **Casarosa, P., Y. K. Gruijthuijsen, D. Michel, P. S. Beisser, J. Holl, C. P. Fitzsimons, D. Verzijl, C. A. Bruggeman, T. Mertens, R. Leurs, C. Vink, and M. J. Smit.** 2003. Constitutive signaling of the human cytomegalovirus-encoded receptor UL33 differs from that of its rat cytomegalovirus homolog R33 by promiscuous activation of G proteins of the Gq, Gi, and Gs classes. J Biol Chem **278:**50010-23.

30. **Cesarman, E., Y. Chang, P. S. Moore, J. W. Said, and D. M. Knowles.** 1995. Kaposi's sarcoma-associated herpesvirus-like DNA sequences in AIDS-related body-cavity-based lymphomas. N Engl J Med **332:**1186-91.

31. **Cesarman, E., E. A. Mesri, and M. C. Gershengorn.** 2000. Viral G protein-coupled receptor and Kaposi's sarcoma: a model of paracrine neoplasia? J Exp Med **191:**417-22.

32. **Cesarman, E., R. G. Nador, F. Bai, R. A. Bohenzky, J. J. Russo, P. S. Moore, Y. Chang, and D. M. Knowles.** 1996. Kaposi's sarcoma-associated herpesvirus contains G protein-coupled receptor and cyclin D homologs which are expressed in Kaposi's sarcoma and malignant lymphoma. J Virol **70:**8218-23.

33. **Chang, J., and D. Ganem.** 2000. On the control of late gene expression in Kaposi's sarcoma-associated herpesvirus (human herpesvirus-8). J Gen Virol **81:**2039-47.

34. **Chang, Y., E. Cesarman, M. S. Pessin, F. Lee, J. Culpepper, D. M. Knowles, and P. S. Moore.** 1994. Identification of herpesvirus-like DNA sequences in AIDS-associated Kaposi's sarcoma. Science **266:**1865-9.

35. **Chiou, C. J., L. J. Poole, P. S. Kim, D. M. Ciufo, J. S. Cannon, C. M. ap Rhys, D. J. Alcendor, J. C. Zong, R. F. Ambinder, and G. S. Hayward.** 2002. Patterns of gene expression and a transactivation function exhibited by the vGCR (ORF74) chemokine receptor protein of Kaposi's sarcoma-associated herpesvirus. J Virol **76:**3421-39.

36. **Chung, Y. H., R. E. Means, J. K. Choi, B. S. Lee, and J. U. Jung.** 2002. Kaposi's sarcoma-associated herpesvirus OX2 glycoprotein activates myeloid-lineage cells to induce inflammatory cytokine production. J Virol **76:**4688-98.

37. **Clemens, M. J., M. Bushell, and S. J. Morley.** 1998. Degradation of eukaryotic polypeptide chain initiation factor (eIF) 4G in response to induction of apoptosis in human lymphoma cell lines. Oncogene **17:**2921-31.

38. **Cornali, E., C. Zietz, R. Benelli, W. Weninger, L. Masiello, G. Breier, E. Tschachler, A. Albini, and M. Sturzl.** 1996. Vascular endothelial growth factor regulates angiogenesis and vascular permeability in Kaposi's sarcoma. Am J Pathol **149:**1851-69.

39. **Couty, J. P., E. Geras-Raaka, B. B. Weksler, and M. C. Gershengorn.** 2001. Kaposi's sarcoma-associated herpesvirus G protein-coupled receptor signals through multiple pathways in endothelial cells. J Biol Chem **276:**33805-11.

40. **Cross, D. A., D. R. Alessi, P. Cohen, M. Andjelkovich, and B. A. Hemmings.** 1995. Inhibition of glycogen synthase kinase-3 by insulin mediated by protein kinase B. Nature **378:**785-9.

41. **Damania, B., M. DeMaria, J. U. Jung, and R. C. Desrosiers.** 2000. Activation of lymphocyte signaling by the R1 protein of rhesus monkey rhadinovirus. J Virol **74:**2721-30.

42. **Damania, B., and R. C. Desrosiers.** 2001. Simian homologues of human herpesvirus 8. Philos Trans R Soc Lond B Biol Sci **356:**535-43.

43. **Damania, B., M. Li, J. K. Choi, L. Alexander, J. U. Jung, and R. C. Desrosiers.** 1999. Identification of the R1 oncogene and its protein product from the rhadinovirus of rhesus monkeys. J Virol **73:**5123-31.

44. **Desrosiers, R. C., V. G. Sasseville, S. C. Czajak, X. Zhang, K. G. Mansfield, A. Kaur, R. P. Johnson, A. A. Lackner, and J. U. Jung.** 1997. A herpesvirus of rhesus monkeys related to the human Kaposi's sarcoma-associated herpesvirus. J Virol **71:**9764-9.

45. **DeWire, S. M., M. A. McVoy, and B. Damania.** 2002. Kinetics of expression of rhesus monkey rhadinovirus (RRV) and identification and characterization of a polycistronic transcript encoding the RRV Orf50/Rta, RRV R8, and R8.1 genes. J Virol **76:**9819-31.

46. **Dictor, M., E. Rambech, D. Way, M. Witte, and N. Bendsoe.** 1996. Human herpesvirus 8 (Kaposi's sarcoma-associated herpesvirus) DNA in Kaposi's sarcoma lesions, AIDS Kaposi's sarcoma cell lines, endothelial Kaposi's sarcoma simulators, and the skin of immunosuppressed patients. Am J Pathol **148:**2009-16.

47. **Dupin, N., T. L. Diss, P. Kellam, M. Tulliez, M. Q. Du, D. Sicard, R. A. Weiss, P. G. Isaacson, and C. Boshoff.** 2000. HHV-8 is associated with a plasmablastic variant of Castleman disease that is linked to HHV-8-positive plasmablastic lymphoma. Blood **95:**1406-12.

48. **Dupin, N., C. Fisher, P. Kellam, S. Ariad, M. Tulliez, N. Franck, E. van Marck, D. Salmon, I. Gorin, J. P. Escande, R. A. Weiss, K. Alitalo, and C. Boshoff.** 1999. Distribution of human herpesvirus-8 latently infected cells in

Kaposi's sarcoma, multicentric Castleman's disease, and primary effusion lymphoma. Proc Natl Acad Sci U S A **96:**4546-51.

49. **Emery, V. C.** 2001. Cytomegalovirus and the aging population. Drugs Aging **18:**927-33.

50. **Ensoli, B., C. Sgadari, G. Barillari, M. C. Sirianni, M. Sturzl, and P. Monini.** 2001. Biology of Kaposi's sarcoma. Eur J Cancer **37:**1251-69.

51. **Estep, R. D., M. K. Axthelm, and S. W. Wong.** 2003. A G protein-coupled receptor encoded by rhesus rhadinovirus is similar to ORF74 of Kaposi's sarcoma-associated herpesvirus. J Virol **77:**1738-46.

52. **Fickenscher, H., and B. Fleckenstein.** 2001. Herpesvirus saimiri. Philos Trans R Soc Lond B Biol Sci **356:**545-67.

53. **Fields, B. N., and D. M. Knipe.** 1990. Fields virology, 2nd ed. Raven Press, New York.

54. **Fields, B. N., D. M. Knipe, and P. M. Howley.** 1996. Fundamental virology, 3rd ed. Lippincott-Raven, Philadelphia.

55. **Flore, O., S. Rafii, S. Ely, J. J. O'Leary, E. M. Hyjek, and E. Cesarman.** 1998. Transformation of primary human endothelial cells by Kaposi's sarcoma-associated herpesvirus. Nature **394:**588-92.

56. **Gaidano, G., and A. Carbone.** 2001. Primary effusion lymphoma: a liquid phase lymphoma of fluid-filled body cavities. Adv Cancer Res **80:**115-46.

57. **Gao, J. L., and P. M. Murphy.** 1994. Human cytomegalovirus open reading frame US28 encodes a functional beta chemokine receptor. J Biol Chem **269:**28539-42.

58. **Gao, S. J., C. Boshoff, S. Jayachandra, R. A. Weiss, Y. Chang, and P. S. Moore.** 1997. KSHV ORF K9 (vIRF) is an oncogene which inhibits the interferon signaling pathway. Oncogene **15:**1979-85.

59. **Gao, S. J., L. Kingsley, D. R. Hoover, T. J. Spira, C. R. Rinaldo, A. Saah, J. Phair, R. Detels, P. Parry, Y. Chang, and P. S. Moore.** 1996. Seroconversion to antibodies against Kaposi's sarcoma-associated herpesvirus-related latent nuclear antigens before the development of Kaposi's sarcoma. N Engl J Med **335:**233-41.

60. **Geras-Raaka, E., A. Varma, I. Clark-Lewis, and M. C. Gershengorn.** 1998. Kaposi's sarcoma-associated herpesvirus (KSHV) chemokine vMIP-II and human SDF-1alpha inhibit signaling by KSHV G protein-coupled receptor. Biochem Biophys Res Commun **253:**725-7.

61. **Geras-Raaka, E., A. Varma, H. Ho, I. Clark-Lewis, and M. C. Gershengorn.** 1998. Human interferon-gamma-inducible protein 10 (IP-10) inhibits constitutive signaling of Kaposi's sarcoma-associated herpesvirus G protein-coupled receptor. J Exp Med **188:**405-8.

62. **Gershengorn, M. C., E. Geras-Raaka, A. Varma, and I. Clark-Lewis.** 1998. Chemokines activate Kaposi's sarcoma-associated herpesvirus G protein-coupled receptor in mammalian cells in culture. J Clin Invest **102:**1469-72.

63. **Giddens, W. E., Jr., C. C. Tsai, W. R. Morton, H. D. Ochs, G. H. Knitter, and G. A. Blakley.** 1985. Retroperitoneal fibromatosis and acquired immunodeficiency syndrome in macaques. Pathologic observations and transmission studies. Am J Pathol **119:**253-63.

64. **Goldenberg, D., A. Golz, A. Netzer, E. Rosenblatt, A. Rachmiel, R. F. Goldenberg, and H. Z. Joachims.** 2001. Epstein-Barr virus and cancers of the head and neck. Am J Otolaryngol **22:**197-205.

65. **Gompels, U. A., J. Nicholas, G. Lawrence, M. Jones, B. J. Thomson, M. E. Martin, S. Efstathiou, M. Craxton, and H. A. Macaulay.** 1995. The DNA sequence of human herpesvirus-6: structure, coding content, and genome evolution. Virology **209:**29-51.

66. **Gorczynski, R. M., M. S. Cattral, Z. Chen, J. Hu, J. Lei, W. P. Min, G. Yu, and J. Ni.** 1999. An immunoadhesin incorporating the molecule OX-2 is a potent immunosuppressant that prolongs allo- and xenograft survival. J Immunol **163:**1654-60.

67. **Greensill, J., J. A. Sheldon, N. M. Renwick, B. E. Beer, S. Norley, J. Goudsmit, and T. F. Schulz.** 2000. Two distinct gamma-2 herpesviruses in African green monkeys: a second gamma-2 herpesvirus lineage among old world primates? J Virol **74:**1572-7.

68. **Griffiths, P. D., D. A. Clark, and V. C. Emery.** 2000. Betaherpesviruses in transplant recipients. J Antimicrob Chemother **45 Suppl T3:**29-34.

69. **Guo, H. G., P. Browning, J. Nicholas, G. S. Hayward, E. Tschachler, Y. W. Jiang, M. Sadowska, M. Raffeld, S. Colombini, R. C. Gallo, and M. S. Reitz, Jr.** 1997. Characterization of a chemokine receptor-related gene in human herpesvirus 8 and its expression in Kaposi's sarcoma. Virology **228:**371-8.

70. **Guo, H. G., M. Sadowska, W. Reid, E. Tschachler, G. Hayward, and M. Reitz.** 2003. Kaposi's sarcoma-like tumors in a human herpesvirus 8 ORF74 transgenic mouse. J Virol **77:**2631-9.

71. **Gutkind, J. S.** 1998. The pathways connecting G protein-coupled receptors to the nucleus through divergent mitogen-activated protein kinase cascades. J Biol Chem **273:**1839-42.

72. **Harrington, W., Jr., L. Sieczkowski, C. Sosa, S. Chan-a-Sue, J. P. Cai, L. Cabral, and C. Wood.** 1997. Activation of HHV-8 by HIV-1 tat. Lancet **349:**774-5.

73. **Hasegawa, H., Y. Utsunomiya, M. Yasukawa, K. Yanagisawa, and S. Fujita.** 1994. Induction of G protein-coupled peptide receptor EBI 1 by human herpesvirus 6 and 7 infection in CD4+ T cells. J Virol **68:**5326-9.

74. **Hildebrandt, J. D.** 1997. Role of subunit diversity in signaling by heterotrimeric G proteins. Biochem Pharmacol **54:**325-39.

75. **Ho, H. H., D. Du, and M. C. Gershengorn.** 1999. The N terminus of Kaposi's sarcoma-associated herpesvirus G protein-coupled receptor is necessary for high affinity chemokine binding but not for constitutive activity. J Biol Chem **274:**31327-32.

76. **Ho, H. H., N. Ganeshalingam, A. Rosenhouse-Dantsker, R. Osman, and M. C. Gershengorn.** 2001. Charged residues at the intracellular boundary of transmembrane helices 2 and 3 independently affect constitutive activity of Kaposi's sarcoma-associated herpesvirus G protein-coupled receptor. J Biol Chem **276:**1376-82.

77. **Hoek, R. M., S. R. Ruuls, C. A. Murphy, G. J. Wright, R. Goddard, S. M. Zurawski, B. Blom, M. E. Homola, W. J. Streit, M. H. Brown, A. N. Barclay, and J. D. Sedgwick.** 2000. Down-regulation of the macrophage lineage through interaction with OX2 (CD200). Science **290:**1768-71.

78. **Holst, P. J., M. M. Rosenkilde, D. Manfra, S. C. Chen, M. T. Wiekowski, B. Holst, F. Cifire, M. Lipp, T. W. Schwartz, and S. A. Lira.** 2001. Tumorigenesis induced by the HHV8-encoded chemokine receptor requires ligand modulation of high constitutive activity. J Clin Invest **108:**1789-96.

79. **Isegawa, Y., Z. Ping, K. Nakano, N. Sugimoto, and K. Yamanishi.** 1998. Human herpesvirus 6 open reading frame U12 encodes a functional beta-chemokine receptor. J Virol **72:**6104-12.

80. **Jacobson, L. P., F. J. Jenkins, G. Springer, A. Munoz, K. V. Shah, J. Phair, Z. Zhang, and H. Armenian.** 2000. Interaction of human immunodeficiency virus type 1 and human herpesvirus type 8 infections on the incidence of Kaposi's sarcoma. J Infect Dis **181:**1940-9.

81. **Kaleeba, J. A., E. P. Bergquam, and S. W. Wong.** 1999. A rhesus macaque rhadinovirus related to Kaposi's sarcoma-associated herpesvirus/human herpesvirus 8 encodes a functional homologue of interleukin-6. J Virol **73:**6177-81.

82. **Kedes, D. H., E. Operskalski, M. Busch, R. Kohn, J. Flood, and D. Ganem.** 1996. The seroepidemiology of human herpesvirus 8 (Kaposi's sarcoma-associated herpesvirus): distribution of infection in KS risk groups and evidence for sexual transmission. Nat Med **2:**918-24.

83. **Kennedy, P. G.** 2002. Key issues in varicella-zoster virus latency. J Neurovirol **8 Suppl 2:**80-4.

84. **Kim, O., and S. J. Yi.** 2003. Lytic replication of Human herpesvirus 8 and induction of apoptosis. Acta Virol **47:**91-5.

85. **Kirshner, J. R., K. Staskus, A. Haase, M. Lagunoff, and D. Ganem.** 1999. Expression of the open reading frame 74 (G-protein-coupled receptor) gene of Kaposi's sarcoma (KS)-associated herpesvirus: implications for KS pathogenesis. J Virol **73:**6006-14.

86. **Kledal, T. N., M. M. Rosenkilde, and T. W. Schwartz.** 1998. Selective recognition of the membrane-bound CX3C chemokine, fractalkine, by the human cytomegalovirus-encoded broad-spectrum receptor US28. FEBS Lett **441:**209-14.

87. **Lacoste, V., P. Mauclere, G. Dubreuil, J. Lewis, M. C. Georges-Courbot, and A. Gessain.** 2000. KSHV-like herpesviruses in chimps and gorillas. Nature **407:**151-2.

88. **Lacoste, V., P. Mauclere, G. Dubreuil, J. Lewis, M. C. Georges-Courbot, and A. Gessain.** 2001. A novel gamma 2-herpesvirus of the Rhadinovirus 2 lineage in chimpanzees. Genome Res **11:**1511-9.

89. **Lacoste, V., P. Mauclere, G. Dubreuil, J. Lewis, M. C. Georges-Courbot, J. Rigoulet, T. Petit, and A. Gessain.** 2000. Simian homologues of human gamma-2 and betaherpesviruses in mandrill and drill monkeys. J Virol **74:**11993-9.

90. **Landolfo, S., M. Gariglio, G. Gribaudo, and D. Lembo.** 2003. The human cytomegalovirus. Pharmacol Ther **98:**269-97.

91. **Lebbe, C., P. de Cremoux, G. Millot, M. P. Podgorniak, O. Verola, R. Berger, P. Morel, and F. Calvo.** 1997. Characterization of in vitro culture of HIV-negative Kaposi's sarcoma-derived cells. In vitro responses to alfa interferon. Arch Dermatol Res **289:**421-8.

92. **Lee, B. J., U. H. Koszinowski, S. R. Sarawar, and H. Adler.** 2003. A gammaherpesvirus G protein-coupled receptor homologue is required for increased viral replication in response to chemokines and efficient reactivation from latency. J Immunol **170:**243-51.

93. **Levy, J. A.** 1997. Three new human herpesviruses (HHV6, 7, and 8). Lancet **349:**558-63.

94. **Lin, S. F., D. R. Robinson, J. Oh, J. U. Jung, P. A. Luciw, and H. J. Kung.** 2002. Identification of the bZIP and Rta homologues in the genome of rhesus monkey rhadinovirus. Virology **298:**181-8.

95. **Liu, C., G. Sandford, G. Fei, and J. Nicholas.** 2004. Galpha protein selectivity determinant specified by a viral chemokine receptor-conserved region in the C tail of the human herpesvirus 8 g protein-coupled receptor. J Virol **78:**2460-71.

96. **Liu, X., and M. A. Gorovsky.** 1993. Mapping the 5' and 3' ends of Tetrahymena thermophila mRNAs using RNA ligase mediated amplification of cDNA ends (RLM-RACE). Nucleic Acids Res **21:**4954-60.

97. **Luttrell, L. M., and R. J. Lefkowitz.** 2002. The role of beta-arrestins in the termination and transduction of G-protein-coupled receptor signals. J Cell Sci **115:**455-65.

98. **M. Zuker, D. H. M. a. D. H. T.** 1999. Algorithms and thermodynamics for RNA secondary structure prediction: a practical guide in RNA Biochemistry and Biotechnology. Kluwer Academic Publishers, Norwell MA.

99. **Macsween, K. F., and D. H. Crawford.** 2003. Epstein-Barr virus-recent advances. Lancet Infect Dis **3:**131-40.

100. **Mansfield, K. G., S. V. Westmoreland, C. D. DeBakker, S. Czajak, A. A. Lackner, and R. C. Desrosiers.** 1999. Experimental infection of rhesus and pig-tailed macaques with macaque rhadinoviruses. J Virol **73:**10320-8.

101. **Marinissen, M. J., and J. S. Gutkind.** 2001. G-protein-coupled receptors and signaling networks: emerging paradigms. Trends Pharmacol Sci **22:**368-76.

102. **Martin, J. N., D. E. Ganem, D. H. Osmond, K. A. Page-Shafer, D. Macrae, and D. H. Kedes.** 1998. Sexual transmission and the natural history of human herpesvirus 8 infection. N Engl J Med **338:**948-54.

103. **Masood, R., J. Cai, T. Zheng, D. L. Smith, Y. Naidu, and P. S. Gill.** 1997. Vascular endothelial growth factor/vascular permeability factor is an autocrine growth factor for AIDS-Kaposi sarcoma. Proc Natl Acad Sci U S A **94:**979-84.

104. **Melendez, L. V., M. D. Daniel, F. G. Garcia, C. E. Fraser, R. D. Hunt, and N. W. King.** 1969. Herpesvirus saimiri. I. Further characterization studies of a new virus from the squirrel monkey. Lab Anim Care **19:**372-7.

105. **Messerle, M., I. Crnkovic, W. Hammerschmidt, H. Ziegler, and U. H. Koszinowski.** 1997. Cloning and mutagenesis of a herpesvirus genome as an infectious bacterial artificial chromosome. Proc Natl Acad Sci U S A **94:**14759-63.

106. **Mettenleiter, T. C.** 2002. Herpesvirus assembly and egress. J Virol **76:**1537-47.

107. **Miller, A. D., and C. Buttimore.** 1986. Redesign of retrovirus packaging cell lines to avoid recombination leading to helper virus production. Mol Cell Biol **6:**2895-902.

108. **Miller, G., L. Heston, E. Grogan, L. Gradoville, M. Rigsby, R. Sun, D. Shedd, V. M. Kushnaryov, S. Grossberg, and Y. Chang.** 1997. Selective switch between latency and lytic replication of Kaposi's sarcoma herpesvirus and Epstein-Barr virus in dually infected body cavity lymphoma cells. J Virol **71:**314-24.

109. **Montaner, S., A. Sodhi, A. Molinolo, T. H. Bugge, E. T. Sawai, Y. He, Y. Li, P. E. Ray, and J. S. Gutkind.** 2003. Endothelial infection with KSHV genes in vivo reveals that vGPCR initiates Kaposi's sarcomagenesis and can promote the tumorigenic potential of viral latent genes. Cancer Cell **3:**23-36.

110. **Montaner, S., A. Sodhi, S. Pece, E. A. Mesri, and J. S. Gutkind.** 2001. The Kaposi's sarcoma-associated herpesvirus G protein-coupled receptor promotes endothelial cell survival through the activation of Akt/protein kinase B. Cancer Res **61:**2641-8.

111. **Moore, P. S., C. Boshoff, R. A. Weiss, and Y. Chang.** 1996. Molecular mimicry of human cytokine and cytokine response pathway genes by KSHV. Science **274:**1739-44.

112. **Moore, P. S., and Y. Chang.** 1995. Detection of herpesvirus-like DNA sequences in Kaposi's sarcoma in patients with and without HIV infection. N Engl J Med **332:**1181-5.

113. **Moore, P. S., S. J. Gao, G. Dominguez, E. Cesarman, O. Lungu, D. M. Knowles, R. Garber, P. E. Pellett, D. J. McGeoch, and Y. Chang.** 1996. Primary characterization of a herpesvirus agent associated with Kaposi's sarcomae. J Virol **70:**549-58.

114. **Moses, A. V., K. N. Fish, R. Ruhl, P. P. Smith, J. G. Strussenberg, L. Zhu, B. Chandran, and J. A. Nelson.** 1999. Long-term infection and transformation of dermal microvascular endothelial cells by human herpesvirus 8. J Virol **73:**6892-902.

115. **Munshi, N., R. K. Ganju, S. Avraham, E. A. Mesri, and J. E. Groopman.** 1999. Kaposi's sarcoma-associated herpesvirus-encoded G protein-coupled receptor activation of c-jun amino-terminal kinase/stress-activated protein kinase and lyn kinase is mediated by related adhesion focal tyrosine kinase/proline-rich tyrosine kinase 2. J Biol Chem **274:**31863-7.

116. **Murakami-Mori, K., S. Mori, and B. Bonavida.** 2000. Molecular pathogenesis of AIDS-associated Kaposi's sarcoma: growth and apoptosis. Adv Cancer Res **78:**159-97.

117. **Murga, C., S. Fukuhara, and J. S. Gutkind.** 2000. A novel role for phosphatidylinositol 3-kinase beta in signaling from G protein-coupled receptors to Akt. J Biol Chem **275:**12069-73.

118. **Murga, C., L. Laguinge, R. Wetzker, A. Cuadrado, and J. S. Gutkind.** 1998. Activation of Akt/protein kinase B by G protein-coupled receptors. A role for alpha and beta gamma subunits of heterotrimeric G proteins acting through phosphatidylinositol-3-OH kinasegamma. J Biol Chem **273:**19080-5.

119. **Nador, R. G., E. Cesarman, A. Chadburn, D. B. Dawson, M. Q. Ansari, J. Sald, and D. M. Knowles.** 1996. Primary effusion lymphoma: a distinct clinicopathologic entity associated with the Kaposi's sarcoma-associated herpes virus. Blood **88:**645-56.

120. **Nador, R. G., L. L. Milligan, O. Flore, X. Wang, L. Arvanitakis, D. M. Knowles, and E. Cesarman.** 2001. Expression of Kaposi's sarcoma-associated herpesvirus G protein-coupled receptor monocistronic and bicistronic transcripts in primary effusion lymphomas. Virology **287:**62-70.

121. **Nakano, K., Y. Isegawa, P. Zou, K. Tadagaki, R. Inagi, and K. Yamanishi.** 2003. Kaposi's sarcoma-associated herpesvirus (KSHV)-encoded vMIP-I and vMIP-II induce signal transduction and chemotaxis in monocytic cells. Arch Virol **148:**871-90.

122. **Neer, E. J.** 1995. Heterotrimeric G proteins: organizers of transmembrane signals. Cell **80:**249-57.

123. **Neipel, F., and B. Fleckenstein.** 1999. The role of HHV-8 in Kaposi's sarcoma. Semin Cancer Biol **9:**151-64.

124. **Nielsen, H., J. Engelbrecht, S. Brunak, and G. von Heijne.** 1997. Identification of prokaryotic and eukaryotic signal peptides and prediction of their cleavage sites. Protein Eng **10:**1-6.

125. **Oksenhendler, E., E. Boulanger, L. Galicier, M. Q. Du, N. Dupin, T. C. Diss, R. Hamoudi, M. T. Daniel, F. Agbalika, C. Boshoff, J. P. Clauvel, P. G. Isaacson, and V. Meignin.** 2002. High incidence of Kaposi sarcoma-associated

herpesvirus-related non-Hodgkin lymphoma in patients with HIV infection and multicentric Castleman disease. Blood **99:**2331-6.

126. **Osborne, J., P. S. Moore, and Y. Chang.** 1999. KSHV-encoded viral IL-6 activates multiple human IL-6 signaling pathways. Hum Immunol **60:**921-7.

127. **Pap, M., and G. M. Cooper.** 1998. Role of glycogen synthase kinase-3 in the phosphatidylinositol 3-Kinase/Akt cell survival pathway. J Biol Chem **273:**19929-32.

128. **Pari, G. S., D. AuCoin, K. Colletti, S. A. Cei, V. Kirchoff, and S. W. Wong.** 2001. Identification of the rhesus macaque rhadinovirus lytic origin of DNA replication. J Virol **75:**11401-7.

129. **Pati, S., M. Cavrois, H. G. Guo, J. S. Foulke, Jr., J. Kim, R. A. Feldman, and M. Reitz.** 2001. Activation of NF-kappaB by the human herpesvirus 8 chemokine receptor ORF74: evidence for a paracrine model of Kaposi's sarcoma pathogenesis. J Virol **75:**8660-73.

130. **Pati, S., J. S. Foulke, Jr., O. Barabitskaya, J. Kim, B. C. Nair, D. Hone, J. Smart, R. A. Feldman, and M. Reitz.** 2003. Human herpesvirus 8-encoded vGPCR activates nuclear factor of activated T cells and collaborates with human immunodeficiency virus type 1 Tat. J Virol **77:**5759-73.

131. **Pelchen-Matthews, A., N. Signoret, P. J. Klasse, A. Fraile-Ramos, and M. Marsh.** 1999. Chemokine receptor trafficking and viral replication. Immunol Rev **168:**33-49.

132. **Polson, A. G., D. Wang, J. DeRisi, and D. Ganem.** 2002. Modulation of host gene expression by the constitutively active G protein-coupled receptor of Kaposi's sarcoma-associated herpesvirus. Cancer Res **62:**4525-30.

133. **Reed, C. J.** 2000. Apoptosis and cancer: strategies for integrating programmed cell death. Semin Hematol **37:**9-16.

134. **Renne, R., D. Blackbourn, D. Whitby, J. Levy, and D. Ganem.** 1998. Limited transmission of Kaposi's sarcoma-associated herpesvirus in cultured cells. J Virol **72:**5182-8.

135. **Renne, R., W. Zhong, B. Herndier, M. McGrath, N. Abbey, D. Kedes, and D. Ganem.** 1996. Lytic growth of Kaposi's sarcoma-associated herpesvirus (human herpesvirus 8) in culture. Nat Med **2:**342-6.

136. **Renwick, N., T. Halaby, G. J. Weverling, N. H. Dukers, G. R. Simpson, R. A. Coutinho, J. M. Lange, T. F. Schulz, and J. Goudsmit.** 1998. Seroconversion for human herpesvirus 8 during HIV infection is highly predictive of Kaposi's sarcoma. Aids **12:**2481-8.

137. **Rose, T. M., J. T. Ryan, E. R. Schultz, B. W. Raden, and C. C. Tsai.** 2003. Analysis of 4.3 kilobases of divergent locus B of macaque retroperitoneal fibromatosis-associated herpesvirus reveals a close similarity in gene sequence and genome organization to Kaposi's sarcoma-associated herpesvirus. J Virol **77:**5084-97.

138. **Rose, T. M., K. B. Strand, E. R. Schultz, G. Schaefer, G. W. Rankin, Jr., M. E. Thouless, C. C. Tsai, and M. L. Bosch.** 1997. Identification of two homologs

of the Kaposi's sarcoma-associated herpesvirus (human herpesvirus 8) in retroperitoneal fibromatosis of different macaque species. J Virol **71:**4138-44.

139. **Rosenkilde, M. M., T. N. Kledal, H. Brauner-Osborne, and T. W. Schwartz.** 1999. Agonists and inverse agonists for the herpesvirus 8-encoded constitutively active seven-transmembrane oncogene product, ORF-74. J Biol Chem **274:**956-61.

140. **Rosenkilde, M. M., T. N. Kledal, P. J. Holst, and T. W. Schwartz.** 2000. Selective elimination of high constitutive activity or chemokine binding in the human herpesvirus 8 encoded seven transmembrane oncogene ORF74. J Biol Chem **275:**26309-15.

141. **Russo, J. J., R. A. Bohenzky, M. C. Chien, J. Chen, M. Yan, D. Maddalena, J. P. Parry, D. Peruzzi, I. S. Edelman, Y. Chang, and P. S. Moore.** 1996. Nucleotide sequence of the Kaposi sarcoma-associated herpesvirus (HHV8). Proc Natl Acad Sci U S A **93:**14862-7.

142. **Said, J. W., K. Chien, T. Tasaka, and H. P. Koeffler.** 1997. Ultrastructural characterization of human herpesvirus 8 (Kaposi's sarcoma-associated herpesvirus) in Kaposi's sarcoma lesions: electron microscopy permits distinction from cytomegalovirus (CMV). J Pathol **182:**273-81.

143. **Sarid, R., S. J. Olsen, and P. S. Moore.** 1999. Kaposi's sarcoma-associated herpesvirus: epidemiology, virology, and molecular biology. Adv Virus Res **52:**139-232.

144. **Sarid, R., T. Sato, R. A. Bohenzky, J. J. Russo, and Y. Chang.** 1997. Kaposi's sarcoma-associated herpesvirus encodes a functional bcl-2 homologue. Nat Med **3:**293-8.

145. **Schulz, T. F.** 2000. KSHV (HHV8) infection. J Infect **41:**125-9.

146. **Schulz, T. F.** 2001. KSHV/HHV8-associated lymphoproliferations in the AIDS setting. Eur J Cancer **37:**1217-26.

147. **Schulz, T. F., and P. S. Moore.** 1999. Kaposi's sarcoma-associated herpesvirus: a new human tumor virus, but how? Trends Microbiol **7:**196-200.

148. **Schwarz, M., and P. M. Murphy.** 2001. Kaposi's sarcoma-associated herpesvirus G protein-coupled receptor constitutively activates NF-kappa B and induces proinflammatory cytokine and chemokine production via a C-terminal signaling determinant. J Immunol **167:**505-13.

149. **Searles, R. P., E. P. Bergquam, M. K. Axthelm, and S. W. Wong.** 1999. Sequence and genomic analysis of a Rhesus macaque rhadinovirus with similarity to Kaposi's sarcoma-associated herpesvirus/human herpesvirus 8. J Virol **73:**3040-53.

150. **Shepard, L. W., M. Yang, P. Xie, D. D. Browning, T. Voyno-Yasenetskaya, T. Kozasa, and R. D. Ye.** 2001. Constitutive activation of NF-kappa B and secretion of interleukin-8 induced by the G protein-coupled receptor of Kaposi's sarcoma-associated herpesvirus involve G alpha(13) and RhoA. J Biol Chem **276:**45979-87.

151. **Simas, J. P., and S. Efstathiou.** 1998. Murine gammaherpesvirus 68: a model for the study of gammaherpesvirus pathogenesis. Trends Microbiol **6:**276-82.

152. **Smit, M. J., D. Verzijl, P. Casarosa, M. Navis, H. Timmerman, and R. Leurs.** 2002. Kaposi's sarcoma-associated herpesvirus-encoded G protein-coupled receptor ORF74 constitutively activates p44/p42 MAPK and Akt via G(i) and phospholipase C-dependent signaling pathways. J Virol **76:**1744-52.

153. **Sodeik, B., M. W. Ebersold, and A. Helenius.** 1997. Microtubule-mediated transport of incoming herpes simplex virus 1 capsids to the nucleus. J Cell Biol **136:**1007-21.

154. **Sodhi, A., S. Montaner, V. Patel, M. Zohar, C. Bais, E. A. Mesri, and J. S. Gutkind.** 2000. The Kaposi's sarcoma-associated herpes virus G protein-coupled receptor up-regulates vascular endothelial growth factor expression and secretion through mitogen-activated protein kinase and p38 pathways acting on hypoxia-inducible factor 1alpha. Cancer Res **60:**4873-80.

155. **Soulier, J., L. Grollet, E. Oksenhendler, P. Cacoub, D. Cazals-Hatem, P. Babinet, M. F. d'Agay, J. P. Clauvel, M. Raphael, L. Degos, and et al.** 1995. Kaposi's sarcoma-associated herpesvirus-like DNA sequences in multicentric Castleman's disease. Blood **86:**1276-80.

156. **Spear, P. G., R. J. Eisenberg, and G. H. Cohen.** 2000. Three classes of cell surface receptors for alphaherpesvirus entry. Virology **275:**1-8.

157. **Spear, P. G., and R. Longnecker.** 2003. Herpesvirus entry: an update. J Virol **77:**10179-85.

158. **Stine, J. T., C. Wood, M. Hill, A. Epp, C. J. Raport, V. L. Schweickart, Y. Endo, T. Sasaki, G. Simmons, C. Boshoff, P. Clapham, Y. Chang, P. Moore, P. W. Gray, and D. Chantry.** 2000. KSHV-encoded CC chemokine vMIP-III is

a CCR4 agonist, stimulates angiogenesis, and selectively chemoattracts TH2 cells. Blood **95:**1151-7.

159. **Streblow, D. N., C. Soderberg-Naucler, J. Vieira, P. Smith, E. Wakabayashi, F. Ruchti, K. Mattison, Y. Altschuler, and J. A. Nelson.** 1999. The human cytomegalovirus chemokine receptor US28 mediates vascular smooth muscle cell migration. Cell **99:**511-20.

160. **Swanton, C., D. J. Mann, B. Fleckenstein, F. Neipel, G. Peters, and N. Jones.** 1997. Herpes viral cyclin/Cdk6 complexes evade inhibition by CDK inhibitor proteins. Nature **390:**184-7.

161. **Talbot, S. J., R. A. Weiss, P. Kellam, and C. Boshoff.** 1999. Transcriptional analysis of human herpesvirus-8 open reading frames 71, 72, 73, K14, and 74 in a primary effusion lymphoma cell line. Virology **257:**84-94.

162. **Taylor, J. F., A. C. Templeton, C. L. Vogel, J. L. Ziegler, and S. K. Kyalwazi.** 1971. Kaposi's sarcoma in Uganda: a clinico-pathological study. Int J Cancer **8:**122-35.

163. **Thome, M., P. Schneider, K. Hofmann, H. Fickenscher, E. Meinl, F. Neipel, C. Mattmann, K. Burns, J. L. Bodmer, M. Schroter, C. Scaffidi, P. H. Krammer, M. E. Peter, and J. Tschopp.** 1997. Viral FLICE-inhibitory proteins (FLIPs) prevent apoptosis induced by death receptors. Nature **386:**517-21.

164. **Trus, B. L., J. B. Heymann, K. Nealon, N. Cheng, W. W. Newcomb, J. C. Brown, D. H. Kedes, and A. C. Steven.** 2001. Capsid structure of Kaposi's sarcoma-associated herpesvirus, a gammaherpesvirus, compared to those of an

alphaherpesvirus, herpes simplex virus type 1, and a betaherpesvirus, cytomegalovirus. J Virol **75:**2879-90.

165. **Veikkola, T., and K. Alitalo.** 1999. VEGFs, receptors and angiogenesis. Semin Cancer Biol **9:**211-20.

166. **Verma, S. C., and E. S. Robertson.** 2003. Molecular biology and pathogenesis of Kaposi sarcoma-associated herpesvirus. FEMS Microbiol Lett **222:**155-63.

167. **Verzijl, D., C. P. Fitzsimons, M. Van Dijk, J. P. Stewart, H. Timmerman, M. J. Smit, and R. Leurs.** 2004. Differential activation of murine herpesvirus 68- and Kaposi's sarcoma-associated herpesvirus-encoded ORF74 G protein-coupled receptors by human and murine chemokines. J Virol **78:**3343-51.

168. **Virgin, H. W. t., P. Latreille, P. Wamsley, K. Hallsworth, K. E. Weck, A. J. Dal Canto, and S. H. Speck.** 1997. Complete sequence and genomic analysis of murine gammaherpesvirus 68. J Virol **71:**5894-904.

169. **Wagner, E. K., and D. C. Bloom.** 1997. Experimental investigation of herpes simplex virus latency. Clin Microbiol Rev **10:**419-43.

170. **Wakeling, M. N., D. J. Roy, A. A. Nash, and J. P. Stewart.** 2001. Characterization of the murine gammaherpesvirus 68 ORF74 product: a novel oncogenic G protein-coupled receptor. J Gen Virol **82:**1187-97.

171. **Whitley, R. J., and B. Roizman.** 2001. Herpes simplex virus infections. Lancet **357:**1513-8.

172. **Wong, S. K.** 2003. G protein selectivity is regulated by multiple intracellular regions of GPCRs. Neurosignals **12:**1-12.

173. **Wong, S. W., E. P. Bergquam, R. M. Swanson, F. W. Lee, S. M. Shiigi, N. A. Avery, J. W. Fanton, and M. K. Axthelm.** 1999. Induction of B cell hyperplasia in simian immunodeficiency virus-infected rhesus macaques with the simian homologue of Kaposi's sarcoma-associated herpesvirus. J Exp Med **190:**827-40.

174. **Wright, G. J., M. J. Puklavec, A. C. Willis, R. M. Hoek, J. D. Sedgwick, M. H. Brown, and A. N. Barclay.** 2000. Lymphoid/neuronal cell surface OX2 glycoprotein recognizes a novel receptor on macrophages implicated in the control of their function. Immunity **13:**233-42.

175. **Wu, L., P. Lo, X. Yu, J. K. Stoops, B. Forghani, and Z. H. Zhou.** 2000. Three-dimensional structure of the human herpesvirus 8 capsid. J Virol **74:**9646-54.

176. **Yang, T. Y., S. C. Chen, M. W. Leach, D. Manfra, B. Homey, M. Wiekowski, L. Sullivan, C. H. Jenh, S. K. Narula, S. W. Chensue, and S. A. Lira.** 2000. Transgenic expression of the chemokine receptor encoded by human herpesvirus 8 induces an angioproliferative disease resembling Kaposi's sarcoma. J Exp Med **191:**445-54.

177. **Yen-Moore, A., S. D. Hudnall, P. L. Rady, R. F. Wagner, Jr., T. O. Moore, O. Memar, T. K. Hughes, and S. K. Tyring.** 2000. Differential expression of the HHV-8 vGCR cellular homolog gene in AIDS-associated and classic Kaposi's sarcoma: potential role of HIV-1 Tat. Virology **267:**247-51.

178. **Zhang, L., J. Chiu, and J. C. Lin.** 1998. Activation of human herpesvirus 8 (HHV-8) thymidine kinase (TK) TATAA-less promoter by HHV-8 ORF50 gene product is SP1 dependent. DNA Cell Biol **17:**735-42.

179. **Zimmermann, K. C., C. Bonzon, and D. R. Green.** 2001. The machinery of programmed cell death. Pharmacol Ther **92:**57-70.

180. **Zlotnik, A., and O. Yoshie.** 2000. Chemokines: a new classification system and their role in immunity. Immunity **12:**121-7.